Optimization of heating and cooling systems consisting of PVT collectors, seasonal storage and heat pumps

MSc. Thesis report

Divye Nikhil Kanawala

TU Delft

Optimization of heating and cooling systems consisting of PVT collectors, seasonal storage and heat pumps

Thesis report

by

Divye Nikhil Kanawala

To obtain the degree of Master of Science at the Delft University of Technology.
To be defended publicly on: 28th August, 2024

Thesis committee:	Rudi Santbergen, Zain Ul Abdin, Arthur Weeber, Emanuele Zanetti
Main Supervisor:	Rudi Santbergen
Daily Supervisor	Zain Ul Abdin
Project Duration	November 2023 - August 2024
Student number	5857988

Sustainable Energy Technology (SET)
TU Delft
August 28th, 2024

Preface

The completion of this thesis represents a pivotal moment in my academic and personal journey. The research undertaken in this thesis—focused on optimizing integrated energy systems involving Photovoltaic thermal (PVT) collectors, Aquifer thermal energy storage (ATES), heat pumps and heat exchangers has been a subject of profound interest and engagement. The process has been intellectually stimulating and personally rewarding, allowing me to deepen my understanding of sustainable energy systems and contribute to the ongoing discourse in this evolving field.

I would like to extend my deepest gratitude to my supervisors, Rudi Santbergen and Zain Ul Abdin, whose expertise, guidance, and constructive feedback have been instrumental in shaping the direction and quality of this work. Their support has not only enriched the research but also significantly enhanced my learning experience.

Special thanks to my colleagues in the research group, particularly Aron van Rossum and David E. Martinez Aguilera. Their collaborative spirit provided a stimulating environment that was both challenging and supportive, fostering a culture of excellence and mutual respect.

During my time in the Netherlands, I was fortunate to be surrounded by a close-knit group of friends who became my support system. I am deeply grateful to Rupesh Yellamraju, Zeba Rahaman, Abhiroop Bhowmik, Manali Shah, Shubham Litke, Shreya Kejriwal, Neel Lodha, Anand Mahajan and Pankaj Upadhyay whose companionship, encouragement, and shared experiences made my time in the Netherlands truly enjoyable. Their presence played a crucial role in helping me balance the demands of academic work and the need for social and emotional well-being.

Furthermore, I wish to acknowledge the broader community at TU Delft. The resources, intellectual environment, and collaborative spirit within the university have been critical to the successful completion of this thesis. I am also grateful to the administrative staff for their assistance and the faculty members whose courses and lectures laid the foundation for my research.

I would like to give my JIP mentors: Smith Rutger and Maarten Oevering a special thanks, whose guidance laid the foundation of my interest in heat networks during my internship at Eneco. I continued that interest to pursue this as my Thesis topic.

Finally, I extend my heartfelt thanks to my parents, sister, brother-in-law, grandparents and friends back home, whose unwavering support and belief in my capabilities have been a constant source of strength. This thesis is a reflection of the collective effort, guidance, and encouragement I have received from all those around me. It is dedicated to them with deep appreciation and gratitude.

Abstract

Interest in incorporating renewable energy systems into current infrastructure has surged as a result of the growing need for sustainable energy solutions in urban settings. This thesis investigates the optimization of a heating and cooling system designed for residential and commercial buildings, with a focus on Dutch climate conditions. The system consists of photovoltaic thermal (PVT) collectors, aquifer thermal energy storage (ATES), heat exchanger and heat pumps. By using these technologies, buildings will be able to satisfy energy demand sustainably without the need for fossil fuels.

Through dynamic simulations, the research aims to optimize the energy system's performance while taking into account a range of operational scenarios and parameter values. Critical components, including the ATES and PVT collectors, are modeled to evaluate their working and performance with heat pumps to provide heating and with heat exchanger for cooling.

The Photovoltaic Materials and Devices research group at TU Delft uses the PVMD Toolbox, a sophisticated modeling tool. Few models from the toolbox are utilised in developing an integrated model, which is later implemented in the toolbox. Later on, it is optimized to improve its effectiveness through dynamic sizing of collectors and aquifers, and implementation of operational modes, making overall the integrated system more robust and redundant. The performance of the integrated system is then studied for a base scenario with 10 PVT collectors and 27,000 m^3 aquifer volume for the current scenario. It showcases promising results. To assess its applicability, the system is analysed under various scenarios. The first scenario is a season-wise performance assessment, where it is showcased that PVT produce energy during summer months and the rest of the year there is a consistent performance by ATES. On comparing the performance of different insulation levels of the buildings, it is found that the future scenarios require half or one-fourth of the energy as compared to the current scenario and the system performs better for them in terms of power consumption by heat pumps. The system's performance under different flow rates of water from PVT and ST is assessed. It is found that at a higher flow rate, a higher amount of energy is generated by both of the collectors, while ST shows better performance than PVT.

For the case when the system provides underfloor heating, it shows that the heat pumps require almost 25% of the energy required for radiator heating. The integrated system is then compared to that of conventional energy systems, demonstrating similar costs but almost no environmental impact and better energy efficiency.

The research findings present a compelling argument for the implementation of such energy systems in urban environments, as they indicate the possibility of substantial energy savings and a decrease in carbon emissions. The report also offers suggestions for future work, such as the application of advanced software, location feasibility studies, and various ATES to precisely model and scale such systems in various real-world circumstances.

This thesis contributes significant insights into the subject of renewable energy systems and lays the groundwork for further study and development of sustainable heat networks by offering a thorough analysis of an innovative method of sustainable energy management.

Contents

List of Figures

List of Tables

Nomenclature

Abbreviations

Abbreviation	Definition
ATES	Aquifer Thermal Energy Storage
AQSYST	Aquifer System Simulation for Test Scenarios
BTES	Borehole Thermal Energy Storage
CAPEX	Capital Expenditure
CO_2	Carbon Dioxide
COP	Coefficient of Performance
DHW	Domestic Hot Water
EIA	Environmental Impact Assessment
EPBP	Energy Payback Period
GWhth	GWh of Thermal energy
GWhe	GWh of Electrical energy
HT	High Temperature
HE	Heat Exchanger
HP	Heat Pump
hp	Horsepower
HRF	Heat Recovery Factor
HVAC	Heating, Ventilation, and Air Conditioning
IEA	International Energy Agency
kWhth	kWh of Thermal Energy
kWhe	kWh of Electrical Energy
LT	Low Temperature
LCOC	Levelized Cost of Cooling
LCOE	Levelized Cost of Electricity
LCOH	Levelized Cost of Heating
MT	Medium Temperature
MWp	Peak Electrical Power in MW
MWth	Peak Thermal Power in MW
NOA	Number of Apartments in each Building
NZEB	Nearly Zero-Emission Building
OPEX	Operational Expenditure
PCM	Phase Change Materials
PTES	Pit Thermal Energy Storage
PV	Photovoltaic
PVT	Photovoltaic Thermal
PVMD	Photovoltaic Materials and Devices
ROI	Return on Investment
SPF	Seasonal Performance Factor

Abbreviation	Definition
SPB	Simple Payback Period
ST	Solar Thermal
TRNSYS	Transient System Simulation Tool
TTES	Tank Thermal Energy Storage
ULT	Ultra-low Temperature

Symbols

Symbol	Definition	Unit
$\dot{Q}$	Heat Transfer Rate	$[W]$
$\dot{m}$	Mass Flow Rate	$[g/s]$
$c_{p,w}$	Specific Heat Capacity of Water	$[J/g.K]$
ΔT	Temperature Difference	[°C]
Q	Energy Heat Transfer	$[J]$
kW	Power	$[kW]$
kW_p	Peak Power	$[kW]$
m	Mass of Water	$[kg]$
R_{th}	Thermal Radius	$[m]$
V	Volume of the Aquifer	$[m^3]$
$c_{p,aq}$	Specific Heat Capacity of the Aquifer	$[J/g.K]$
L	Screen Length	$[m]$
W	Work	$[J]$
T_{b}	Building Temperature	[°C]
$T_{\text{c,out}}$	Outlet Temperature of Heat exchanger	[°C]
$T_{\text{w,aq}}$	Warm Aquifer Temperature	[°C]
$T_{\text{c,aq}}$	Cold Aquifer Temperature	[°C]
η_{he}	Heat exchanger efficiency	(%)
$\dot{m}_b$	Mass flow rate of water	$[kg/s]$

1

Introduction

Solar energy generation has risen over the past two or three decades due to a global shift toward renewable sources. This shift is an attempt to address environmental concerns by reducing greenhouse gas emissions and mitigating the impact of climate change. Renewable energy sources like solar, wind, hydro, and geothermal are being preferred over fossil fuels due to their high availability, low environmental impact and long-term sustainability.

Buildings are a major source of carbon emissions and require a lot of energy for their electricity as well as heating/ cooling needs. Therefore, there is a need to develop an energy system which delivers the growing demand, in a sustainable manner. Such a type of energy system is being modeled in this thesis to check its applicability, and performance energy-wise and compare it economically to the conventional district heating systems.

This chapter will delve into topics such as photovoltaic (PV) modules, solar thermal (ST) collectors, photovoltaic thermal (PVT) collectors, heat pumps, storage tanks, aquifer thermal energy storage (ATES) systems as a seasonal storage tank which is a part of the energy system. Later on, the degradation of PV modules performance and key research gaps in the optimization of ATES systems integrated with solar collectors will be briefly discussed.

1.1 Background

An overview of the fundamental components of the energy system modeled in this thesis is presented in this section. PV modules are the first in the line; they use the photovoltaic effect to directly convert sunlight into electricity. Next, ST collectors are devices that extract heat from sunlight for a variety of uses—are described. PVT collectors are the next topic covered in this section. These collectors combine PV and ST technologies to produce heat and energy from a single unit. They offer better efficiency with the utilisation of less space. The topic of heat pumps is then discussed. Heat pumps are machinery that utilise a small amount of external power to transport thermal energy from a source of lower temperature to a sink of higher temperature. In many renewable energy systems, particularly those that combine PVT and ATES, heat pumps are essential components. Utilising them, the low-temperature heat from ATES systems or PVT collectors can be raised to temperatures suitable for space heating or domestic hot water applications. This section provides a basic understanding of their working and the need to use them in integrated energy systems.

1.1.1 PV modules

Photovoltaic modules, also known as solar modules, are devices that convert sunlight into electricity through a process called the photovoltaic effect. PV modules are formed by combining

several solar cells which generate electricity through the release of electrons by absorbing energy from the photons present in sunlight. The efficiency of PV modules, which refers to how effectively they convert sunlight to electricity, has been improved over time. Currently, the modules available in the market have around 20-21% efficiency. These systems can be integrated with energy storage technologies like batteries, allowing excess power generated during peak sunlight hours or summer to be stored and utilized during periods of low or no solar irradiation, such as at night or in winter. This integration enhances system reliability and efficiency, providing a more consistent energy supply that better aligns with demand patterns, thus addressing solar energy's intermittent nature. Figure 1.1a depicts a PV module which generates electricity from sunlight.

(a) (b)

Figure 1.1: Schematic representation of a PV module and a solar thermal collector

1.1.2 Solar thermal collectors

Solar thermal collectors are devices that collect heat by absorbing sunlight and converting that into heat. The sunlight is absorbed by the absorber part of the collector and the heat generated is transferred to the cooling fluid such as air, water, phase change materials (PCM), and nanofluids (EIA, 2022). The main components of solar collectors include the absorber, glazing/enclosure materials, heat transfer piping, and insulation. Various types of these collectors exist, including flat plate solar collectors, concentrating solar collectors, evacuated tube solar collectors, and parabolic solar collectors.

Tian and Zhao (2013) classify solar thermal collectors depending on applications and environments. Unglazed collectors, used for pool heating or in mild climates, have black surfaces absorbing sunlight directly. Glazed collectors, enclosed in glass or plastic covers, are efficient for domestic hot water systems or space heating. Air-based collectors circulate air to capture and transfer heat, while water-based collectors use a fluid to absorb solar energy for heating water in various settings. Each type of solar thermal collector has unique advantages for diverse energy needs, harnessing sunlight's power extensively.

Ul Abdin and Rachid (2021) mention that these collectors collect, store, and utilize heat for various applications, such as domestic hot water (DHW), space heating, space cooling, and supplying industrial heat for processes like drying and desalination. Figure 1.1b shows a solar thermal collector which converts sunlight into thermal energy by heating the fluid travelling inside its tubes.

1.1.3 Introduction to photovoltaic thermal systems

A PVT is a device which combines PV and ST modules into one unit where PV generates electricity and ST generates heat energy. Generally, the electrical and thermal efficiency of this collector is higher compared to stand-alone conventional modules. Only 15-20% of the incident solar radiation is absorbed. The rest of the radiation is converted into thermal energy by the absorber at the back of the PV module. The PVT collector utilizes the waste heat going into the environment to heat the fluid and produce thermal energy which can be used for space heating, cooling and DHW. The components of the PVT system mainly include:

- PV module integrated with solar thermal collector
- Storage tank for storing the generated heat
- Heat pump for elevating the temperature of water
- Pump for circulating the water
- Controller for controlling the flow of water

According to Sharaf et al. (2022), one advantageous outcome of this process is the lowered temperature of the solar cell module, depending on the inlet temperature, size and extraction medium. This is a result of the efficient heat transfer to the cooling fluid, leading to improved operational efficiency and prolonged lifespan. Therefore, the PVT collectors achieve more specific surface energy than standard PV modules.

Kalogirou (2019) found out that the thermal conductivity between the heat absorption unit and the PV module can increase electrical and thermal efficiency. The cooling liquid can be of various types such as air, water, refrigerants, nanofluids, and bi-fluid (a combination of liquid and air). Air cooling offers the advantage of an increase in overall efficiency with less cost but low performance as compared to water cooling (Prasad & Bansal, 2021). Zhao et al. (2019) highlighted that the design, climate and operational elements are the main parameters affecting the performance of PVT collectors.

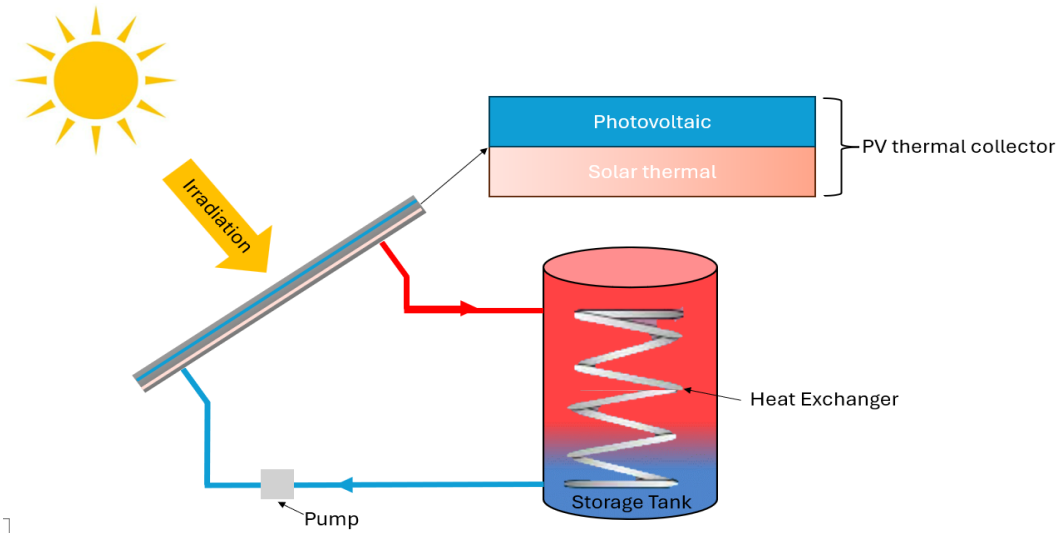

Figure 1.2: Visual representation of PVT collector system

Figure 1.2 shows the overall layout of a PVT system. The output temperature from the PVT collector can vary from 30 °C up to 80 °C depending on the type of the collector (Sadeghi et al.,

2022).

Flat-plate PVT collectors can be classified into different categories based on the type of working fluid employed, namely water type, air type, or a combination of both (water/air) type, indicated by Ibrahim et al. (2011). Zondag et al. (2003) mentioned various configurations of flat-plate PVT collectors which include sheet-and-tube, channel, free-flow, and dual-absorber designs. Among these, the channel-below-transparent PV design demonstrated the highest efficiency.

Compared to liquid-based systems, air-based PVT collectors generally exhibit lower efficiency levels and have lower manufacturing costs, as found by Aste et al. (2008). Ibrahim et al. (2011) states that these flat-plate PVT collectors have the flexibility of functioning either as grid-connected systems or as standalone systems. Research conducted by Talavera et al. (2007) highlighted that grid-connected PVT systems prove to be more financially advantageous investments under specific economic circumstances.

Concentrating PVT collectors play a crucial role in the cost reduction of electricity generated by PV modules through the concentration of sunlight, thereby enabling the utilization of a smaller module area, quoted by Kribus et al. (2006). However, the elevated concentration levels result in increased PV module temperatures, emphasizing the importance of maintaining low temperatures to uphold efficiency levels, found out by Othman et al. (2005), Singh et al. (2008), Katz et al. (2001) and Radziemska and Klugmann (2002).

Unglazed and glazed PVT collectors exhibit distinct characteristics in terms of thermal efficiency and cost-effectiveness. Huang et al. (1999) and Huang et al. (2001) have developed unglazed PVT collectors which typically showcase lower thermal efficiencies compared to glazed systems but prove to be more economical. On the contrary, Chow et al. (2009) found out that glazed PVT collectors generally yield higher thermal outputs at the expense of potential electrical efficiency losses due to heightened operating temperatures.

PVT can be combined with storage mediums such as underground tanks, aquifers, and pit storage to store the hot water, which can be directly used to supply heating and cooling to buildings or as an input to heat pumps which can raise the water to the desired temperature and supply it. The heat pumps can be run through the electricity produced from the PVT collectors, improving the overall system's self-sufficiency (Weiss & Spörk-Dür, 2023).

Chow et al. (2012) investigated PVTs in-depth and addressed issues such as the high costs of the collectors, product standardization, installation training, and product reliability. The study conducted by (Matuška, 2014) concluded that the cost of PVT collectors is higher than its counterpart PV modules and solar thermal collectors, due to more material requirements and complex design. However, there has been significant growth in the global market of these collectors in recent years, since they have higher efficiency than their counterparts. Weiss and Spörk-Dür (2023) in the annual study of IEA's Solar Heating and Cooling Programme stated that there has been an increase of 57% in sales in the year 2021 from a 20% increase in the year 2020. Countries like Israel, Netherlands, France, Germany and Spain are the largest markets of PVT collectors in the world. Weiss and Spörk-Dür (2023) estimated that the cumulative installed PVT collector area in the world is 1.50 million m^2, producing 789 MWth in thermal capacity and 276 MWp in electrical capacity.

1.1.4 Heat pumps

Heat pumps utilize electricity to increase the temperature of the source and supply it to the sink, defined by (Union, 2009). Simply, they are the reverse of heat engines transferring heat from low-temperature regions to high-temperature regions. Dinçer et al. (2017) mentions the process of heat transfer is executed by pumping a fluid (such as refrigerant) through the system. There are various types of heat pumps air-to-water, water-to-water, brine-to-water, air–to–air,

water–to–air, brine–air and ground source heat pumps. Figure 1.3 illustrates the refrigeration cycle of a water-source heat pump. The cycle involves the circulation of a refrigerant through various components to transfer heat between a water source (such as an underground aquifer) and a building and the cycle is reversed when cooling is required (Association, 2018).

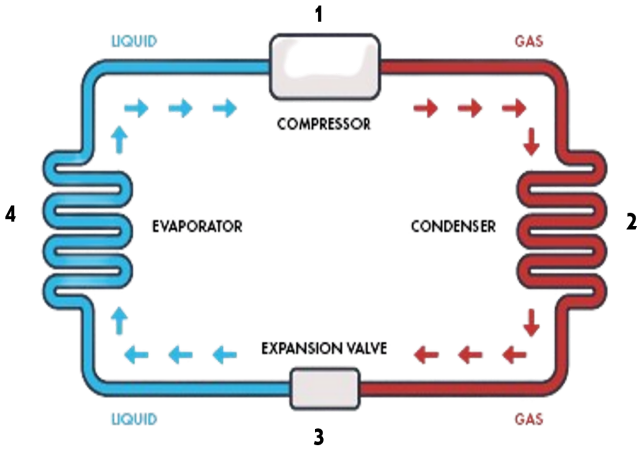

Figure 1.3: Water-based heat pump, "Heating and Cooling Systems" (2022)

Working principle of heat pumps

1. Compressor: The refrigerant vapour is compressed, increasing its pressure and temperature.

2. Condenser: In heating mode, the hot refrigerant vapour releases heat to the building loop, condensing it into a liquid. In cooling mode, it releases heat to the water loop.

3. Expansion Valve: The liquid refrigerant's pressure drops, turning it into a low-pressure liquid-vapour mixture.

4. Evaporator: In heating mode, the low-pressure refrigerant absorbs heat from the water loop, evaporating into a vapour. In cooling mode, it absorbs heat from the building loop.

5. Water loop: This loop carries heat between the water source (lake, pond, or well) and the heat pump. In heating mode, it provides heat to the evaporator. In cooling mode, it dissipates heat from the condenser.

6. Building loop: This loop circulates a heat transfer fluid between the heat pump and the building's heating or cooling system, delivering or removing heat as needed.

Electricity from the grid or a renewable energy source is taken as input to transfer the energy absorbed from the outside environment to the heating water through coolant liquid in the evaporator. This liquid is compressed at high pressure, in turn increasing its temperature above the heated water and then condensing it in the condenser where the heat is transferred to heating water.

The performance of these systems is influenced by various factors such as ambient conditions, type of installation and the conditions of buildings where these systems are installed. Vorushylo et al. (2018) found out that heat pumps have higher efficiency, lower costs, and low carbon emissions compared to direct heating. These systems decrease the reliance on non-renewable sources for home heating thereby improving energy security. The number of heat pumps sold in

Europe has increased from 7.5 million units in 2014 to 11.8 million units in 2018, (Zhang et al., 2022).

The efficiency of the heat pumps is evaluated by finding out the ratio of the amount of heat energy (Q) given out by the heat pump to the amount of energy (W) injected. This ratio is generally referred to as the Coefficient of Performance (COP) as mentioned in the Equation 1.1.

$$COP = \frac{Q}{W} \tag{1.1}$$

1.1.5 Storage tanks

A pivotal component within PVT systems is the storage tank, which accumulates surplus thermal energy to be utilized during periods of high demand. These storage tanks serve as short-term storage such as hot water tanks, as well as long-term storage in seasonal tanks like ATES. Storage tanks have different designs and can be made of various materials (for example stainless steel, reinforced concrete, carbon steel, and nickel-plated copper) which can affect the overall performance, efficiency, cost, and effectiveness of PVT systems (Danehkar & Yousefi, 2022). Pang et al. (2020) states that materials like polyethene, fibreglass and thermoplastic are becoming increasingly popular due to the lower build costs. Alsaqoor et al. (2023) mentions that selecting an appropriate storage tank is critical for enhancing the operational efficacy of PVT systems.

Rahimi-Ahar et al. (2023) investigated the effect of stratified water thermal storage having a phase change material (PCM) ball-packed bed connected to unglazed PVT collectors. This resulted in expanding the thermal capacity of storage and increasing the overall efficiency of the system. Sun et al. (2022) evaluated the performance of a PVT collectors integrated with a phase change material-water storage system and found that the lower melting point PCM increases the performance of PVT collectors but the temperature of water in the tank is lower than the required for DHW. Ul Abdin et al. (2022) proposed and modelled an integrated photovoltaic thermal collector and storage tank system to enable optimization of the design parameters. Their key findings included increased temperatures with an air gap, limited returns beyond 0.1 m insulator thickness, thinner absorbers and copper materials improving heat transfer, water-glycol mixes outperforming pure water, and recycled engine oil as an absorber reducing environmental impact. Overall, the integrated model provided a robust platform for determining the sensitivity of system performance to various design choices.

Seasonal storage can mitigate the mismatch between supply and demand of thermal energy over the year. In winter, when there is low radiation, the PVT collectors will produce less thermal and electrical energy which is also the period with high thermal load. In such cases, seasonal storage can supply the excess demand required. Yang et al. (2021) examined 60 case studies, of which 51 employed seasonal storage to increase the utilisation of solar technology to solve the seasonal mismatch. The seasonal storage offers the advantage of having low capital costs compared to electrical and domestic thermal storage (Sarbu & Sebarchievici, 2018). On a scale of per kWh, it is 100 times cheaper for large installations (Lund et al., 2016). The capital costs majorly include land costs, storage and site availability.

Bird et al. (2016) discusses that due to the rapid installations of renewable energy sources and their issue of intermittency, electrical grids have become unreliable and the excess power is curtailed. seasonal storage can utilize the excess power to provide the mismatch in thermal energy, though the seasonal cost difference needs to be large enough to accommodate for seasonal storage. These storages are a natural way to shift the peak demands and to improve thermal energy efficiency (Nordell & Snijders, 2015). ATES can be used to store cold from winter months and heat from summer months, to cool buildings in summer and heat them in winter respectively.

1.1.6 Aquifer thermal energy storage as seasonal storage

Aquifer thermal energy storage systems utilize underground water-bearing layers, known as aquifers, to store either heat or cold. van der Roest et al. (2021) mentions that a typical ATES comprises of multiple cold and warm aquifers. The groundwater is used as working fluid which is injected and extracted from the aquifer to store and extract the thermal energy, respectively. ATES system can have two aquifers at different depths, or two aquifers separated by radial distance, or three aquifers with the third aquifer used as a buffer to store water at intermediate temperature. Generally, an ATES system has two aquifers: warm and cold. Figure 1.4 shows the different types of aquifer systems for the two modes, heating and cooling. The ATES system consists of a set of aquifers, water-to-water heat pumps, heat exchangers and the piping network. ATES system can be constructed in places where there are unconsolidated sands, gravel or fractured rocks.

Fleuchaus et al. (2020) found out that the loss of heat source and varying demand are the two main drawbacks of ATES. It is advantageous to use ATES since they have low CO_2 emissions but there might be unwanted interaction between ATES and the subsurface which can lead to degradation in performance. The drilling of aquifers for ATES is the main cost parameter. Also, the Water Board has set various preconditions that must be met when extracting and discharging water, related to thermal effects, management and maintenance, and physico-chemistry. This could increase the complexity of obtaining the permits to extract the water in the area (Blaas, 2022). West (2004) mentions the cost savings and reconfigurability of these systems as their limitations in his study.

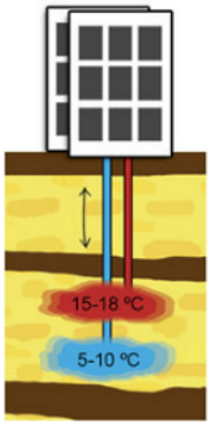

(a) Two aquifers at different depths

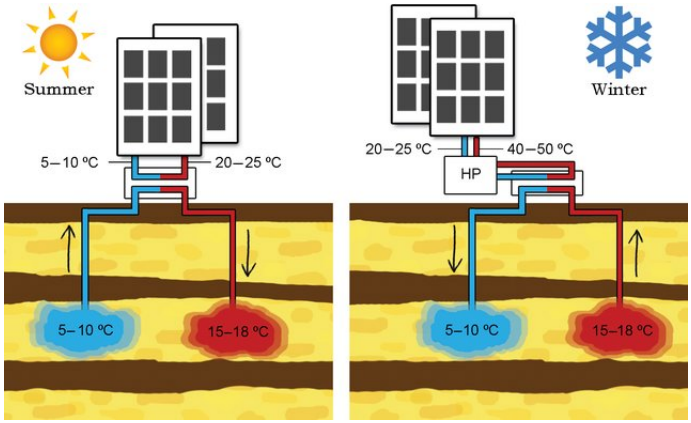

(b) Two aquifers at radial distance

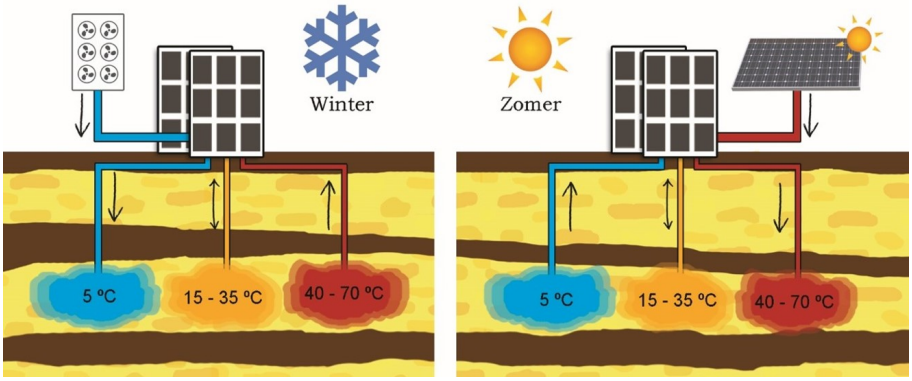

(c) Triple aquifer

Figure 1.4: Different configurations of aquifer system, Bloemendal and Olsthoorn (2018a) and Bloemendal et al. (2022)

ATES is advantageous as water's high specific heat and naturally underground formations are utilized (Lee, 2010). Lyden et al. (2022) mentions that the ATES offers lower installation costs than Tank Thermal Energy Storage (TTES), Borehole Thermal Energy Storage (BTES) and Pit Thermal Energy Storage (PTES). It also has a lower land footprint than all of these storage mediums.

1.2 Role of the energy system in heating grids

The integration of ATES and PVT collectors significantly enhances the sustainability and efficiency of district heating networks. Recent developments have focused on the fourth and fifth generations of district heating grids. Fourth generation grids operate at temperatures below 70°C, while fifth generation systems function at near-ambient temperatures.

ATES plays a crucial role in managing daily and seasonal thermal energy storage within fourth-generation district heating systems, effectively balancing supply and demand fluctuations. It enables dynamic imbalance control by storing excess heat during periods of high supply and releasing it when demand increases. PVT collectors contribute by providing both heat and renewable electricity, allowing for the immediate integration of thermal output into the district heating system.

By combining these technologies, fourth generation networks can achieve improved renewable energy storage and utilization, leading to more efficient and environmentally friendly heating solutions.

The integration of ATES and PVT collectors can play a crucial role in optimizing thermal energy distribution across buildings with diverse heating and cooling demands in fifth-generation district heating systems. ATES allows for the storage of low-grade heat at temperatures that may not be immediately usable. When buildings require heat, they can draw upon this stored thermal energy. Meanwhile, PVT collectors continuously generate heat and renewable electricity, with the thermal output being directly utilized within the district heating system to meet demand.

This synergy enables fifth-generation grids to efficiently manage varying building loads through the storage and flexible use of thermal energy. By combining these technologies, both fourth and fifth-generation thermal grids can significantly enhance their energy efficiency, storage capacity, and renewable energy utilization. The future of district heating systems lies in their ability to be smarter and more sustainable, achievable through the mutually beneficial integration of ATES and PVT systems.

1.3 Energy regulations in the Netherlands

Table 1.1 provides a concise overview of temperature requirements and corresponding provisions for three key residential functions: space heating, domestic hot water, and space cooling. The table illustrates the different temperature requirements across residential energy services and the corresponding technological solutions, highlighting the complexity of designing efficient, multi-purpose energy systems for buildings, as required by the Dutch Government.

1. The High-Temperature (HT) heat network is required to supply heat at 90°C.

2. The Medium-Temperature (MT) heat network needs to supply heat at 70°C.

3. The Low-Temperature (LT) heat network supplies heat at 40°C temperature.

Table 1.1: Dutch regulations for heat and cold demand, European Commission (2020)

Function	**Required temperature**	**Required provision**
Space heating	$>(40-90\,^{\circ}\mathrm{C})$ (depending on insulation)	$>$ HT(90 °C), MT(70 °C) or LT(40 °C) heat network
Space cooling	$<(18\,^{\circ}\mathrm{C})$ (in newly built houses)	$>$ Ultra Low Temperature (ULT) heat network
Domestic hot water	$>(55-65\,^{\circ}\mathrm{C})$ (legionella prevention)	$>$ HT(90 °C) or MT(70 °C) heat network

1.4 Performance degradation of the collectors

Solar modules harness the energy from sunlight through the photovoltaic phenomenon, transforming sunlight into electricity. Researchers have extensively studied their performance, efficiency and cost-effectiveness. Klampaftis et al. (2009) and Branker et al. (2011) state that several factors such as module temperature, sunlight levels and environmental conditions can impact the efficiency of cells. Singh et al. (2008) and Razak et al. (2016) found that solar module's efficiency declines as the module's temperature rises, aligning with Ali et al. (2016) assertion that solar modules display lower electrical efficiency in peak summer compared to winter. Similarly, Zaini et al. (2015) and Ali et al. (2016) state that these modules tend to work efficiently under cooler temperatures. Moreover, prolonged exposure to temperatures, beyond thresholds can lead to long-term degradation of cells as investigated by Rahman et al. (2023).

Gagliano and Aneli (2017) observed during their experimental investigation that the PV cells generate less voltage at higher temperatures with no change in current resulting in decreased power produced. There is an approximate 4.50% increase in power with a drop of 10 °C in PV cells temperature. To improve solar module's output power and efficiency, researchers introduced cooling methods for PV modules and the figure 1.5 shows the variation in I and V values with cell temperature.

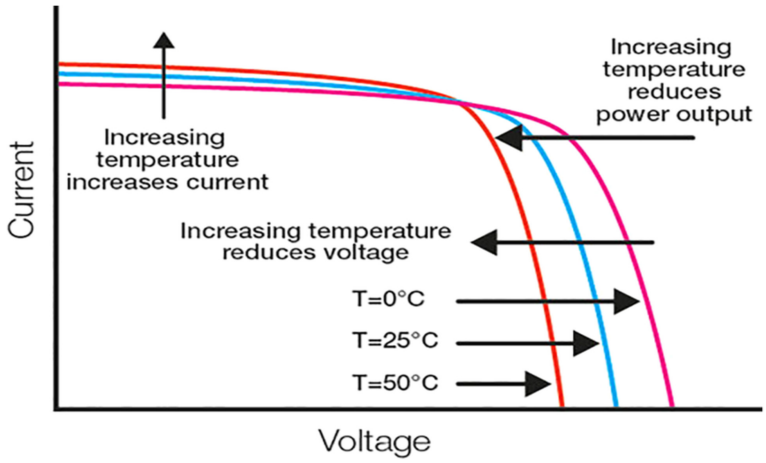

Figure 1.5: Variation in the I-V curve with temperature for PV module, Curve Tracing (2024)

Rosa-Clot et al. (2010) conducted a pioneering experiment where the PV modules were partially immersed in water, which increased efficiency by 10-20%. Odeh and Behnia (2009) studied the effect of water cooling through a water trickling mechanism, resulting in a 15% improvement in solar module system output. The use of water cooling in PV modules can increment the electrical power output by nearly five times (Kolhe et al., 2012). Kozak-Jagieła et al. (2023) in their recent paper found out that water cooling is a better option than air cooling of PV

modules. Another finding is that the high operating temperature of the PV modules results in their degradation, leading to a loss in efficiency and lifetime. Matias et al. (2017) designed a setup for cooling PV modules and found the best flow rate of water to be 0.60 L/min and an energy gain of about 23% compared to PV modules without a cooling system.

In a study conducted by Moharram et al. (2013) for PV modules with 1.25 m^2 area and front surface cooling, there was an increase of 1.50% efficiency. The cooling system utilized a 1 hp pump with a water flow rate of approximately 0.50 kg/s and a cooling rate of 2 °C/min was observed. Smith et al. (2014) observed that the monocrystalline PV modules cooled at around 0.12 kg/s water flow rate gave a net energy gain (including pump) of nearly 5%. Moreover, when water near 0 °C was used it resulted in a 24% power increment. Nižetić et al. (2016) developed a cooling technique for both the front and back sides of PV modules. Experimental variation of the flow rate of water from 0.01 kg/s to 0.060 kg/s, resulted in an increase in efficiency nearly by 15%, 19%, and 20% for back side, front side, and simultaneous back-and-front cooling, respectively. The paper published by Grubišić-Čabo et al. (2016) mentions active water cooling as the best method to cool PV modules or PVT collectors. One of the drawbacks of using this method is the evaporation of water from the storage tank. By the utilisation of ATES as seasonal storage tanks, cooling of PVT collectors can result in an increase in performance and the lifetime of such systems with no loss of water from the aquifers.

Huang et al. (2001) in Taiwan investigated the performance of PVT collectors with water pumps and storage tanks. It was found that the daily thermal efficiency reached 38% and the primary energy savings exceeded 60% indicating the overall efficiency of the system to be better than conventional PVT collectors. The PVT system usage can depend on the location as well as the application required (Chow, 2010). For locations with low irradiation levels, it can be used for space heating which is needed all around the year. For locations with high irradiation levels, the PVT system can provide a hot water supply, space heating, and natural ventilation in colder months. The Energy Payback Period (EPBP) of the PVT system was found to be less than 3 years for Hong Kong. The paper also mentions that these systems can capture 90% of the commercial market.

Bakker et al. (2005), in his study concluded that the PVT collectors could be combined with space and tap water heating systems. TRNSYS simulation results revealed that they can act as an independent energy system since all of the energy requirements were met by the system itself. The initial investment would be needed for such integration but it would pay back in a few years and the benefits were much more. Buonomano et al. (2016) observed that the cooling system installed on the PVT collector resulted in a maximum temperature drop of 10° C with a Simple Payback period (SPB) of 4 years. It was found that the electrical and thermal energy generated by the system can save about 650 €/year. Dubey and Tiwari (2008) assessed the life cycle of the PVT system in Delhi with the hot water application. It was found out that if the system is operational for 300 days of a year then the SPB was nearly 5 years and the EPBP was little more than 1 year.

1.5 Optimization of integrated energy system

ATES systems enhance building energy efficiency by storing excess heat and cold through underground geology. These systems need to be optimized, which is a challenging process that calls for achieving a balance between multiple factors. ATES's full potential can be realised by more investigation into modelling and optimisation strategies. ATES may provide load shifting, increased system flexibility, and sustained energy cost reductions if it is optimized.

In the year 2000, in the German city of Rostock, a solar heating plant with ATES as seasonal storage was installed to power about 108 flats covering an area of 7000 m^2. Only 50% demand for space heating and DHW was met through the system. Pinel et al. (2011) reviewed available

methods for seasonal storage in residential applications. They discussed methods for improving stratification and reducing losses while analysing computational methods for simulating and optimising sensible heat storage systems. The limitation of their study is that they didn't discuss methods for modelling seasonal storage within energy system tools or co-simulation methods. Cole et al. (2012) stated that thermal storage can be integrated with the thermal and power systems of buildings. Optimization of such storage can lead to an increase in the efficiency of such a system as well as of the combined system. It also improves the economics along with giving the system flexibility to deal with the loads. Sauty et al. (1982) in their study measured the temperature of a single aquifer over time which is used as a thermal energy storage. The paper recommended a few solutions to improve energy storage in such a system. Nordbotten (2017) studied the ATES storage in detail and gave out model equations to optimize them for different locations and sizes. Such storage option can have energy recovery from 66-89% depending on the size, location and application.

Kranz and Bartels (2010) investigated the ATES system installed for the German parliament in Berlin using two numerical models and operational data. The study focused on determining the parameters that improved the heat recovery factor (HRF). It was found that the lower temperature of the cold aquifer while discharging and the higher temperature of the hot aquifer improved the HRF. Also, the injection temperature of a cold aquifer should be as close to the temperature inside it since it is directly proportional to HRF.

Kranz et al. (2015) investigated the parameters which affect the performance of ATES and concluded that there is a research gap on optimising such systems in combination with other energy sources like PVT collectors. Carotenuto et al. (1990) in their paper evaluated a combined system of ATES and an air conditioning system for space heating and cooling. The study optimized the system with the preliminary design for applications of heating and cooling. However, it lacked the integration of PVT or any other solar-based system into the studied system.

Kangas and Lund (1994) described a computer simulation model in Aquifer System Simulation for Test Scenarios (AQSYST) for thermal storage in ATES. The model can input a large number of parameters but has not been studied in detail and it is unclear on the part of the accuracy of the results published by the model. Xie et al. (2018) found out that the depleted oil wells can be used as underground thermal energy storage. For a depth of about 2000 m, they were able to store and extract heat without affecting the temperature and other parameters of the aquifer. Methods like the Monte Carlo method were used to perform sensitivity analysis to find a correlation between storage efficiency and five other parameters. Bloemendal et al. (2022), in his research, proposed an area for future investigation involving the integration of PVT with ATES to provide heating and cooling for buildings. The new system would be more self-sufficient due to the generation of electricity by itself. Hoekstra et al. (2020) in their study of ATES, integrated PVT for combining heat and electricity generation. PVT collectors of 119 m^2 area were used on the roof of office buildings, generating slightly over 18 kWp. The calculated heat extraction was found to be 3000 MJ/m^2/year on utilising 10 °C ATES water and 1100 MJ/m^2/year heat discharge. The annual energy output of PVT was approximately 18.50 GWhe and marginally close to 10.40 GWhth. This study published some important results which need to be analyzed further in detail.

1.6 Research gap

A literature gap exists in the optimization of energy systems integrated with PVT, ATES and heat pumps. There is a need for multi-objective optimization which considers the mismatch in energy production and number of PVTs and sizing of ATES systems, taking into consideration the technical and economical limitations. Therefore, this study optimizes several parameters of the system such as the sizing of the aquifers, and the number of collectors required to meet the building demand. It forms a base for an integrated energy system driven by sustainable energy

sources.

Recent advancements in Aquifer thermal energy storage (ATES) system design have been made by van-Rossum (2024), a student from the Photovoltaic Materials and Devices (PVMD) Research Group at Delft University of Technology. However, the thermal system modeling approach exhibited several notable limitations.

First of all, because heat pumps must deliver water at high temperatures (over 50 °C), they are an essential part of many energy systems and were not included in the model. Second, it showed the aquifer system—which serves as a storage medium by default—as a continuous loop for the transport of water. Furthermore, the model was only calibrated for one kind of demand, so figuring out the right aquifer size for a variety of input demands required some trial and error. The model's usefulness is severely limited by this lack of flexibility. In addition, the modeling approach for the heat exchanger was unique in that it omitted any indication of the input or output temperature.

Furthermore, the aquifer porosity used in the model was 0.15, which is not representative of typical aquifer conditions in The Netherlands, where a porosity of 0.30 is generally observed. This discrepancy could lead to inaccurate predictions of system performance and storage capacity.

Given these limitations, there is a clear need to develop and validate an improved thermal energy system model. Such a model should comprehensively cover all aspects of ATES systems, including heat pumps and accurate aquifer characteristics. Moreover, it should be flexible enough to accommodate varying demand profiles and reflect real-life heat networks more accurately. This enhanced model would provide a more reliable tool for designing and optimizing ATES systems in diverse geological and operational contexts.

Parameters like the number of PVTs, the number of aquifers as seasonal storage and aquifer size for the modeled building demands are part of the optimization problem. The dynamic models of the solar collectors are developed with varying configurations and heat extraction mediums (Ul-Abdin et al., 2024). However, due to the complexity and time-consuming nature of dynamic simulations, a reduced temperature approach is employed, using specific coefficients for thermal and electrical components. This method remains accurate and enhances the efficiency of system modeling. For the integrated system, an improved heat pump model, a part of the toolbox is utilized (Aguilera, 2024). to account for several changes throughout the year. The integrated system is categorized into several operational modes to account for various changes throughout the year. The study also aims to find out the economic aspects of the system to compare the applicability and scalability of the system with the conventional energy system.

1.7 Objectives

The main objective of this thesis is to optimize the integrated energy system consisting of PVT collectors and ATES. With an emphasis on the climate conditions in the Netherlands. This offers a sustainable thermal energy solution for the buildings of Amsterdam. This main objective will be fulfilled by accomplishing the following sub-objectives:

1. Develop the integrated system of aquifers, heat pumps, heat exchanger and solar collectors with dynamic demand and variable inputs. Optimize the system to account for varying changes in the inputs making it more robust and redundant (Chapter 3).

2. Validate the existing model of the aquifer and PVT system developed by van-Rossum (2024), part of PVMD Toolbox. Through analyzing parameters such as screen length and radius of the aquifer (Chapter 3).

3. Examine the integrated system's performance in various scenarios to understand its applicability under various scenarios. Furthermore, compare its cost and carbon emissions with current commercial heat systems (Chapter 4).

Finally, as a result of this thesis, the optimized system consisting of PVT, ATES, heat exchanger and heat pump will be incorporated into the PVMD toolbox.

1.8 Structure

This thesis report is structured as follows: Chapter 2 outlines the methodology, including PVMD Toolbox usage for modeling energy yield (thermal and electrical), and system inputs (weather data, demand, aquifer properties, etc). Chapter 3 focuses on the development of the heat exchanger and aquifer systems model, as well as their integration into a comprehensive ATES system. Subsequently, Chapter 4 presents the integrated system optimization while discussing the primary results and findings of the thesis and presenting several case studies. The research conclusions drawn throughout the thesis are summed up in Chapter 5. Based on the study's findings, Chapter 6 offers suggestions and recommendations for further research.

2

Overview of components

Designing an energy system that integrates renewable sources and storage technologies requires a comprehensive understanding of the various components and their interactions. The methodology employed in this study aims to address the complexities associated with optimizing a system comprising PVT collectors, ATES, heat pumps and heat exchangers. The proposed approach leverages dynamic simulations to capture the time-varying nature of energy yield, demands of the building, and weather patterns throughout the year.

The methodology section discusses each component within the energy system in detail. Section 2.1 discusses the PVMD Toolbox and its several modules in detail. This toolbox provides weather data as well as a few models like the heat pump model, which are then combined in the integrated system to model the demand. Later on, the system is added as a part of the toolbox. Section 2.2 discusses the solar collectors, which serve as the primary source of thermal energy. The role of water-to-water heat pumps is to facilitate efficient heat transfer and temperature elevation which is elaborated upon in Section 2.3. Additionally, Section 2.4 focuses on the heat exchanger component, responsible for facilitating the transfer of thermal energy between various system components such as aquifers and heat pumps. Section 2.5 explores ATES and its working, a key aspect of the seasonal storage of thermal energy.

Furthermore, the methodology outlines the essential system inputs required for accurate modeling and optimization. Section 2.6 delves into the weather data, including irradiance and ambient temperature profiles, which significantly influence energy generation and demand patterns. The impact of building types and their respective heating, cooling, and domestic hot water demands are discussed, as these factors play an essential role in determining the system's sizing and performance requirements.

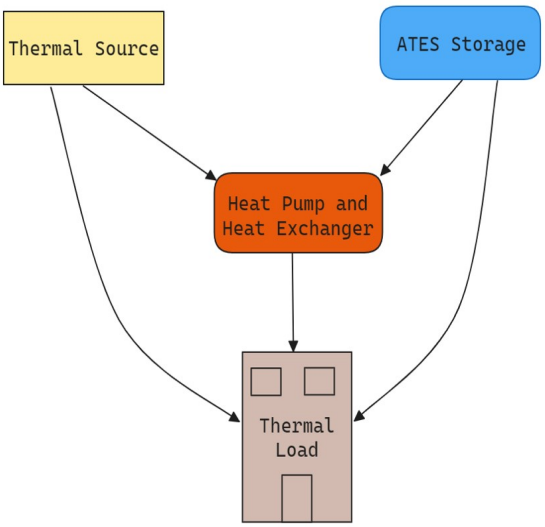

Figure 2.1: Basic elements of Energy Model

2.1 PVMD Toolbox

Several software tools, including MATLAB, have been used to model PV energy yield, as stated by Patel and Agarwal (2008). This project seeks to extend the capabilities of the PVMD Toolbox, a software tool developed by the Photovoltaic Materials and Devices (PVMD) research group at the Delft University of Technology for modeling and estimating solar system energy output, Vogt et al. (2022).

The toolbox facilitates a comprehensive analysis through a series of sub-functions, each tailored to specific aspects of PV system performance.

1. CELL: Evaluates the performance of different solar cell chemistries.
2. MODULE: Visualizes the optical performance of a defined PV system.
3. WEATHER: Determines the energy absorbed by the solar cells before conversion.
4. THERMAL: Calculates the operational temperatures of the PV system.
5. ELECTRIC: Computes the DC energy output of the PV system.
6. DEGRADATION: Analyzes the degradation performance of the solar cells and PV system.
7. CONVERSION: Calculates the AC energy output of the PV system with the chosen inverter.
8. FINANCIALS: Computes and visualizes the LCOE for the system.

The workflow starts with cell simulations and progresses through each sub-function in a specific order, as represented in a workflow diagram in Figure 2.2. Intermediate outputs are generated at each step, leading to the final outputs.

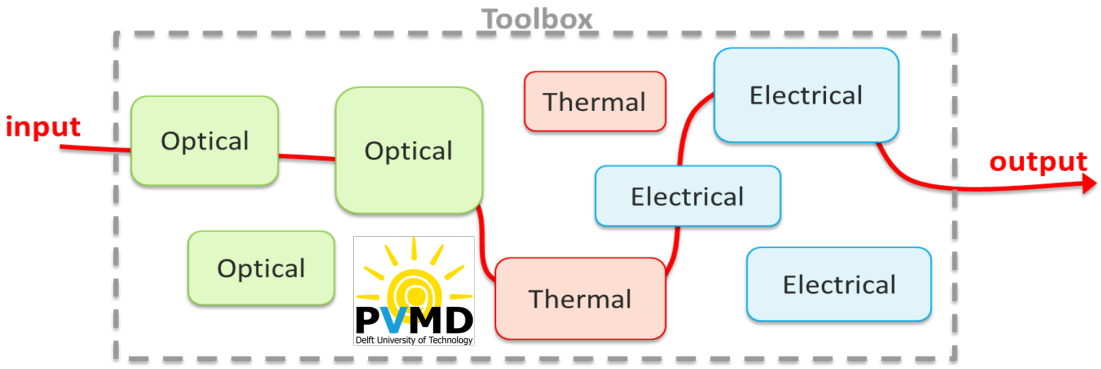

Figure 2.2: Modules of PVMD Toolbox

There is constant work going on with the PVMD Toolbox, with the addition of regular new features. With the help of this toolkit, data can be produced for database usage. This thesis, once completed, will be added to the PVMD Toolbox and will improve the modeling of integrated systems as already developed and added by van-Rossum (2024) and Aguilera (2024). The PVMD Toolbox provides a robust framework for detailed PV system analysis, making it a valuable tool for researchers and engineers in the field of photovoltaics.

2.2 Solar collector

A PVT collector as explained in subsection 1.1.3 combines PV modules and ST collectors to convert sunlight into electricity and capture solar radiation as heat. Only 15-20% of solar radiation is turned into electrical energy by PV cells, with excess energy absorbed by a thermal absorber for generating thermal energy. The collector's ability to produce both electrical and thermal energy utilizing the same area makes it more efficient than standard PV modules and ST collectors. The thermal energy can be used for building space heating, cooling, and hot water production, improving overall energy efficiency. The modeled system utilizes the PVT or ST collector to generate electrical and thermal or only thermal energy, respectively depending on the demand of the buildings being modeled.

PV Module

The diode equation for a single cell, as outlined in equation 2.1 and given by Díaz (2022), serves as a fundamental correlation that characterizes the electrical characteristics of a photovoltaic (PV) cell. Understanding and simulating the efficacy of PV modules, comprised of interconnected PV cells, relies heavily on this equation. It suggests that the current output of a PV cell is determined not only by the photo-generated current but also by the diverse electrical and physical attributes of the cell.

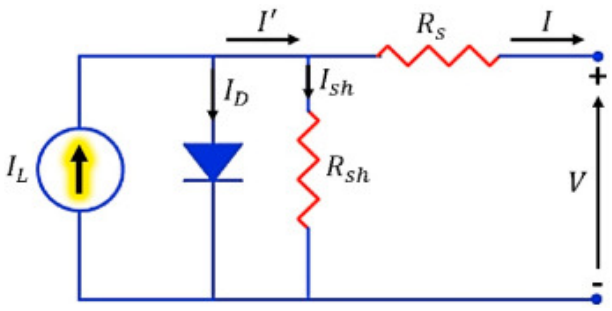

Figure 2.3: Equivalent circuit of a solar cell considering the single diode model, Díaz (2022)

$$I = I_{\text{ph}} - I_0 \left(\exp\left(\frac{V + IR_s}{nV_t} \right) - 1 \right) - \frac{V + IR_s}{R_p} \tag{2.1}$$

In equation 2.1, I represents the output current of the PV cell in A, I_{ph} denotes the photo-generated current in A, I_0 signifies the saturation current of the diode in A, V stands for the output voltage of the PV cell in V, R_s and R_p denotes the series and shunt resistance of the PV cell in Ω, respectively. n is the diode ideality factor (dimensionless), k represents the Boltzmann constant (1.38×10^{-23} J/K), T stands for the absolute temperature of the PV cell in K, and q signifies the elementary charge of an electron (1.602×10^{-19} C) and the thermal voltage is given by V_t.

Solar thermal collector

The modeled system utilizes a flat plate solar thermal collector to produce the thermal energy. The equation 2.2 characterizes the efficiency (η^{th}) of a solar thermal collector considering various operational parameters, including baseline efficiency (η_0^{th}) and temperature-dependent loss coefficient (a_1). It demonstrates that collector efficiency diminishes with increasing temperature disparity between the inlet (T_i) and ambient (T_{amb}) temperatures relative to solar irradiance (I).

The thermal energy (Q_{th}) of the collector can be calculated by Equation 2.3 which is based on its thermal efficiency (η^{th}), collector area (A_g), and incident solar irradiance (I). This equation establishes the crucial link between input solar energy and the thermal energy extracted.

Ul-Abdin et al. (2024) found a simple approach as discussed earlier in section 1.6 where the reduced temperature is used to find out the unique coefficient (a_1) and through that the efficiency of the collector. It was determined the slope of the efficiency curve, allows the thermal efficiency to be predicted for different operating conditions. The nonlinear nature of these equations reflects the complex heat transfer and thermodynamic processes occurring within the solar thermal collector system.

The temperature of the outflow water from PVT is governed by Equation 2.4, based on the initial temperature of water (T_i) and the heat added (Q_{th}).

$$\eta^{\text{th}} = \eta_0^{\text{th}} - a_1 \cdot \left(\frac{T_i - T_{\text{amb}}}{I} \right) \tag{2.2}$$

$$Q_{\text{th}} = \eta^{\text{th}} \cdot A_g \cdot I \tag{2.3}$$

$$T_{\text{out}} = T_i + \frac{Q_{\text{thermal}}}{m \cdot c_{\text{p,water}}} \tag{2.4}$$

Photovoltaic thermal collector

PVT collectors generate thermal and electrical energy. The thermal part of these collectors is already presented in subsection 2.2, where Equations 2.2 and 2.3. In this section, equations 2.5 and 2.6 present the formulas for the electrical energy and efficiency, respectively. Equation 2.5 showcases the relation between electric efficiency at standard temperature and ambient and inlet temperature, with the coefficient (b_1), as found out by Ul-Abdin et al. (2024). The electrical energy (Q_{el}) of the collector can be calculated by Equation 2.6 which is based on its electrical

efficiency (η^{E}), collector area (A_g), and incident solar irradiance (I). This equation establishes the fundamental relationship between incoming solar energy and the extracted electrical energy.

$$\eta^{\mathrm{E}} = \eta_0^{\mathrm{E}} - b_1 \cdot \left(\frac{T_i - T_{\mathrm{amb}}}{I} \right) \tag{2.5}$$

$$Q_{\mathrm{el}} = \eta^{\mathrm{E}} \cdot A_g \cdot I \tag{2.6}$$

2.3 Heat pumps

Heat pumps utilize electricity to transfer heat from one location to another, rather than generating heat directly. This mechanism allows them to achieve significantly higher energy efficiency compared to conventional electric resistance water heaters. According to Connection (2024), heat pumps can be two to three times more energy efficient than auxiliary heaters. In the modeled system for this study, heat pumps are employed as the primary method of water heating. This choice is based on their superior energy efficiency and ability to provide adequate heating capacity without the need for auxiliary heating systems. By focusing solely on heat pump technology, the model aims to maximize energy efficiency and minimize electricity consumption in the water heating process.

Mustafa Omer (2008) reported that water-based heat pumps are more efficient than air-based heat pumps due to the higher thermal capacity of water. They are quieter, save space and are also less prone to icing issues in cold climates. Moreover, these heat pumps are chosen for the modeled system since they have higher efficiency due to their heat source being a warm aquifer whose temperature remains stable throughout the year. Redko et al. (2020) states that these heat pumps are less susceptible to weather-related performance making them more reliable than their alternatives since they transfer heat from one source to another and do not generate them. If the thermal and electrical energy is provided to the heat pump through a sustainable source then they have almost negligible environmental impact.

2.4 Heat exchanger

Heat exchangers are devices designed to facilitate the transfer of thermal energy (heat) between two or more fluids, such as liquids or gases, without mixing them. Their application lies in industrial heating, cooling, and heat recovery processes. They are an important component of modern-day HVAC systems for air conditioning and ventilation. They play a key role in power generation, refrigeration, and air conditioning applications, facilitating efficient heat transfer and energy management.

The most common types of heat exchangers are shell-and-tube, plate, and compact heat exchangers with also different types of fluid flows like parallel, counter-current, etc. Counter-flow heat exchangers are used in the modeled system. In this configuration, the hot and cold fluids move in opposite directions. Figure 2.4 shows the general layout of the heat transfer in a counter-flow type heat exchanger.

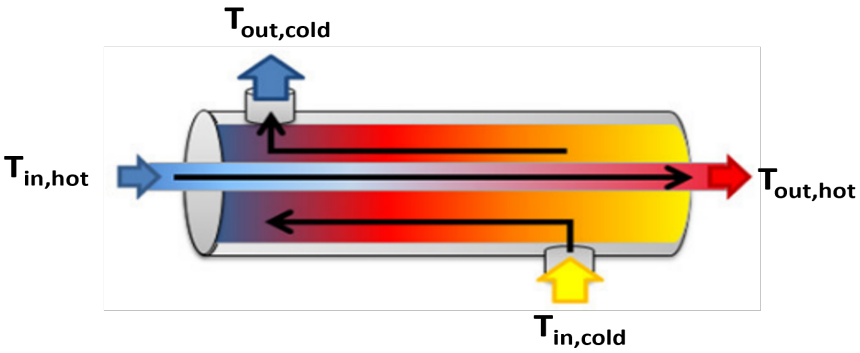

Figure 2.4: Heat transfer in counter-flow type heat exchanger, Adapted from Ronquillo (2023)

2.5 Aquifer system

ATES as explained in subsection 1.1.6 is a system to store heat underground in water-bearing layers known as aquifers. In the system modeled, there are two aquifers separated by a radial distance, one to store cold water and the other to store warm water. This configuration is chosen since it minimizes cross-contamination risks, and potential for thermal energy storage and improves heating and cooling system efficiency.

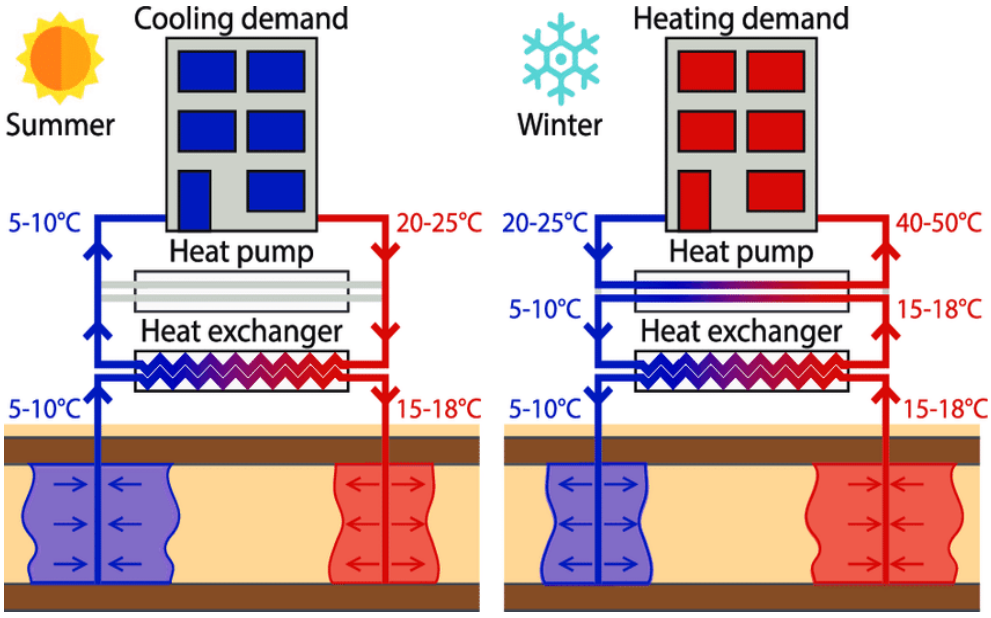

Figure 2.5: Representation of aquifer system with heat exchanger and heat pump for summer (cooling demand) and winter (heating demand) season of the year, Duijff et al. (2021)

The ATES system works in the following way, when cooling is required, cold water ($5 - 10\,^{\circ}\mathrm{C}$) from the cold aquifer of ATES will be passed through a heat exchanger. The water coming from the building gets cooled due to heat transfer with cold water and is sent back to the building. The cold water whose temperature has been raised is sent to the warm aquifer. During winter, when heating is required the hot water ($15 - 18\,^{\circ}\mathrm{C}$) from the hot aquifer is circulated through the heat exchanger to supply the water coming from the building to heat it. The warm water after passing through the heat exchanger is injected into the cold water at a low temperature. In this way, ATES can be used as a seasonal storage. The heat stored in each of the aquifers will change over the year but at the end of the year, there should be a net balance of energy in the system. Furthermore, the technology is combined with PVT/ST collectors in this project

to store the excess heat generated by PVTs in summer and supply it back to the buildings in winter.

2.6 Modeled system inputs

In this section, the various system inputs essential for accurately modeling and simulating the performance of an integrated energy system for a residential building in Amsterdam are discussed. Key parameters such as weather data, building type and insulation, heating and cooling demands, and domestic hot water demands are analyzed. These inputs are pivotal for optimizing the design and operation of the integrated system, ensuring it meets the energy needs of the building while minimizing environmental impact.

2.6.1 Weather data

To gather precise and representative weather data, the Meteonorm data is used to simulate accurate weather conditions for a typical meteorological year at the chosen location. This process involves compiling comprehensive datasets on various meteorological parameters, including all solar irradiation components (direct, diffuse and ground-reflected), ambient temperatures, wind speed, and other relevant factors. Obtaining this detailed weather information is pivotal, as it significantly impacts the performance of solar photovoltaic and thermal modules, as well as the heating and cooling load calculations for buildings. The data for Amsterdam has been taken from Meteonorm.

Irradiance
Irradiance which is the measure of the amount of solar radiation reaching a surface, is an important parameter to accurately predict the energy output of solar collectors which include PV modules, PVT and ST collectors. PVT collectors convert solar energy into both electricity (through the photovoltaic component) and thermal energy (through the thermal component). The amount of electricity generated and heat captured depends heavily on the intensity of the solar irradiation reaching the collectors. Having accurate irradiance data allows for precise modeling and forecasting of the PVT collectors' energy production capabilities under different conditions. This data is essential for optimizing the integrated system design and the sizing of the components appropriately, to ensure a reliable supply of heating, cooling, and hot water demand to the buildings.

Figure 2.6 shows the solar irradiance over the year in Amsterdam which is a significant factor in determining the energy production from the PVT collectors. Higher irradiance levels during certain periods of the year may require a smaller number of these collectors or a larger aquifer to effectively capture and store the thermal energy.

Ambient Temperature
Ambient temperature data is another critical input for properly designing and operating a PVT collector system for buildings. The ambient temperature (T_{am}) affects both the electrical and thermal performance of the PVT collectors. On the electrical side, PV cells operate more efficiently at lower temperatures, so higher ambient temperatures can reduce the amount of electricity generated. On the thermal side, the temperature differential between the PVT collector and ambient air drives the rate of heat transfer and thermal energy capture.

Figure 2.6 shows the temperature profile exhibiting a clear seasonal pattern, with higher temperatures during the summer months and lower temperatures during the winter months. The outside temperature variations can influence the sizing and performance of the aquifer and PVT combined system, which affects the heating and cooling demands of the building.

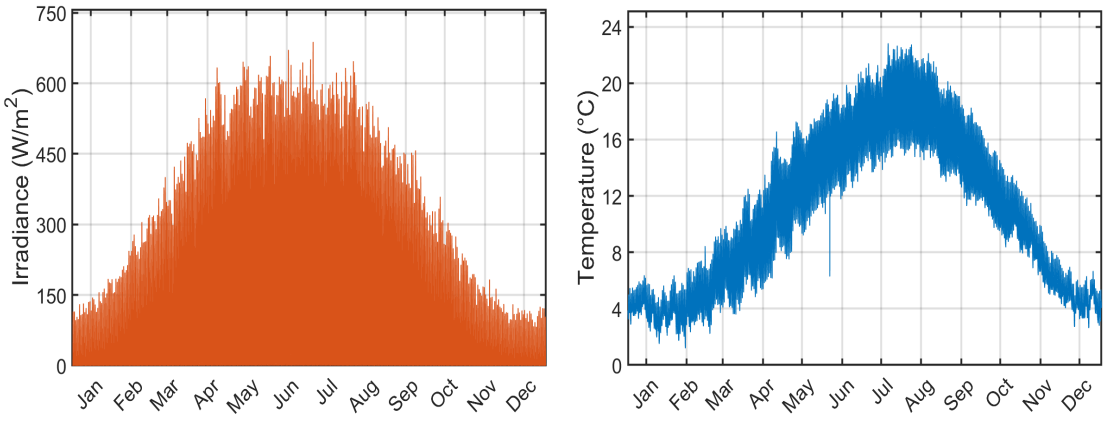

Figure 2.6: Irradiance and ambient temperature throughout the year for Amsterdam

2.6.2 Type of building and insulation

The impact of residential building construction type and level of insulation on heating, cooling, and domestic hot water energy demands is profound, (Van Doorninck, 2020). Buildings with good insulation display notably lower heating demands in comparison to older or inadequately insulated structures. Specifically, whereas historic buildings necessitate 94.70 kWh/m^2 for heating space, well-insulated homes have a much lower demand of 69.60 kWh/m^2, marking a decrease of around 26%. Moreover, proper insulation enables the use of cooling systems, illustrated by a cooling demand of 13.90 kWh/m^2 in well-insulated buildings, a requirement absent in older or less insulated homes. Notably, the domestic hot water demand remains relatively steady across different types of buildings, varying from 16.60 to 17.60 kWh/m^2, indicating that insulation levels have a minor influence on this specific energy need. The data clearly shows that building type plays a great role in determining the demand values for heating, cooling, and hot water. Well-insulated residential buildings exhibit significantly lower heating demands and increased cooling demands compared to historic or insulated buildings.

Figure 2.7 shows the temperature inside a well-insulated residential apartment in Amsterdam without heating and cooling. A well-designed system can help maintain a comfortable and stable indoor temperature by providing heating and cooling as needed, potentially reducing the size or number of PVT collectors and the size of aquifers required.

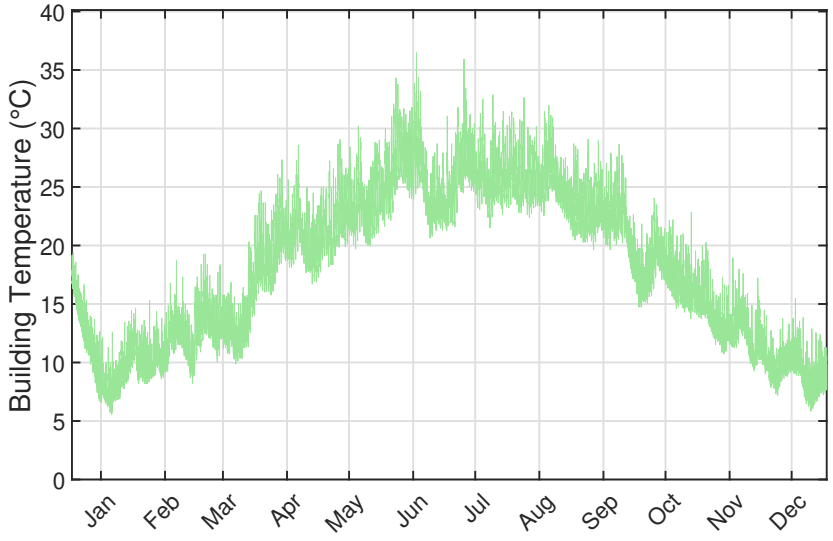

Figure 2.7: Temperature of a well-insulated residential building of Amsterdam throughout the year

2.6.3 Heating and cooling demand

Figure 2.8 shows the space heating and space cooling demand for the four buildings modeled of Amsterdam. The red area represents the heating demand, while the blue area represents the cooling demand.

The modeled system is designed to meet these heating and cooling demands, where a larger aquifer can potentially provide more thermal energy storage capacity and reduce the number of PVT collectors required.

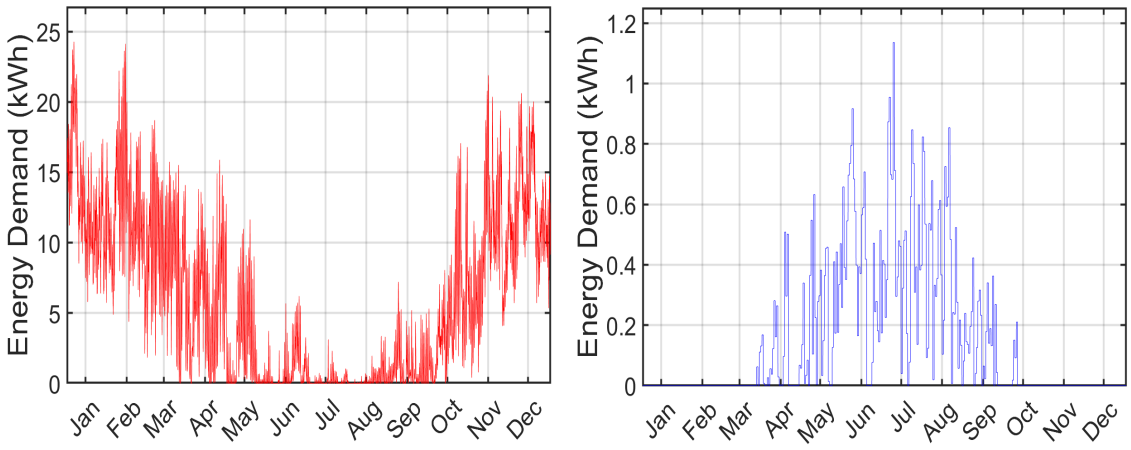

Figure 2.8: Heating and cooling demand of four buildings modeled of Amsterdam

2.6.4 Domestic hot water demand

Figure 2.9 shows the domestic hot water consumption for the four buildings modeled.

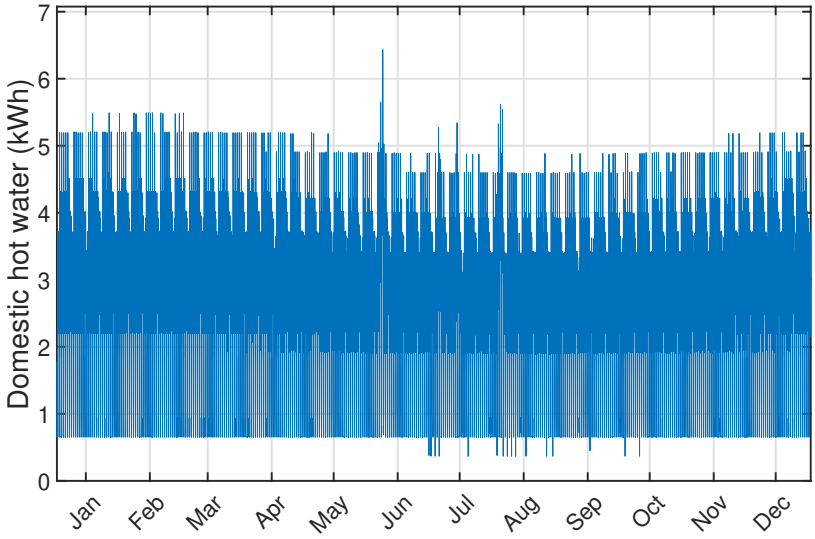

Figure 2.9: Domestic hot water consumption of four buildings modeled of Amsterdam

In summary, the dimensions of the aquifer and the quantity of PVT collectors needed for a specific structure rely on different factors, such as heating and cooling requirements, hot water usage, outside temperature, sunlight exposure, and the preferred level of heat storage. A bigger aquifer may offer a higher capacity for storing thermal energy, potentially decreasing the necessary number of PVT collectors. In contrast, a greater quantity of PVT collectors can enhance the system's thermal energy generation and storage capabilities.

2.7 Conclusion

This chapter has provided a comprehensive overview of the main components of the integrated system. There is a complex interaction between these components to deliver the thermal demand, which is highlighted by explaining the need of each of the component and their working. This understanding helps to model each of the components individually and the integrated system. System inputs such as irradiance, ambient temperature, etc which are pivotal in the modeling and optimization of the system are discussed at the end of the chapter.

In the following chapters, modeling of these components is covered along with the development of an integrated system to deliver the energy demand. The optimization strategy is also explored which is then implemented and the findings are discussed for the several case studies modeled.

3

Development and integration of models

In this chapter, the detailed modeling approach is addressed for the integrated energy system under investigation. This work directly responds to one of the sub-objectives outlined in Section 1.7 namely: Develop the integrated system of aquifers, heat pumps, heat exchanger and solar collectors with dynamic demand and variable inputs. Optimize the system to account for varying changes in the inputs making it more robust and redundant. The next sub-objective of the thesis which is to validate the existing model of the aquifer and PVT system, a part of the PVMD Toolbox is also accomplished in this chapter.

Section 3.1 provides an overview of the chapter's overall system architecture, while Section 3.2 describes the mathematical models for each component. The optimization approach is then explained and applied to improve the system's performance in a variety of dynamic and operational situations.

The approach incorporates the complexities of intermittent renewable energy sources, fluctuating energy demands, and the thermal dynamics of aquifer thermal energy storage, Section 3.5. The next section presents a comprehensive overview of the energy flows within the integrated system, highlighting the interactions between all components. The chapter concludes with section 3.7, the validation of the existing model, which is a part of the toolbox.

This chapter lays the foundation for the results and discussions that follow in subsequent chapters, providing a robust analytical framework for evaluating the performance and potential of this integrated energy system.

3.1 Model architecture

The diagram depicted in Figure 3.1 illustrates the fundamental components of the modeled energy system. It provides an overview of the inputs, predefined data and outputs within the system, presenting a general understanding of its functionality.

This system architecture illustrates a MATLAB-based approach for modeling and optimizing building energy management. Weather and building data are fed as system inputs. These inputs, along with predefined aquifer data such as aquifer capacity, are utilized by the Energy model to estimate the energy demand and constraints.

The optimization model receives the output from the energy model and uses it to optimize

several parameters, including the number of PVT/ST collectors and the size of the aquifer (both warm and cold). Together with the aquifer system's balancing, the optimization model considers several building demands, including space heating, domestic hot water, and cooling needs.

To maximize building energy demand and use, this architecture makes it easier to integrate various data sources and models within the MATLAB environment. This could lead to the development of more affordable and energy-efficient solutions when compared to gas-powered district heating networks.

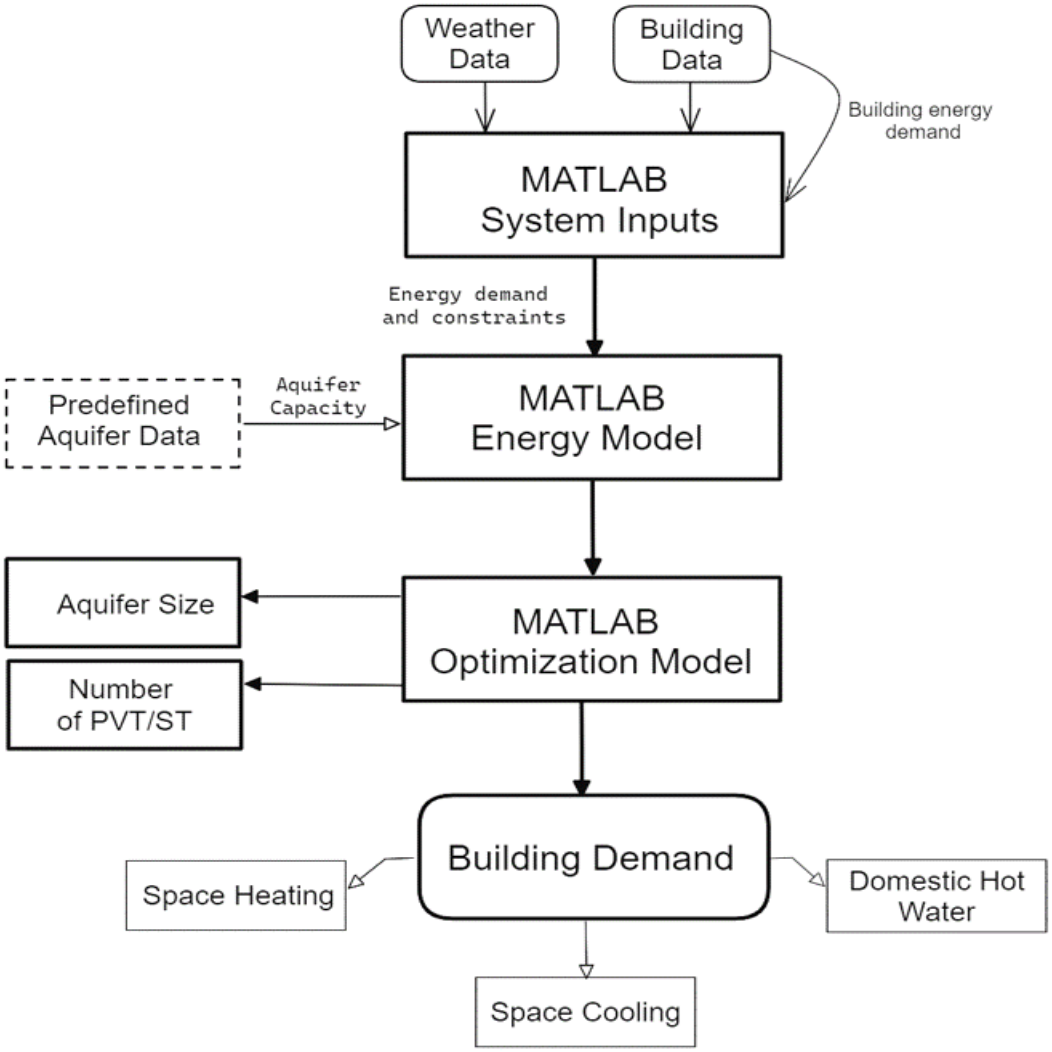

Figure 3.1: Flowchart of the MATLAB-based system architecture for energy modeling and optimization. The model takes weather and building data as inputs to simulate energy demand and optimize system performance based on the demand

3.2 Existing component models

This section briefly describes different models used throughout the energy system modeling. A comprehensive analysis of each model, encompassing its formulation, governing equations, and relevant parameters is presented in this section. The aim is to explain the underlying modeling methodology and facilitate a thorough understanding of the analytical approach.

3.2.1 Photovoltaic thermal collectors

There exist models for these collectors in the PVMD Toolbox which have been used to build the integrated system. Table 3.1 outlines the default parameters of a flat-plate water-based PVT collector. It has a thermal efficiency of 47% and electrical efficiency of 20%, at a mass-flow rate of 0.027 kg/s and zero reduced temperature.

Table 3.1: Parameters of PVT collector

Parameter	**Value**
m_w	0.027 kg/s
A_c	2.0 m^2
β	0.0045 1/°C
T_{STC}	25 °C
NOCT	48 °C
G_{STC}	1000 W/m^2
$c_{p,w}$	4186 (J/kg°C)
$\eta_{o,tha}$	0.47
a_{1a}	7.31 W/(m^2K)
e_{1a}	0.33 W/(m^2K)
$\eta_{o,ele}$	0.20

3.2.2 Solar thermal collectors

Solar thermal collectors which produce thermal energy are also a part of the modeled system. Specifically, flat plate collectors and evacuated tube collectors are considered. Table 3.2 presents the default values of the parameters of the evacuated type with a thermal efficiency of 50% and 75% for the flat plate type, with a mass-flow rate of 0.01 kg/s, at a reduced temperature of zero. Figure 3.2 showcases the relation of thermal efficiency with varying reduced temperatures.

Table 3.2: Parameters for evacuated and flat plate solar thermal collectors

Parameter	**Evacuated solar thermal collector**	**Flat plate solar thermal collector**
m_w	0.01 kg/s	0.01 kg/s
A_c	2.0 m^2	2.0 m^2
T_{STC}	25 °C	25 °C
NOCT	48 °C	48 °C
G_{STC}	1000 W/m^2	1000 W/m^2
$c_{p,w}$	4186 (J/kg°C)	4186 (J/kg°C)
a_{1a}	1.25 W/(m^2K)	3.67 W/(m^2K)
$\eta_{o,tha}$	0.50	0.75

For modeling of the ST collectors the flat-plate type was chosen due to its superior performance compared to the evacuated type.

To quantify the heat generation by the PVT/ST collector, a reduced-temperature approach is employed to estimate the thermal efficiency of these collectors. This thermal efficiency metric is a function of the inlet temperature (T_i) of the working fluid entering the collector to absorb thermal energy in relation to the ambient temperature (T_{amb}) and the incident solar irradiance, as illustrated in Figure 3.2.

Consequently, when the inlet temperature approximates the ambient temperature, the thermal efficiency approaches its maximum value (zero reduced temperature). The reduced temperature approach facilitates the determination of thermal efficiency by accounting for the temperature

differential between the inlet fluid and the ambient environment, thereby enabling accurate estimation of the heat production capabilities of the PVT/ST collector under varying operating conditions.

The reduced temperature (tmp), can be calculated using the formula:

$$tmp = \left(\frac{T_i - T_{\text{amb}}}{G} \right)$$

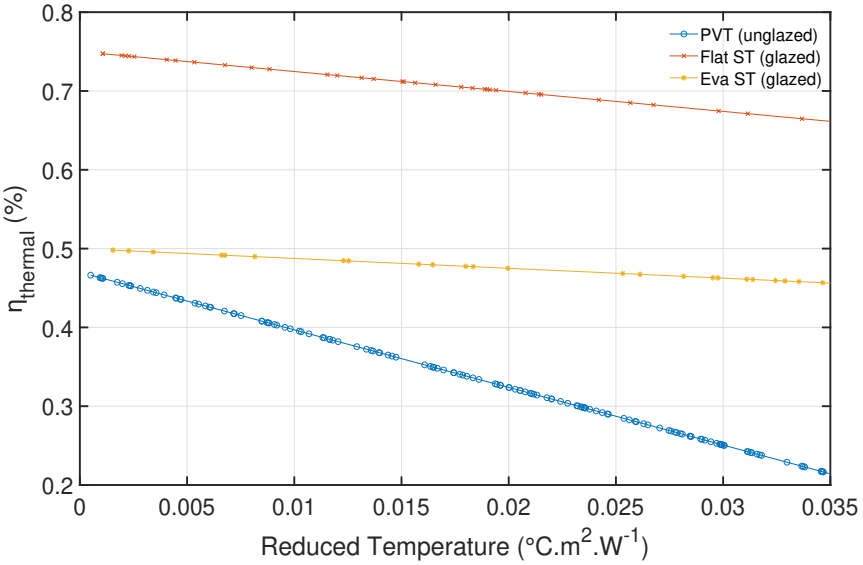

Figure 3.2: Plot of thermal efficiency vs reduced temperature for PVT and ST collectors, Efficiency (η_{tha}) decreases with increasing reduced temperature (tmp), least of PVT, followed by evacuated ST whose (η_{tha}) is moderate and for flat plate ST, it is high around 65%.

The thermal efficiency of PVT collectors is the lowest among the three collectors since it is an unglazed collector, where there are high thermal losses, which reduces the cell temperature in turn increasing the electrical efficiency. The flat-plate and evacuated tube solar thermal collectors are glazed type so their thermal losses are less compared to unglazed PVT due to which their thermal efficiency is more compared to the latter.

3.2.3 Heat pump

The performance of heat pumps depends on the temperatures and heat transfer conditions of the heat source and sink. These conditions vary depending on the location and the time of the year, creating a need to develop a dynamic model for these systems. A generic approach for modeling the performance of heat pumps is provided by Fischer et al. (2017) which utilises quadratic regression.

The PVMD Toolbox proposed a heat pump model which accurately simulates the space heating and domestic hot water demands, based on the equations developed by Ruhnau et al. (2019). The method used to model the thermodynamic cycle for each hour of the year accounts for the fluctuating thermal conditions required for space heating and domestic hot water.

$$\text{COP} = 9.97 - 0.2 \cdot \Delta T + 0.0012 \cdot \Delta T^2 \tag{3.1}$$

where ΔT is the difference between sink (T_{sink}) and source temperature (T_{source}).

T_{sink} (°C) is the temperature needed for water for space heating through radiators or domestic hot water. While T_{source} (°C) is the temperature of the water entering the heat pump which provides the thermal energy to the refrigerant of the heat pump.

Ruhnau et al. (2019) in the paper followed a rigorous approach to validate data accurately and applicability, in formulating the equation for heat pump performance. By utilizing historic time series, validated standard load profiles, and manufacturer data corroborated with field measurements, the study ensures a high degree of reliability. The research encompasses diverse heat demands, sources, and sinks across 16 cold-temperate-climate EU countries over 11 years, providing a comprehensive dataset for weather sensitivity analyses. The authors have meticulously considered spatial aggregation at the national level and temporal resolution at hourly intervals, aligning with European electricity market models. This thorough methodology underpins the credibility of the presented Coefficient of Performance (COP) equation, offering a robust foundation for further academic inquiry and practical applications in the field.

The pressure of liquid refrigerant coming out of the condenser and entering the expansion valve is computed by determining the required sink temperature using Equations 3.2 and 3.3, depending on the type of demand: dhw (T_{dhw}) or space heating (T_{sh}). The condenser approach temperature is denoted as T_{appr}.

$$T_{\text{sink}} = T_{\text{dhw}} + T_{\text{appr}} \tag{3.2}$$

For modeling purposes, $T_{\text{dhw}} = 60°\text{C}$ and $T_{\text{appr}} = 5°\text{C}$ are used, as determined by Østergaard and Svendsen (2017) and Ruhnau et al. (2019)., respectively.

$$T_{\text{sink}} = T_{\text{sh}} \tag{3.3}$$

The chosen temperature for space heating (T_{sh}) is 50°C as determined by Günther et al. (2014). These temperature values are considered constant throughout the simulation of the year.

3.3 Models developed

This section discusses the ATES and heat exchanger models that I constructed for my thesis.

3.3.1 Developement of aquifer model

This subsection discusses the basic parameters required to design an ATES system, its characteristics, performance and the operational parameters of the aquifers.

Designing of aquifers
Aquifer system for a full year and the working is explained in section 2.5. Now, this section focuses on the designing of such systems by calculating the optimal spacing between the aquifers to minimize thermal interference and maximize energy recovery. The thermal interference and energy recovery depend on the geometric shape of the thermal volume of the aquifer as stated by Doughty et al. (1982).

A simplified approach has been taken to design the aquifer. A well injects water into a homogenous aquifer with a horizontal, impermeable and isolating top and bottom with aquifer thickness as H. Dispersion and heat conduction losses are neglected. The injected water forms a cylinder with R_h, known as hydraulic radius. The well is assumed to penetrate fully inside the aquifer

so L is equal to H. The thermal zone is the injected water of the aquifer in thermal equilibrium meaning that the water in this zone is that same temperature. The R_{th} is smaller than R_h due to the fact the surrounding soil absorbs some of the energy.

The sizes of aquifers in real-world applications vary depending on their use, typically ranging from 12,000 to 500,000 m^3, with screen lengths between 5 and 150 m (Bloemendal & Olsthoorn, 2018b).

Figure 3.3 illustrates the cross-section of an aquifer, depicting the key parameters involved in the thermal and hydraulic characteristics of the system.

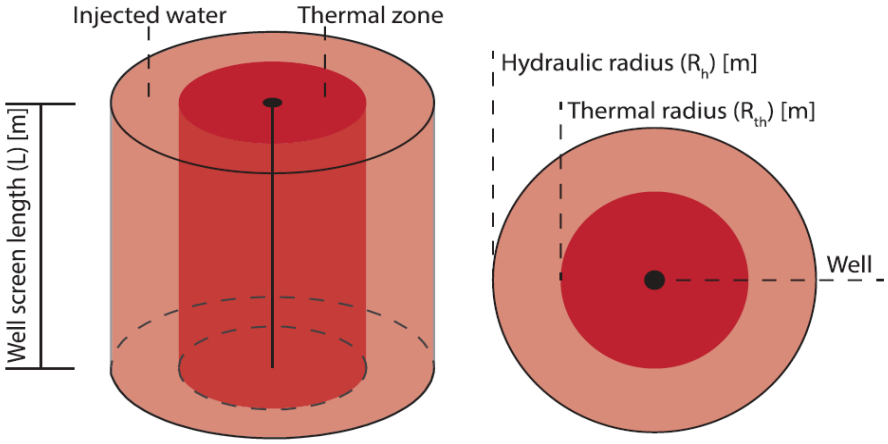

Figure 3.3: Illustration of the cross-section of an aquifer indicating thermal radius (R_{th}), hydraulic radius (R_h) and screen length (L), Duijff et al. (2021)

Bloemendal and Hartog (2018) found an equation to calculate hydraulic radius which represents the radius of the cylinder of injected water, Equation 3.4:

$$R_h = \sqrt{\frac{V}{n\pi L}} \tag{3.4}$$

where V is the injected volume, n is the porosity of the aquifer, and L is the screen length of the aquifer. The aquifer is considered fully penetrating so L is equal to the aquifer thickness H. A relation between hydraulic radius and thermal radius (R_{th}) was approximated by Bloemendal and Hartog (2018).

$$R_{th} = \sqrt{\frac{c_w V}{c_a \pi L}} \approx 0.66 \cdot R_{\mathrm{h}} \tag{3.5}$$

where c_w and c_a are the volumetric heat capacities of water and the aquifer material, respectively. This equation helps determine the spread of thermally influenced zones around the aquifers, which is vital for the placement of aquifers and ensuring no thermal interaction between the aquifers.

The ratio of the aquifer screen length over the thermal radius (L/R_{th}) determines the cylindrical shape of the thermal zone. A small L/R_{th} ratio means that the thermal radius is large compared to the length of the aquifer screen so that the cylinder is short and wide. Doughty et al. (1982) after studying several ATES systems around the world, found out that L/R_{th} ratios vary roughly between 1 and 4.

When infiltration continues, advective heat transport dominates. The increase in infiltration volume overtakes dispersion losses near the aquifer, creating a sharp heat interface. This persists during infiltration as injected heat moves faster than conduction. Storage and extraction make the interface less acute due to conduction. The retained heat enhances efficiency over multiple storage cycles. To reduce losses, there is a need to minimize thermal cylinder surface area (A) compared to stored heat volume (V) by choosing the appropriate screen length for the required storage volume and local conditions, Equation 3.6.

$$\frac{A}{V} = \frac{2\pi R_{\mathrm{h}}^2 + 2\pi R_{\mathrm{h}} L}{\pi R_{\mathrm{h}}^2 L} = \frac{2}{L} + \frac{2}{R_{\mathrm{h}}} \tag{3.6}$$

Bloemendal and Hartog (2018) found out the optimal screen length as a function of storage volume :

$$L = 1.02 \cdot V^{1/3} \tag{3.7}$$

The parameters used in designing the aquifers have been mentioned in Table 3.3. Each parameter has been carefully selected with the specific geographical conditions of The Netherlands.

Table 3.3: Hydraulic and thermal properties of the aquifer and clay layer, Duijff et al. (2021)

Parameter	**Symbol**	**Value**	**Units**
Porosity	n	0.3	-
Horizontal hydraulic conductivity aquifer	$k_{h,s}$	35	m/d
Vertical hydraulic conductivity aquifer	$k_{v,s}$	7	m/d
Horizontal hydraulic conductivity aquitard	$k_{h,c}$	0.05	m/d
Vertical hydraulic conductivity aquitard	$k_{v,c}$	0.01	m/d
Density of sand and clay material	$\rho_{s/c}$	2640	kg/m^3
Density of water	ρ_w	1000	kg/m^3
Thermal conductivity aquifer material	k_s	3	J/(s·m·°C)
Thermal conductivity aquitard material	k_c	1	J/(s·m·°C)
Thermal conductivity water	k_w	0.58	J/(s·m·°C)
Specific heat capacity sand and clay material	$c_{p,aq}$	0.71	kJ/(kg·°C)
Specific heat capacity water	$c_{p,w}$	4.18	kJ/(kg·°C)

Aquifer characteristics
The sizing of aquifers is crucial for the efficient functioning of an ATES system. Key characteristics to consider include hydraulic conductivity, porosity, and aquifer thickness are mentioned in Table 3.3. Hydraulic conductivity determines the rate at which groundwater can be pumped and injected, significantly impacting the system's efficiency. High porosity is desirable as it allows for greater water storage capacity, while a thicker aquifer can store more water, enhancing the system's overall capacity. These factors collectively influence the volume of thermal energy that can be stored and retrieved, thus determining the system's performance.

The influence of temperature on water properties is considered negligible in this model, as the variation is less than 1% of the actual value, which does not significantly impact the system. Comparative simulations performed for the system using temperature-dependent values for water's specific heat capacity and density demonstrated that the system's performance remained unaffected, with aquifer temperatures unchanged to two decimal places. Consequently, static values for water's specific heat capacity ($c_{p,w}$) and density (ρ_w) are employed throughout the model.

This simplification aligns with findings by Ward et al. (2007) and Fossoul et al. (2011), demonstrating that the temperature dependence of groundwater viscosity and density can be disregarded when assessing the performance of ATES systems. This approach allows for the treatment of heat transport processes—including advection, conduction, and dispersion—as linear functions concerning temperature, thereby streamlining the model without compromising its accuracy.

Aquifer placement and configuration
Aquifer placement and configuration are critical for minimizing thermal interference and optimizing system performance. The double-aquifer system, where one aquifer is used for extraction and another for injection, is strategically placed at a distance to reduce thermal interference. Ensuring radial symmetry around the aquifers can further optimize the flow and storage of thermal energy, leading to more efficient energy transfer and system operation. Proper spacing between aquifers helps maintain the thermal integrity of the stored energy and prevents the mixing of warm and cool water, which can degrade system performance. Bloemendal et al. (2018) provided more specific guidelines, stating that both the aquifers should be placed at least 3 times their thermal radius (R_{th}) apart. For aquifers with the same water temperature, the spacing should be 0.5 to 1 times R_{th} apart to avoid thermal interference. This quantitative guidance is crucial for maximizing the number of ATES systems in an area while maintaining efficiency.

Performance of aquifers
The efficiency of an ATES system is influenced by several factors, including the performance of heat exchangers/heat pumps and the long-term sustainability of the system. Above-ground components play a vital role in the overall performance of the system, and minimizing heat losses through these components is essential. Additionally, the system must be designed for long-term operation, typically 20-30 years, considering potential maintenance requirements and system degradation.

The design process also involves considerations of aquifer properties such as permeability, porosity, thermal conductivity, specific heat capacity, and aquifer heterogeneity which affect the thermal conductivity and storage capacity whose values are mentioned in Table 3.3.

3.3.2 Heat exchanger

The system has been modeled for buildings with the demand of space heating/cooling and dhw requirements. The latter demand cannot be fulfilled through PVT/ST collectors, nor warm aquifers, which are utilised to produce thermal energy at much higher temperatures ($30-60\,^{\circ}\mathrm{C}$) than required for cooling ($16-18\,^{\circ}\mathrm{C}$). To satisfy this demand, the cold aquifer can be utilised in which the water is stored at $15\,^{\circ}\mathrm{C}$. The water is pumped to the building, where heat transfer takes place, and in return cools the building. The temperature of the water after heat exchange gets elevated and is stored in the warm aquifer. The process involves no mixing of the two fluids (cold aquifer water and building water), and only the heat is exchanged.

Equation 3.8 forms the base of the equations used to model heat exchanger. Equations 3.9 and 3.10 are used to calculate the flow rate of water extracted from the aquifer and the outlet water temperature after exchanging heat with the building.

$$Q_{\mathrm{in}} = Q_{\mathrm{out}} \tag{3.8}$$

$$\dot{m}_b = \frac{Q_{\mathrm{supplied}}}{(T_{\mathrm{b}} - T_{\mathrm{c}}) \times c_{p,w} \times \eta_{he}} \tag{3.9}$$

$$T_{\mathrm{c,out}} = T_{\mathrm{c,aq}} + \frac{Q_{\mathrm{supplied}}}{\dot{m}_b \times c_{p,w}} \tag{3.10}$$

where the space cooling demand of the building for that hour is represented by Q_{supplied}, being fulfilled through the pumping of cold water from the aquifer. The flow rate of water from the cold aquifer is indicated by $\dot{m}_b$ (kg/s). The building's inside temperature is symbolized as T_{b} ($^{\circ}$C). The space cooling temperature is represented by T_{c} (16 $^{\circ}$C) and the specific heat capacity of water, $c_{p,w}$ (4186 J/kg $^{\circ}$C). Heat exchange efficiency is denoted by η_{he}, which is considered to be 90%. The outlet temperature of water is represented by $T_{\mathrm{c,out}}$ ($^{\circ}$C). Finally, the water returns after exchanging heat with the building and is added to the cold aquifer, which is at $T_{\mathrm{c,aq}}$ ($^{\circ}$C).

Graphs indicating the variation of the pumping rate with changing demand of cooling are presented in Section 4.2.7. Also, the injected water's temperature in the cold aquifer is plotted against time, showing the heat injected per hour of the demand.

3.4 Operational modes of the modeled system

In the previous version of the energy system modeled, the approach followed was to categorize each hour of the year either as energy deficit or energy excess depending on the thermal energy produced by the collectors. However, this approach lacked an accurate representation of the dynamics of such a system.

The new approach categorizes the year into different modes depending on the demand (space heating/space cooling and dhw) and considers the closed cycle of water for each hour, which makes it accurate to the current heat systems in the practical world. The modeled system operates for the full year (8760 hours). The system takes into account the space heating, space cooling and domestic hot water demand on per-hour basis. The whole year is divided into five main cases depending on the requirement: domestic hot water and space heating, domestic hot water only, space cooling and domestic hot water and space heating/cooling with domestic hot water. This means, that are several control points for the system designed to meet demand.

In the context of space heating, the radiator heating is considered. For this, water is the source of energy supplied at 50 $^{\circ}$C, which heats the surrounding environment of the radiator. The domestic hot water demand is met by supplying water at 65 $^{\circ}$C, which prevents the growth of Legionella (bacteria formed when the water temperature is below 60 $^{\circ}$C) as found by Østergaard and Svendsen (2017). The water for space cooling of the buildings is supplied at 16 $^{\circ}$C. These temperatures follow the research and investigation of Rezvanpour and Chen (2023).

The integrated energy system operates in five primary modes which are further divided into three sub-modes depending on the PVT output (kWh). Each mode is designed to meet specific combinations of space heating, space cooling, and domestic hot water demands efficiently. Table 3.4 summarizes these operational modes and mentions the operating condition of each mode.

1. **Mode 1: Space Heating and Domestic Hot Water**
Mode 1 is activated when there is space heating demand as well as DHW. It has sub-cases where the first case is activated when the PVT output is more than 0.5 kWh and the outflow temperature of water from the PVT/ST collector is more than 20 $^{\circ}$C. The outflow water is then transferred to the heat pump which extracts energy from it and elevates the temperature of water to the required space heating temperature (50 $^{\circ}$C). The DHW demand is satisfied by water coming from a heat pump at 65 $^{\circ}$C which takes thermal energy from the water of a warm aquifer (25 $^{\circ}$C). The water after exchanging the energy is cooled and sent to the cold aquifer as shown in Figure 3.4.

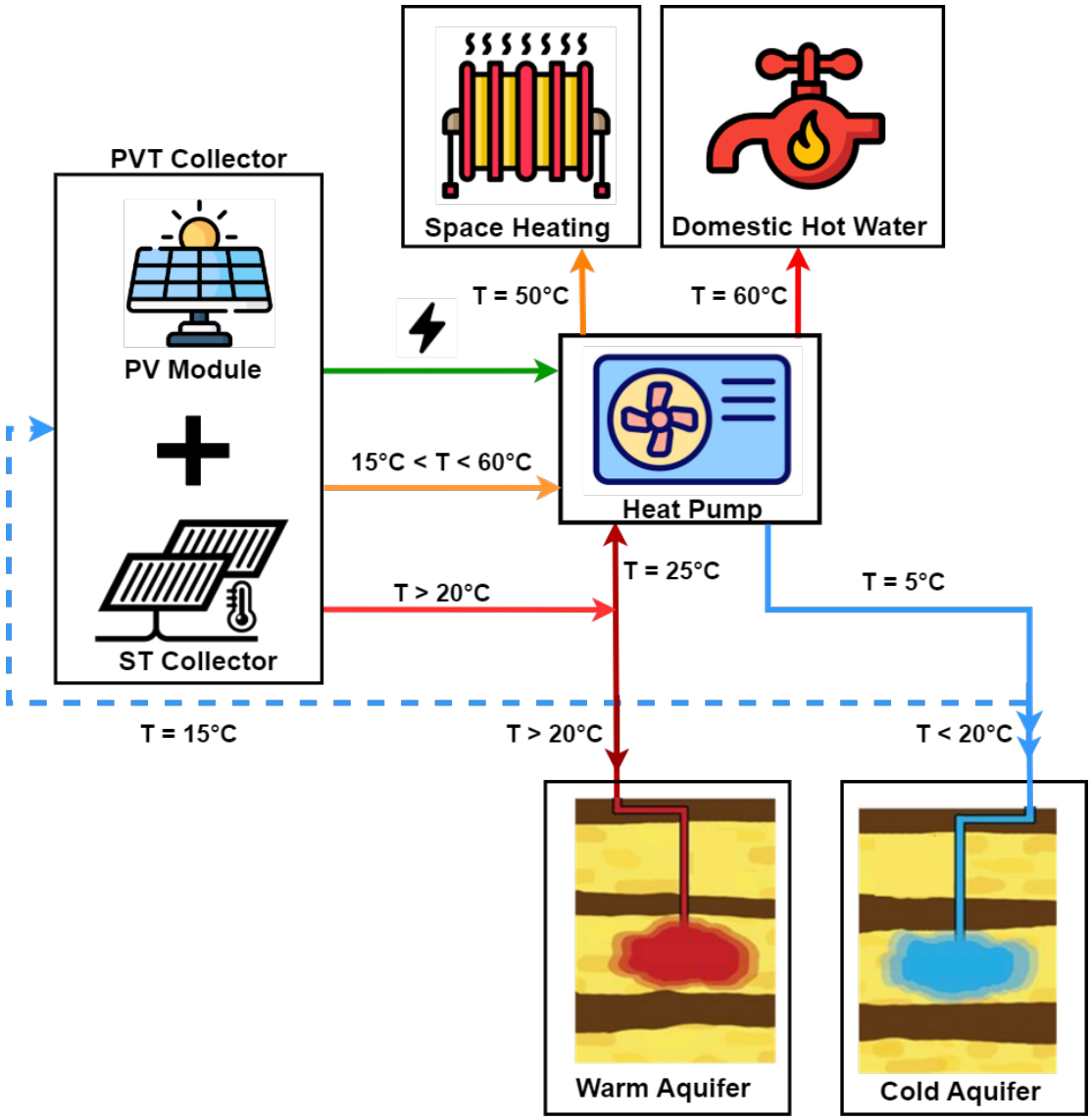

Figure 3.4: Illustration of operational mode 1 where space heating and DHW are the demands met through PVT/ST collectors, warm aquifer and heat pump while electricity is generated through PV modules and PVT collectors. Excess thermal energy from PVT and ST collectors is stored in warm/cold aquifers depending on the temperature of the water.

2. **Mode 2: Space Cooling and Domestic Hot Water**
This mode is activated when there is a need to cool the buildings which utilises the water from the cold aquifer (present at around 15 °C) and is passed through a heat exchanger which cools the building water and then sends the warm after to the warm aquifer as shown in Figure 3.5.

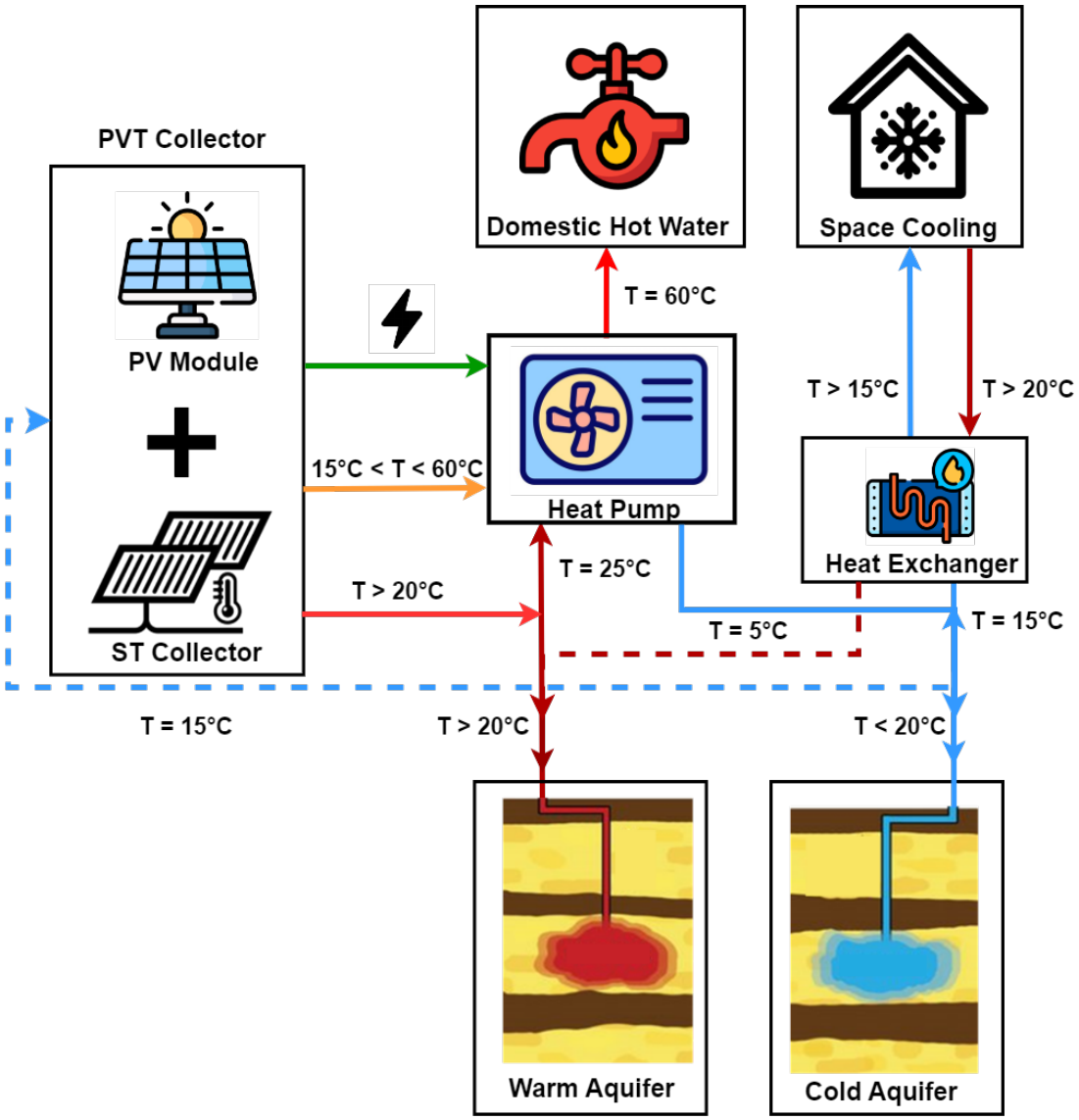

Figure 3.5: Illustration of operational mode 2 where space cooling demand is met through the heat exchanger and cold aquifer. DHW is met through a warm aquifer and heat pump while electricity is generated through PV modules and PVT collectors. Excess thermal energy from PVT and ST collectors is stored in warm/cold aquifers depending on the temperature of the water.

3. **Mode 3: Space Heating > Space Cooling and Domestic Hot Water**
This mode is similar to Mode 1, but the mode has more space heating demand than space cooling demand so space heating is met along with DHW demand, similar as Figure 3.4.

4. **Mode 4: Space Cooling > Space Heating and Domestic Hot Water**
This mode is similar to Mode 2. Still, the mode has more space cooling demand than space heating demand so space cooling is met along with DHW demand, similar to Figure 3.5.

5. **Mode 5: Domestic Hot Water**
This mode is only activated when the space heating or space cooling demand is not present and only DHW demand is satisfied by a warm aquifer and heat pump as shown in Figure 3.6.

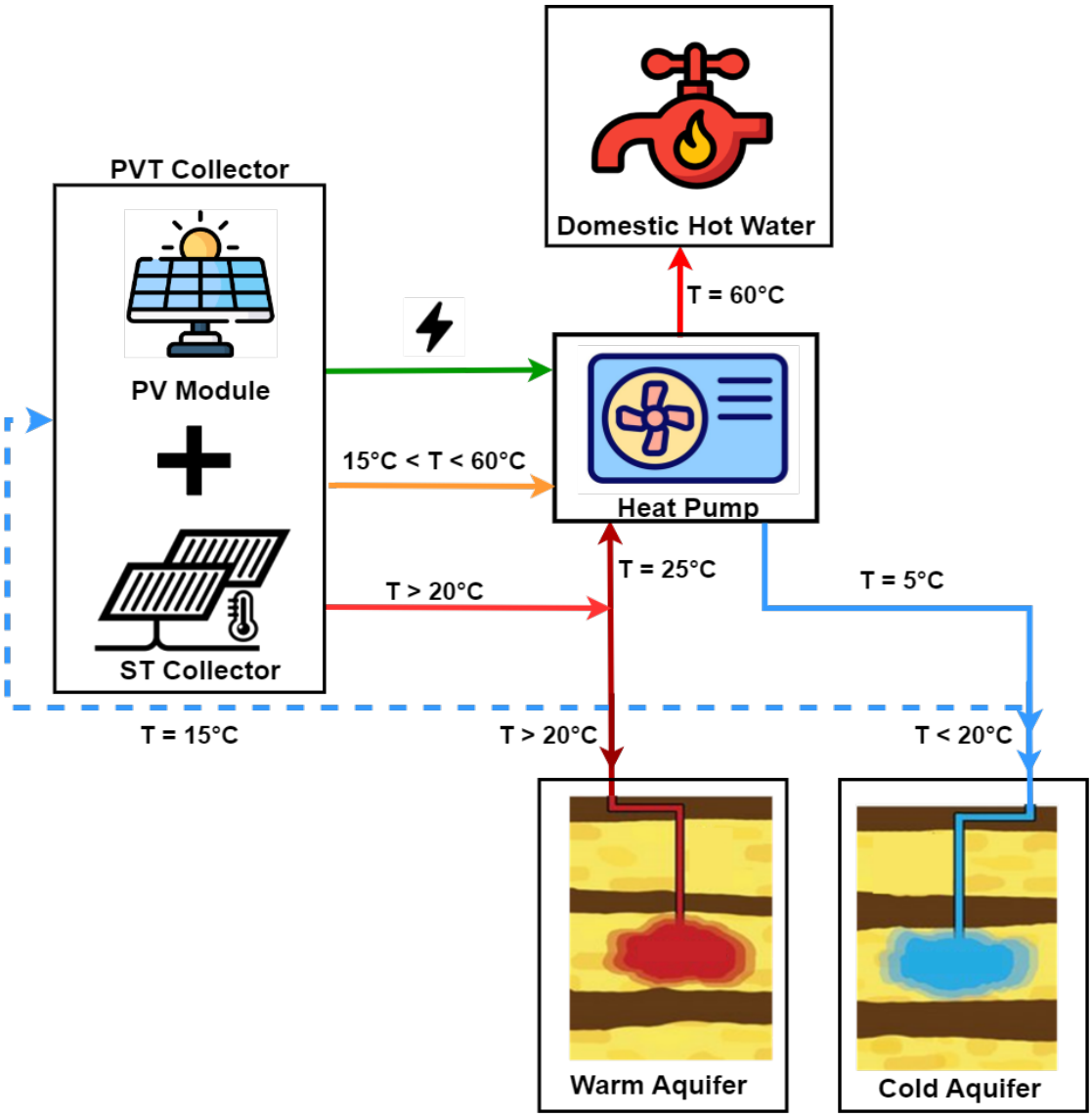

Figure 3.6: Illustration of operational mode 5 where DHW is met through a warm aquifer and heat pump while electricity is generated through PV modules and PVT collectors. Thermal energy from PVT and ST collectors is stored in warm/cold aquifers depending on the temperature of the water.

Table 3.4: Operational Modes of the system for the full year

Requirement	**Mode**	**Activation condition**	**Energy sources**	**Space Heating/Cooling**	**DHW**
Space Heating, DHW	1a	Outflow Temp $> 20°C$, PVT ≥ 0.5 kW	PVT, Warm aquifer	PVT	Warm aquifer
Space Heating, DHW	1b	$14°C \leq$ Outflow Temp $\leq 20°C$, PVT ≥ 0.5 kW	Warm aquifer	PVT, Warm aquifer	Warm aquifer
Space Heating, DHW	1c	PVT < 0.5 kW	Warm aquifer	Warm aquifer	Warm aquifer
Space Cooling, DHW	2a	Outflow Temp $> 20°C$, PVT ≥ 0.5 kW	Cold aquifer, Warm aquifer	Cold aquifer, Building	Warm aquifer
Space Cooling, DHW	2b	$14°C \leq$ Outflow Temp $\leq 20°C$, PVT ≥ 0.5 kW	Cold aquifer, Warm aquifer	Cold aquifer, Building	Warm aquifer
Space Cooling, DHW	2c	PVT < 0.5 kW	Cold aquifer, Warm aquifer	Cold aquifer, Building	Warm aquifer
Heating > Cooling, Space Heating, DHW	3a	Outflow Temp $> 20°C$, PVT ≥ 0.5 kW	PVT, Warm aquifer	PVT	Warm aquifer
Heating > Cooling, Space Heating, DHW	3b	$14°C \leq$ Outflow Temp $\leq 20°C$, PVT ≥ 0.5 kW	PVT, Warm aquifer	PVT, Warm aquifer	Warm aquifer
Heating > Cooling, Space Heating, DHW	3c	PVT < 0.5 kW	Warm aquifer	Warm aquifer	Warm aquifer
Cooling > Heating, Space Heating, DHW	4a	Outflow Temp $> 20°C$, PVT ≥ 0.5 kW	Cold aquifer, Warm aquifer	Cold aquifer, Building	Warm aquifer
Cooling > Heating, Space Heating, DHW	4b	$14°C \leq$ Outflow Temp $\leq 20°C$, PVT ≥ 0.5 kW	Cold aquifer, Warm aquifer	Cold aquifer, Building	Warm aquifer
Cooling > Heating, Space Heating, DHW	4c	PVT < 0.5 kW	Cold aquifer, Warm aquifer	Cold aquifer, Building	Warm aquifer
No demand, DHW only	5a	Outflow Temp $> 20°C$, PVT ≥ 0.5 kW	Warm aquifer	No demand	Warm aquifer
No demand, DHW only	5b	$14°C \leq$ Outflow Temp $\leq 20°C$, PVT ≥ 0.5 kW	Warm aquifer	No demand	Warm aquifer
No demand, DHW only	5c	PVT < 0.5 kW	Warm aquifer	No demand	Warm aquifer

This flexible operational strategy allows the system to adapt to varying weather conditions and energy demands throughout the year, optimizing the use of renewable sources and stored thermal energy. By switching between these modes, the system maintains high efficiency and maximizes the utilization of renewable energy sources under diverse conditions.

3.5 Governing equations of Integrated system

The aquifer system is utilised as a storage system to store excess thermal energy and supply when the thermal collectors are not able to provide or to act as a secondary supply when the collectors are the primary source. Due to the dynamic nature of these energy systems and demand, there was a need to develop such equations which correctly represent the volume and temperature changes in the aquifers for each hour of the year. The existing model for the aquifer system didn't accurately quantify the temperature or volume changes. Therefore, these equations have been developed to make the whole system more realistic.

The equations presented in this section represent the case when water from the warm aquifer is utilized for space heating the buildings for an hour. Equations for the case of space cooling are presented in Appendix A.3.

3.5.1 Volume dynamics of aquifers

The volume changes in both warm and cold aquifers are governed by the following equations:

For the warm aquifer:

$$V1(i) = V_1 - V_{ext}(i) \tag{3.11}$$

For the cold aquifer:

$$V2(i) = V_2 - V_{cc} + V_{inj}(i) \tag{3.12}$$

where:
V_1 and V_2 are the volumes of warm and cold aquifers at time step i, respectively.
$V1$ and $V2$ are the initial volumes of warm and cold aquifers, respectively.
V_{ext} is the volume extracted for space heating and DHW at time step i.
V_{cc} is the volume used for cooling the collectors.
V_{inj} is the volume injected from heat pumps and collectors at time step i.

3.5.2 Temperature dynamics of aquifers

The temperature changes in the aquifers are described by:

For the warm aquifer:

$$T_{\text{aquifer},1}(i) = T_{\text{aquifer},1}(i-1) \tag{3.13}$$

For the cold aquifer:

$$T_{\text{aquifer},2}(i) = \frac{V_2 \cdot T_{\text{aquifer},2}(i-1) + V_{\text{inj}}(i) \cdot T_{\text{inj water}}(i)}{V_2(i)} \tag{3.14}$$

where:
$T_{\text{aquifer},1}(i)$ and $T_{\text{aquifer},2}(i)$ are the temperatures of warm and cold aquifers at time step i.
$T_{\text{aquifer},1}(i-1)$ and $T_{\text{aquifer},2}(i-1)$ are the temperatures of warm and cold aquifers at time step i-1.
$T_{\text{inj water}}(i)$ is the temperature of injected water at time step i.

This equation provides insights into the thermal dynamics of the aquifer system for an hour of the year, indicating how the injection and extraction processes influence the temperature distribution within the cold aquifer.

Equations 3.11 to 3.14 facilitate the analysis of volume and temperature dynamics in response to injection and extraction of water in these aquifers, over the year. They serve as fundamental concepts in understanding the thermal and hydraulic behaviour of these aquifers.

3.6 Energy interactions in the system

Figure 3.7 illustrates the complex energy interactions within the integrated system. The diagram shows how electricity (green arrow) flows from the PV modules and PVT collectors to power the heat pump and meet other electrical demands. Thermal energy (red arrows) is generated by the PVT/ST collectors and the heat pump, then stored in the warm aquifer or used directly for space heating and dhw applications. The cold aquifer provides cooling (blue arrow), which utilises a heat exchanger. The bidirectional arrows between the aquifers and the building systems represent the seasonal storage and retrieval of thermal energy.

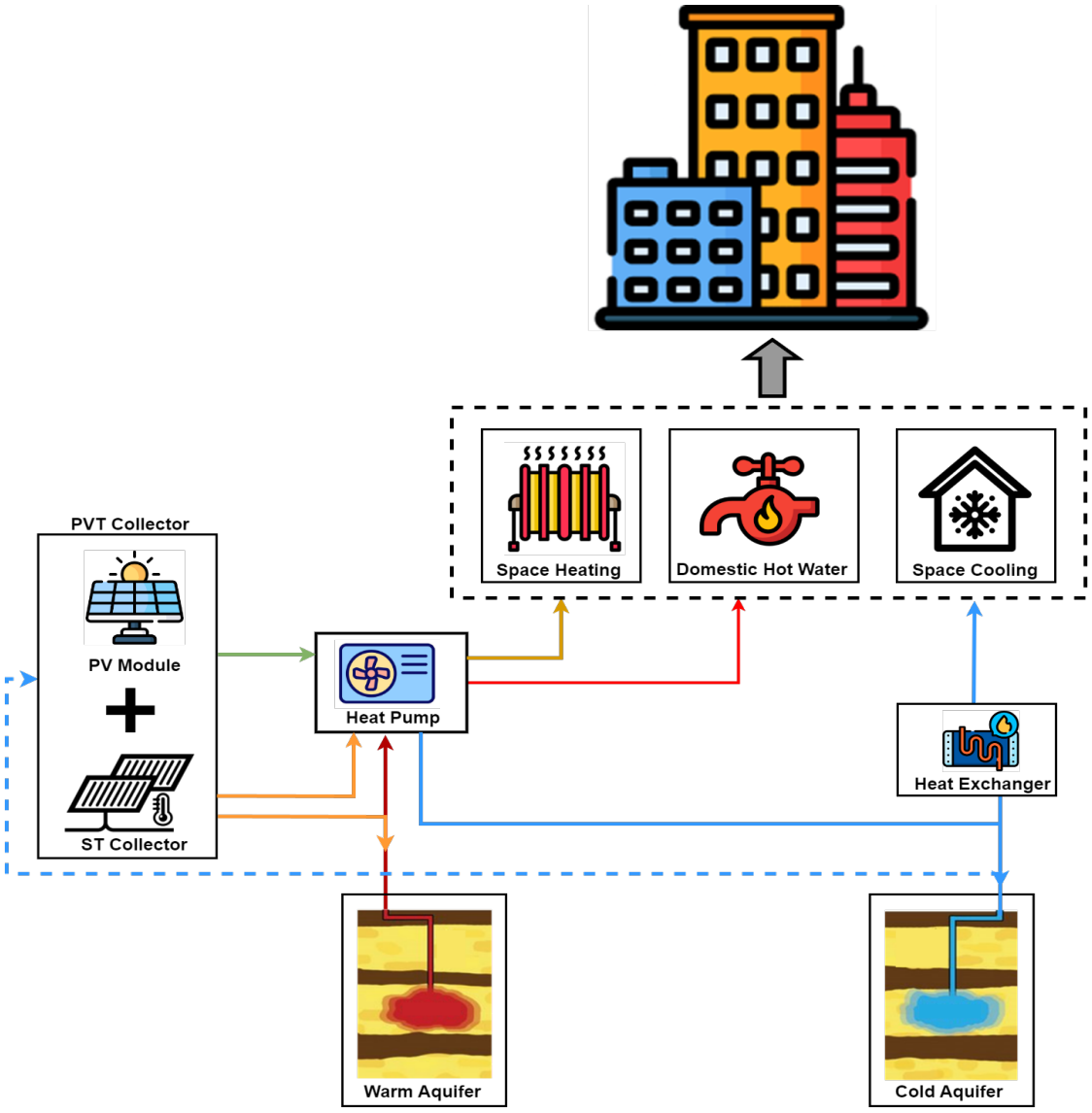

Figure 3.7: Schematic representation of energy interactions in a multi-temperature heat network. The green, red, orange and blue arrows represent the electricity, heating, DHW and cooling networks, respectively. Each arrow indicates the direction of energy flow between components.

The diagram demonstrates how different energy sources and technologies can be integrated to supply multiple demands (heating, cooling, and domestic hot water) while potentially improving overall system efficiency. It maximizes the use of renewable sources and stored energy to meet varying demands throughout the year.

3.7 Validation of previous integrated model

van-Rossum (2024) previously worked on integrated systems with PVT collectors and ATES, which covered a fundamental method to model the number of collectors needed for a given demand and aquifer size. It did not take into account the need for hot water, nor did it accurately represent the heat exchanger and heat pump. As a result, there was scope to model an integrated system in which the number of PVT/ST collectors and aquifer sizes are determined by the demand.

The work has been validated in this section based on L/R_{th} ratio, covered in subsection 3.3. The graph provided for analysis illustrates the parameter L/R_{th} with permit volume (V) parameter which is vital in the evaluation of Low-Temperature (LT) ATES systems.

In the figure 3.8, the relationship between L/R_{th} ratio and permit volume (V) is depicted, where the black line indicates the optimal value, the blue line shows the minimum value and the red line denotes the maximum value of this ratio. The scattered points represent the historical data of ATES systems around the world, with the red dashed line signifying the theoretical value derived from van-Rossum (2024) model which had a value of $L/R_{th} = 1.5$ for a permit volume of 15,000 m^3.

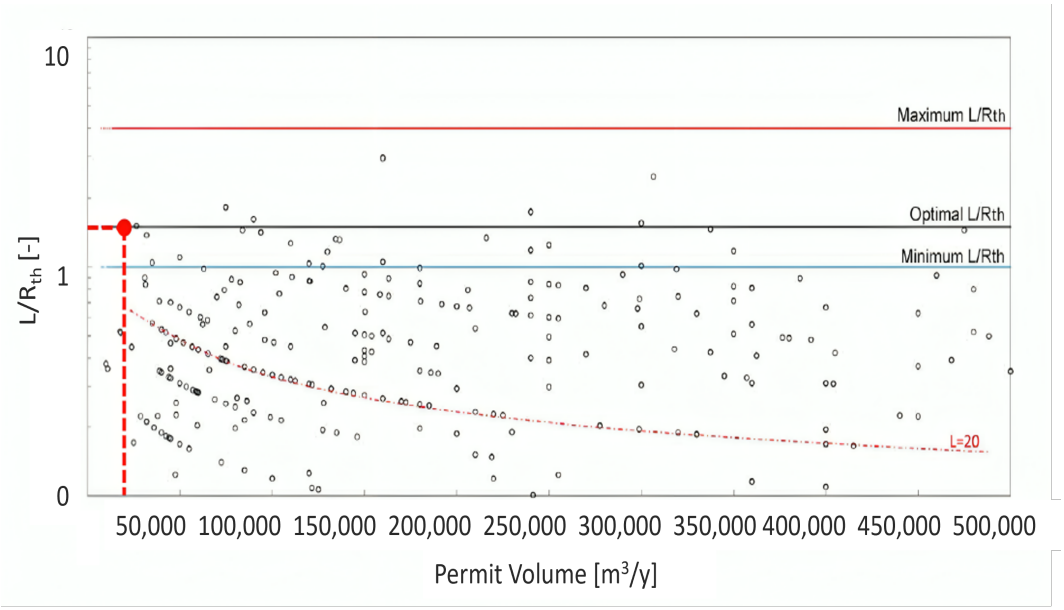

Figure 3.8: L/R_{th}-value relative to permit volume of ATES systems in practice, combined with minimum (L/R_{th}= 1), maximum (L/R_{th}=4) and optimal (L/R_{th}= 1.5) for conduction and dispersion losses, Adapted from Bloemendal and Hartog (2018)

3.8 Conclusion

This chapter concludes by answering the two sub-objectives of the thesis: first, to develop an integrated system model and optimize it. It is presented by modeling each component of the system and also by utilising a few models from the PVMD Toolbox. Then the optimization of the integrated model is performed by dynamically sizing the aquifers and the number of PVT collectors. Also, the system is designed to work all round year and to manage the varying inputs, several operational modes are designed, making it more robust and redundant. The second objective is accomplished by validating previously developed systems of ATES and PVT based on the screen length and thermal radius.

In the next chapter, the last sub-objective of the thesis is covered. It examines the findings of the integrated system for several cases while evaluating the modeled system in various aspects.

4

Results and Discussion

This chapter showcases the working of the integrated model developed. This work directly responds to one of the sub-objectives outlined in Section 1.7: Examine the integrated system's performance in various scenarios to understand its applicability under various scenarios. Furthermore, compare its cost and carbon emissions with current commercial heat systems.

In the first section, general parameters considered while modeling the system are addressed. The next section examines the system under a base case scenario analysing and showcasing the temperature dynamics of several components and their effect on the system's performance. Further diving into the chapter, Section 4.3 provides a seasonal analysis of the system inputs and their effect on the performance of the system.

Section 4.4 discusses the different insulation levels and the changing demands in each case. The effect of the demands on the system is evaluated on several aspects such as power consumed by heat pumps and sizing of the aquifers. The next section discusses varying flow rates of PVT and ST collectors and their effect on the count of operational modes developed to understand the system's dynamics more accurately. It answers the question of choosing of right type of collectors and the flow rate.

Section 4.6 is a comparative analysis of system performance in the case of underfloor heating, a case different from radiator heating which was considered in the previous cases. The next section mentions the costs of such a system refining them into several categories and projecting the levelised cost of thermal energy. The chapter ends with Section 4.8 which discusses the carbon emissions saved by utilisation of the system in comparison with district heating.

4.1 Modeling of integrated system

The modeling methodology for an integrated system with ATES, heat exchangers, heat pump, submersible pumps, PVT/ST collectors, and PV modules is presented in the following section. First, the modeling of residential hot water demands, space heating and cooling demands, and general system parameters are reviewed. The integration of these components aims to optimize energy efficiency and sustainability in meeting the diverse thermal needs of multiple buildings throughout the year.

4.1.1 Modeling of space heating, space cooling and DHW demands

The heating and cooling profiles, specifically the space heating, domestic hot water and space cooling demand for a particular type of building are obtained with the assistance of the Amsterdam Institute for Advanced Metropolitan Solutions (AMS Institute). Generally, ATES systems exhibit a seasonal pattern, operating in heating mode during winter and cooling mode during summer. However, energy demands can fluctuate within a single day, necessitating heating in

the morning and cooling in the afternoon. Despite these short variations, studies by Sommer (2015) have demonstrated that they do not significantly impact the overall thermal efficiency and thermal impact of the system.

In this study, the required capacity was calculated based on the specific heating and cooling needs (W/m^2), provided by AMS Institute. The heat delivered by the ATES must be calculated separately for heating and cooling as the system operates differently in each mode. Figure 4.1 illustrates an ATES system for two different demands: space heating (winter) and space cooling (summer). One of the primary advantages of these systems is the ability to provide cooling without the use of heat pumps. The temperature difference between the cold well and the building temperature makes it possible to cool the building without using the heat pump which translates to a great amount of energy saved, as corroborated by Sommer (2015). Consequently, calculating the energy demand for cooling from the wells does not require additional components, simplifying the process. Each aquifer has a submersible pump to pump the groundwater out of the wells to the heat pumps and heat exchangers (Bakema et al., 1994). All three demands are met by the ATES which ensures that the thermal energy storage system efficiently meets the diverse energy needs of the buildings throughout the year.

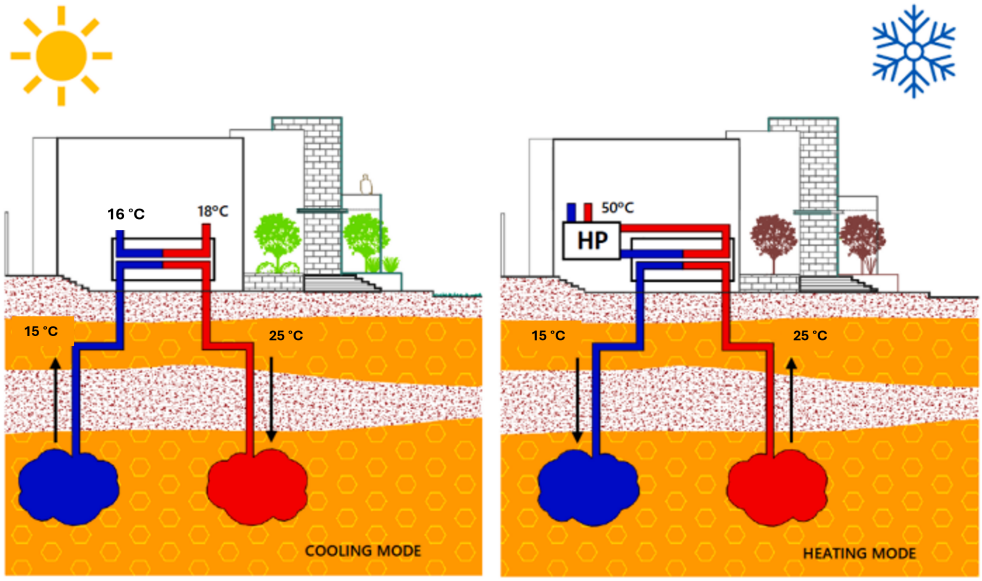

Figure 4.1: Schematic representation of cooling and heating through cold and warm aquifers in a year for building, Adapted from Ruiz Delgado et al. (2010)

4.1.2 General model parameters

The key parameters and design considerations of the integrated system under study are presented in this section. It presents the importance of the specific values and constraints through the tables 4.1 and 4.2.

Table 4.1 outlines the foundational parameters for a dual-aquifer thermal energy storage system designed to serve four buildings: Oudebrugsteeg 3, Beursstraat 5, Beursstraat 21 and Warmoesstraat 96. This system incorporates 10 PVT collectors, each with a collector area of 2.0 m^2, which play a crucial role in harnessing solar energy to meet the buildings' energy demands. The combined heating demand of all buildings is significantly high at 197.21 MWh, compared to a relatively modest cooling demand of 18.04 MWh, indicating a likely colder climate or specific building usage patterns. Additionally, the total domestic hot water demand is 83.14 MWh, further emphasizing the substantial heating requirements.

The warm aquifer's starting temperature is 25 °C, while the cold aquifer's is 15 °C. This creates an initial temperature differential of 10 °C, which is necessary for effective thermal energy storage

and retrieval. The equal volumes of 27,000 m^3 in both aquifers show a balanced design intended to maximize energy storage capacity. This volume is essential to preserving the thermal balance and making sure the buildings' annual energy requirements are satisfied.

By utilizing solar and aquifer energy, the dual-aquifer system with PVT collectors provides a sustainable solution that improves energy efficiency and offers a sustainable option to the current district heating network. The potential for large energy savings is highlighted by the substantial need for heating and the strategic use of renewable energy sources. This base case model's scalability also makes it adaptable to many scenarios, as modeled in Section 4.4, which makes it a flexible foundation for future use in energy systems for sustainable buildings.

Table 4.1: Base case parameters of integrated system

Parameter	**Value**
Number of buildings	4
Total PVT collectors	10
Collector area of a PVT/ST	2.0 m^2
Total heating demand combined of all buildings	197.21 MWh
Total cooling demand combined of all buildings	18.04 MWh
Total domestic hot water demand combined of all buildings	83.14 MWh
Heating power required by all buildings	26.55 kW
Cooling power required by all buildings	2.47 kW
Domestic hot water power required by all buildings	9.49 kW
Starting temperature of the warm aquifer	25 °C
Starting temperature of the cold aquifer	15 °C
Volume of the warm aquifer	27000 m^3
Volume of the cold aquifer	27000 m^3
Heat exchanger efficiency	90%

Table 4.2 presents the key temperature parameters used in modeling the integrated system. The values indicate the operational constraints and design considerations for a dual-aquifer (warm and cold) setup. The maximum temperature fluctuation of 5 °C and a minimum of 0.5 °C represent the allowable range of temperature changes within each aquifer. A minimum temperature difference of 6 °C between aquifers ensures efficient energy storage and retrieval. Both aquifers are designed to have a 5 °C temperature difference between the start and end of the year, accounting for seasonal variations. The warm aquifer's maximum temperature is set at 35 °C, while the cold aquifer's minimum is 5 °C, establishing the system's overall operational temperature range. Above these values, the ATES system's performance changes and also it is not considered a LT-ATES system. These parameters are crucial for optimizing the ATES system's performance, ensuring thermal balance, and maintaining the long-term sustainability of the groundwater resource.

Table 4.2: Temperature constraints for ATES system modeling.

Parameter	**Value**
Maximum temperature fluctuation of each aquifer	5° C
Minimum temperature fluctuation of each aquifer	0.5° C
Minimum temperature difference between aquifers	6° C
Allowed temperature difference (aquifer 1, year start-end)	5° C
Allowed temperature difference (aquifer 2, year start-end)	5° C
Maximum temperature of warm aquifer	35° C
Minimum temperature of cold aquifer	5° C

4.2 Thermal energy system performance: Annual dynamics and component analysis

A comprehensive analysis of the thermal energy system's performance is presented in this section, concentrating on a PVT flow rate of 0.015 kg/s. The following discussion examines various critical aspects of the system, including aquifer temperatures, PVT outlet temperature, heat pump performance, and energy distribution across different components.

By analyzing these parameters, insights into the system's behavior throughout an annual cycle are provided by highlighting the interaction between weather conditions, technological performance, and energy demand. This analysis is crucial for understanding the system's efficiency, identifying potential areas for optimization, and evaluating its effectiveness in meeting space heating and domestic hot water requirements.

The subsequent figures and their interpretations offer a detailed view of temperature variations, energy flows, and system efficiencies. These observations will form the basis for assessing the overall system performance and its ability to adapt to seasonal changes in energy demand and weather conditions.

4.2.1 Aquifer temperature over the year

Figure 4.2 illustrates the annual temperature variations in warm and cold aquifers over a year. Each of the aquifers is sized at 27,000 m^3 each. Two distinct curves are plotted: the warm aquifer (red) and the cold aquifer (blue). The warm aquifer exhibits a temperature range from 25 °C to 26.58 °C, with a notable increase around the middle of the year since the thermal energy generated by the collectors is stored in it. In contrast, the cold aquifer maintains lower temperatures, ranging from 15 °C to 15.62 °C, with less pronounced variations, due to space cooling demand being one-third times less than space heating demand.

Both aquifers show a general warming trend as the year progresses, with the warm aquifer demonstrating a more significant temperature increase. The temperature difference between the two aquifers remains substantial throughout the year, with an average gap of approximately 10 °C.

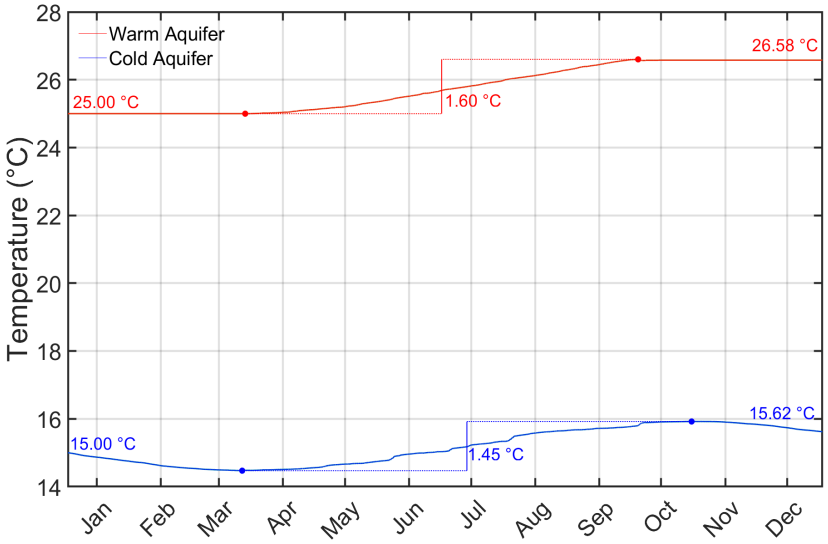

Figure 4.2: Temperature throughout the year of warm and cold aquifers

4.2.2 PVT inflow and outflow temperature over the year

Figure 4.3 presents two subplots showing PVT inflow and outflow temperatures throughout the year. The top graph depicts inflow temperature, ranging from approximately 14.50 °C to 16 °C, with a gradual increase from spring to fall. The bottom graph illustrates outflow temperature, which exhibits more pronounced daily fluctuations and a wider range (roughly 16 °C to 26 °C), with peak temperatures occurring in summer months (May to September). The outlet temperature is dependent on irradiance and mass flow rate of water. The graph of outlet temperature has been modeled in consideration of the climate of Amsterdam, The Netherlands where the maximum irradiance for a year is around 700 W/m^2. If a location near the equator is taken, irradiance peaks at around 2500 W/m^2, then the outlet temperature at the same mass flow rate will be above 40 °C.

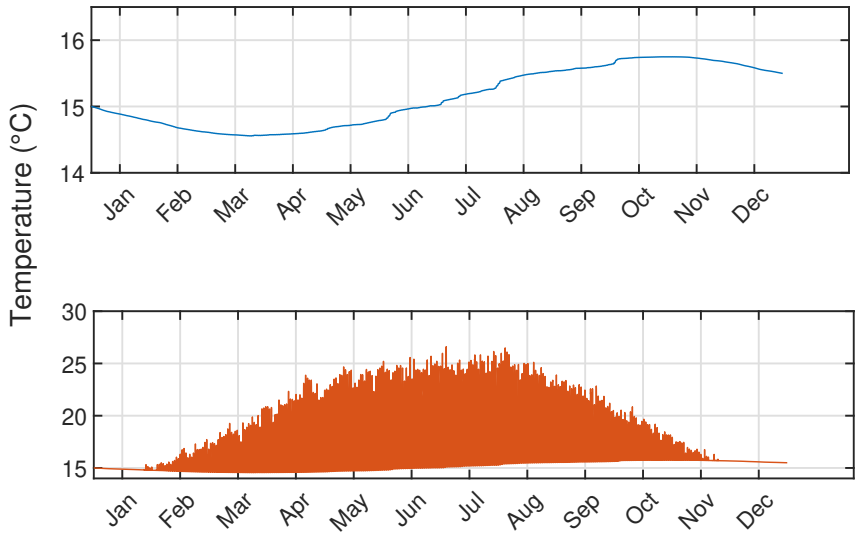

Figure 4.3: PVT inflow and outflow temperatures throughout the year at 0.015 kg/s flow rate.

4.2.3 Peak demands over the year

Peak demand is crucial for component sizing in heating and cooling systems. It represents the maximum load the system must handle, ensuring that the equipment can meet the highest expected demand.

Table 4.3 presents the peak demands for space heating, space cooling, and domestic hot water for the modeled 4 buildings over a year. It includes the number of hours each system needs, the average power consumption, the peak power demand, and the hour of the year when the peak occurs.

Table 4.3: Average and peak demands of space heating, space cooling and hot water during the year of the modeled 4 buildings

Demand	Hours needed	Average power (kW)	Peak power (kW)	Hour of the year
Space heating	7426	26.56	91.25	125
Space cooling	7302	2.46	103.03	3787
Domestic hot water	8760	9.49	24.19	3787

4.2.4 Coefficient of Performance of ATES and PVT during the year

Plot 4.4 displays the COP for three systems: ATES (SH), PVT (SH) and ATES (DHW) for a year. COP is calculated using the formula mentioned in subsection 3.2.3. The performance of the ATES and PVT systems can be evaluated through their COP, as shown in Table 4.4. ATES

systems demonstrate consistent performance, with space heating and DHW maintaining average COPs of 3.55 and 3.47 respectively. In contrast, the PVT system exhibits greater variability, with an average COP of 4.36 but reaching a maximum of 5.20, indicating significant seasonal fluctuations in efficiency.

Table 4.4: COP of heat pump for sources: PVT, ATES for SH and ATES for DHW

System	Average COP	Maximum COP
PVT (SH)	4.36	5.20
ATES (SH)	5.14	5.25
ATES (DHW)	3.47	3.55

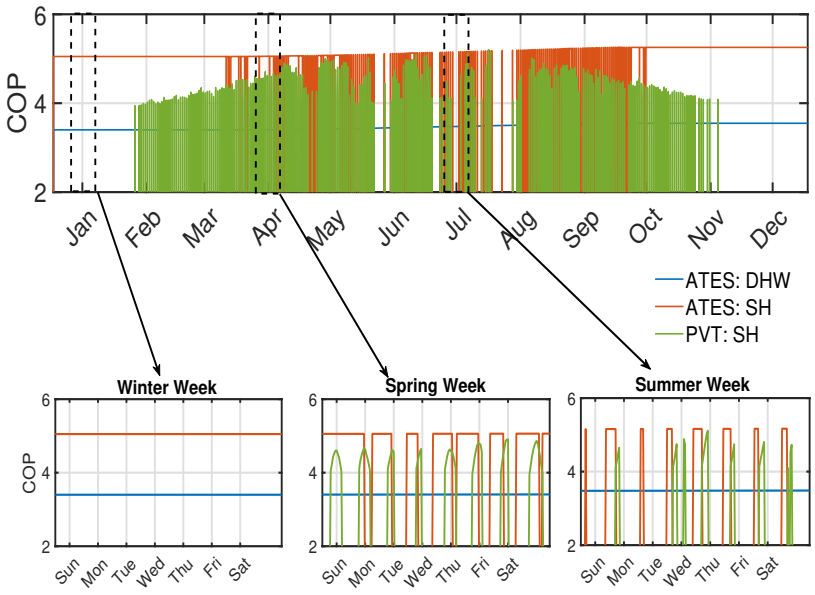

Figure 4.4: COP of heat pump for DHW and SH demands through ATES and PVT across the year for 0.015 kg/s flow rate.

4.2.5 Power consumed by heat pumps

Power consumed by heat pumps to deliver SH and DHW demands through thermal energy provided by PVT and ATES throughout the year is plotted in Figure 4.5. The ATES system generally consumes more power and exhibits greater variability since it meets almost all of the demand, with peak consumption (high demand for space heating) in winter months. The PVT collectors show lower, more consistent power consumption, primarily during the summer months (May to September). The total power consumed by the heat pump for space heating and hot water applications is 68.55 kW.

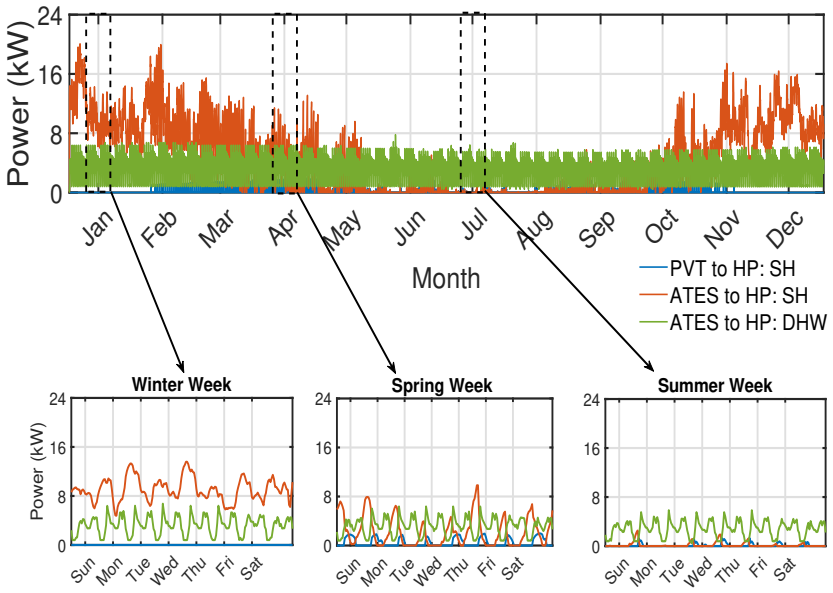

Figure 4.5: Power consumption of heat pumps (kW) for supplying energy from PVT and ATES to meet building's demand throughout the year.

4.2.6 Difference between inlet and outlet water temperature through PVT over the year

Graph 4.6 illustrates the temperature difference of water inlet and outlet from PVT over a year. The plot exhibits a distinct seasonal pattern, with higher temperature differences during summer months (May to September) when irradiance is maximum (above 500 W/m^2) and lower differences in winter due to lower irradiance (below 300 W/m^2). The maximum difference reaches about 11 °C (maximum thermal energy), while the minimum approaches 0 °C (generating no thermal energy).

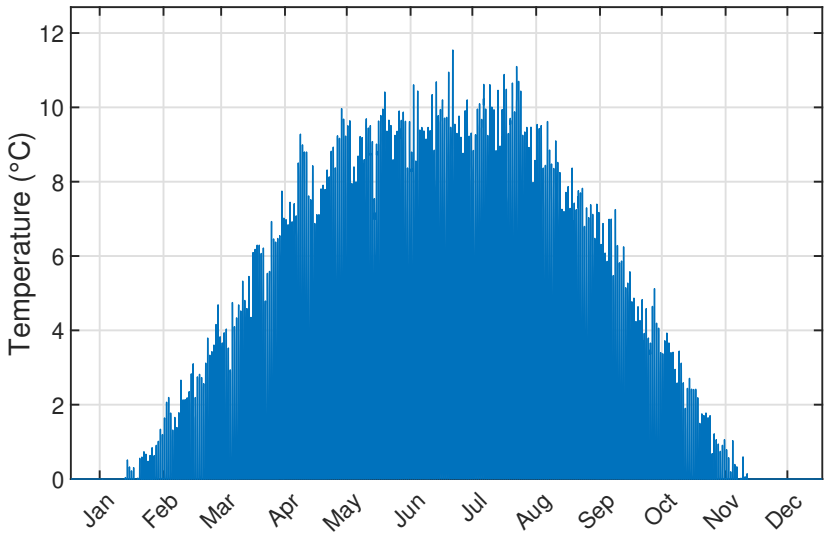

Figure 4.6: Annual temperature difference (°C) between water entering and leaving the collectors at 0.015 kg/s flow rate.

4.2.7 Pumping rate of water through ATES and PVT

Graph 4.7 compares pumping rates for ATES and PVT systems over a year to meet the space heating, cooling and DHW demands. ATES demonstrates higher and more variable pumping rates, particularly in winter months. At the same time, PVT shows lower, more consistent rates primarily during summer, when they produce thermal energy and store it in warm aquifer. Before and after the summer months (May to September) there is the time when they produce thermal energy given to the heat pump to meet the space heating requirement.

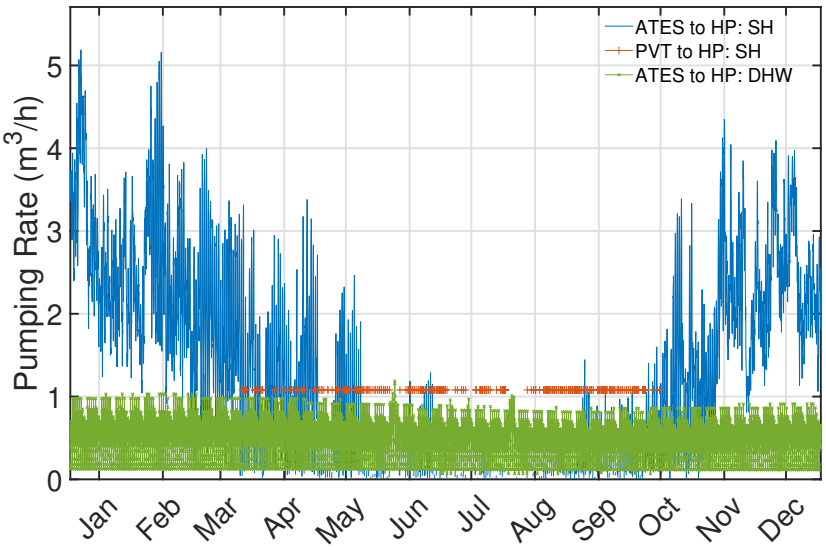

Figure 4.7: Comparison of pumping rate (m^3/h) of water over the year month-wise from ATES and PVT for dhw and space heating application.

The table below indicates the average and maximum pumping rate value for each component and specific application. The variation in the pumping rate for space heating is primarily due to the change in demand over the year and also due to variable energy generation by PVT collectors. The pumping rate for the hot water application doesn't change much since the demand is constant with few peaks during the year due to sudden weather changes as observed from graphs 4.17 and 2.6.

Table 4.5: Average and maximum pumping rates (m^3/h) of PVT to HP for SH, ATES to HP for SH and ATES to HP for DHW over a year

System	Average pumping rate (m^3/h)	Maximum pumping rate (m^3/h)
PVT (SH)	1.08	1.08
ATES (SH)	1.67	5.18
ATES (DHW)	0.457	1.18

4.2.8 Energy supplied by ATES, heat pump and PVT throughout the year

To understand the system dynamics, energy input through the warm aquifer and PVT to satisfy the space heating and DHW demand is shown in Figure 4.8.

The ATES: SH system (blue line) shows significant seasonal variation in energy output. During the winter months (January, February, March, November and December), the energy output is highest, peaking at around 70 kWh/day, showcasing high demand for space heating. From spring to summer (April to September), the energy output decreases drastically, reaching its lowest point below 10 kWh/day around mid-year, due to low SH demand with increased ambient temperatures. The energy output starts to rise again in the autumn months, indicating the return of heating requirements.

The energy output of the PVT collectors to HP (orange line) remains relatively low and consistent throughout the year, with values around 1-2 kWh/day. There is a slight increase during the summer months (May to September), where the output occasionally peaks slightly above 2 kWh/day, likely due to increased solar irradiance. However, the overall contribution of the PVT system remains minimal compared to the other systems.

The ATES: DHW (red line) exhibits a steady energy output due to almost constant DHW demand throughout the year, maintaining values between 5-10 kWh/day. This consistency suggests a relatively constant demand for domestic hot water year-round, with minor fluctuations around the average value.

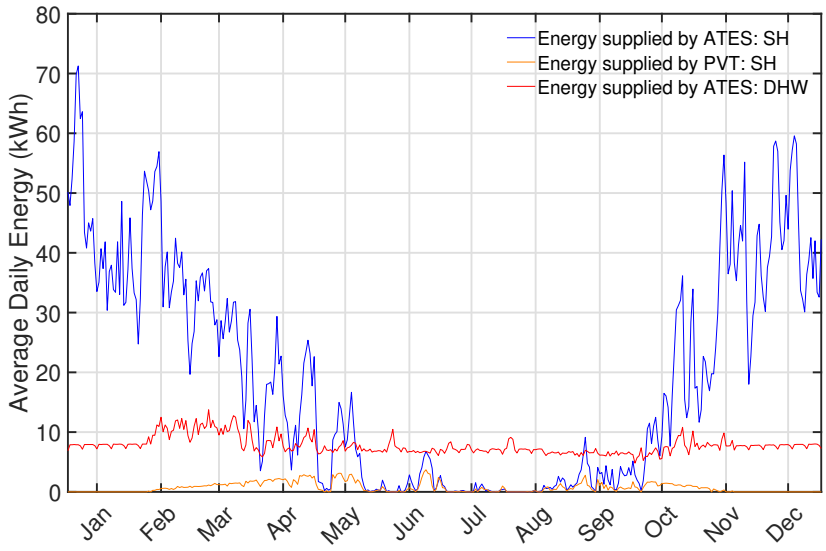

Figure 4.8: Energy output daily to meet SH and DHW demands via ATES and PVT.

The ATES: SH system shows significant seasonal variability with high outputs in winter and low in summer, reflecting the heating demand pattern. The PVT collectors produce more energy in the summer and contribute minimally overall. The ATES: DHW system provides a steady energy output throughout the year, meeting the consistent demand for domestic hot water. The analysis highlights the importance of each system's role and the impact of seasonal changes on their performance.

The developed integrated system is validated similarly as van-Rossum (2024) work. The value of $L/R_{th} = 1.51$ and a permitted volume of 27,000 m^3 is found for the base case scenario. This is in line with the findings of Bloemendal and Hartog (2018).

This comprehensive analysis of the thermal energy system's annual performance reveals complex interactions between various components. The ATES system demonstrates robust performance, providing consistent energy for both space heating and domestic hot water, with COPs averaging at 3.55 and 3.47 respectively. In contrast, the PVT system shows significant seasonal variability, with its effectiveness peaking during the summer months (May to September).

The temperature dynamics of the aquifer show a trend toward gradually warming, with more noticeable differences in the warm aquifer. This trend merits long-term monitoring to ensure system sustainability. Even though it varies, the PVT collector's performance helps the system function more efficiently overall, especially when solar irradiation is high. ATES and PVT systems have dramatically different heat pump efficiency (measured by COP values), with ATES exhibiting more consistent performance. The system's flexibility in responding to varying demands is demonstrated by the examination of power consumption and pumping rates. This is especially noticeable in the way the ATES system responds to the need for winter heating.

These findings provide valuable insights for system optimization, particularly in balancing the contributions of ATES and PVT components to meet varying seasonal demands efficiently.

4.3 Seasonal system dynamics throughout the year

The system modeled is simulated for the current demand of four buildings which correspond to Oudebrugsteeg 3, Beursstraat 5, Beursstraat 21 and Warmoesstraat 96. The current demand, given the existing insulation in these buildings, includes the requirements for space heating (SH), domestic hot water (DHW), and space cooling (SC). The data for these demands is provided by AMS Institute and is recorded on an hourly basis throughout the year.

4.3.1 Winter analysis

Figure 4.9 showcases the winter season, specifically in the second week of January. The outlet temperature of the PVT collector exhibits significant variability influenced by the limited solar irradiance (around 100 W/m^2) and low ambient temperatures (average 5 °C) typical of Amsterdam's winter. Over the full week, the outlet temperature ranges between a minimum of approximately 15 °C, aligning with the inlet temperature from the cold aquifer, and a maximum of around 25 °C. The average outlet temperature hovers around 20 °C, indicating that the system can only slightly elevate the water temperature above the cold aquifer's baseline. This shows that in winter months, the PVT collectors with low flow rates (higher outlet temperatures) also cannot satisfy the space heating demand, indicating that the warm aquifer is the primary source for these months.

A detailed observation of a single day (January 8th) within this week via Figure 4.9 shows distinct fluctuations. Overall, the winter performance of the PVT system is constrained by the low ambient temperatures and limited solar exposure, resulting in moderate increases in outlet temperature.

This indicates that the space heating and DHW demands can't be met alone by PVT+HP and there is a need for Warm Aquifer+HP to satisfy the demands.

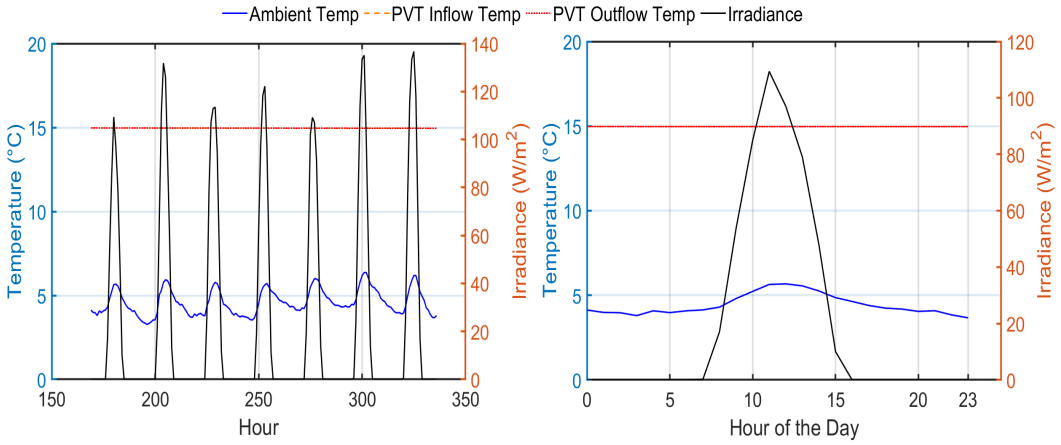

Figure 4.9: Winter season - Ambient temperature, Irradiance, and PVT collector inflow and outflow temperatures in Amsterdam (Week 2, January)

Performance analysis of the system for winter
Figure 4.10 depicts the performance of heat pump for three distinct sources - PVT, ATES (SH) and ATES (DHW) - over varying time scales. Both images consistently show that the ATES system exhibits the highest efficiency with a COP of approximately 5.0, followed by the ATES for DHW at around 3.4. In contrast, the PVT system doesn't meet the demand for space heating. This is observed for one full week timeframe (Week 2) and also for the January 8th.

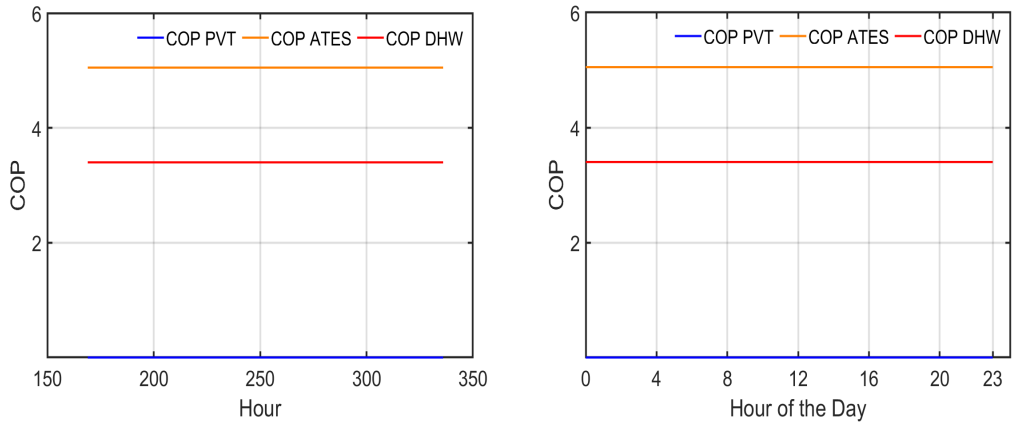

Figure 4.10: Winter season - Coefficient of Performance of heat pump for different sources and different demands (Week 2, January)

4.3.2 Summer analysis

In contrast, the summer season, examined in the 28th week of July, presented in Figure 4.11, shows a more pronounced and sustained increase in the outlet temperature (maximum of 45 °C) of the PVT collector due to higher solar irradiance (maximum of 600 W/m^2) and ambient temperatures (above 15 °C). These values indicate that the conditions are favourable for these collectors to generate enough energy to satisfy the space heating demand for most of the time in the summer months (May to September).

These observations can be seen clearly when plotted for a summer day (July 9th), Figure 4.11. The temperature profile remains relatively stable with high values throughout daylight hours, peaking around midday. This stability is attributed to the consistent and high levels of solar irradiance.

This period shows that the PVT combined with HP can be utilised effectively to satisfy the demands.

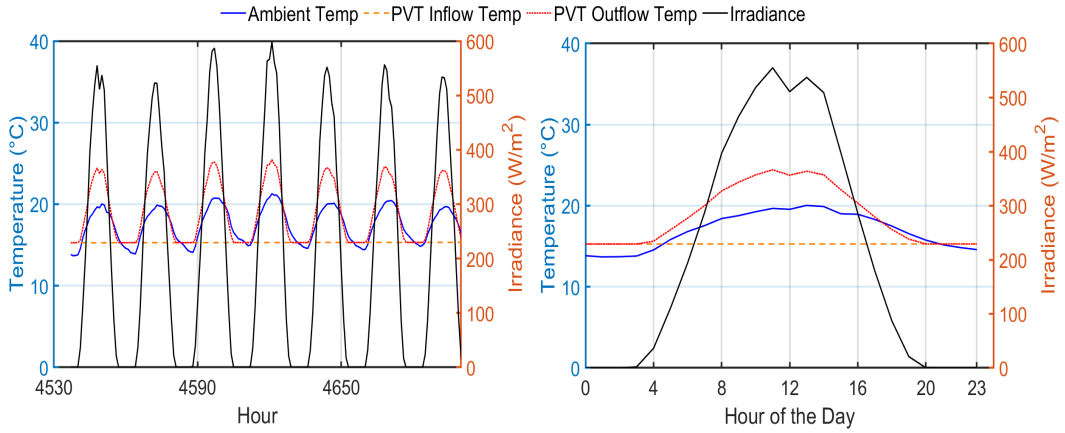

Figure 4.11: Summer season - Ambient temperature, Irradiance, and PVT collector inflow and outflow temperatures in Amsterdam (Week 28, July)

Performance analysis of the system for summer
Figure 4.12 depicts a longer timeframe (a summer week) of hours of the year 4520 to 4720. Here, the DHW system again maintains a steady COP around 3.5 showcasing a constant demand. The ATES system displays a repeating pattern of sharp, high peaks (COP around 5.1) occurring at

regular intervals, likely daily. The PVT system shows more significant activity in this timeframe, with regular peaks reaching a COP of about 4.5, often coinciding with or slightly lagging behind the ATES peaks due to weather conditions supporting the thermal generation.

The right-side graph, plotted in figure 4.12 shows a 24-hour cycle representing a typical summer day. The DHW system maintains a constant COP of about 3.5 throughout the day. The ATES system exhibits a sharp peak between hours 3 and 5, reaching a maximum COP of approximately 5.10, but remains at zero for the rest of the day showing that the demand for space heating is not there. The constant PVT line indicated in blue shows that the thermal energy during the day is not produced since the operating conditions are not satisfied.

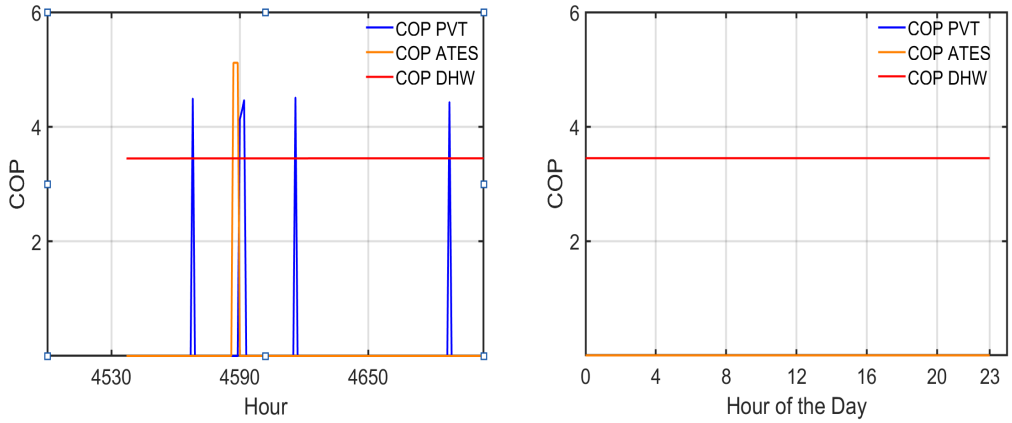

Figure 4.12: Summer season - Coefficient of Performance of heat pump for different sources and different demands (Week 28, July)

4.3.3 Spring analysis

Spring, represented by the 15th week of the year in April through Figure 4.13, offers a transitional scenario between winter and summer. The outlet temperature during this week varies from a minimum of 20 °C to a maximum of 35 °C, with an average temperature of about 27.5 °C. This indicates a moderate improvement in the system's performance compared to winter, benefiting from increased solar irradiance (around 450 W/m^2) and rising ambient temperatures (average 10 °C).

Analyzing a single day (April 9th) through Figure 4.13 within this week, the temperature trend shows a clear daily cycle as seen in Figures 4.9 and 4.11. This season is intermediate Spring serves as a preparatory phase where the system begins to operate more efficiently, setting the stage for the optimal conditions of summer.

This season there is only considerable use of PVT+HP combination and more of the demand is satisfied by warm aquifer and heat pump.

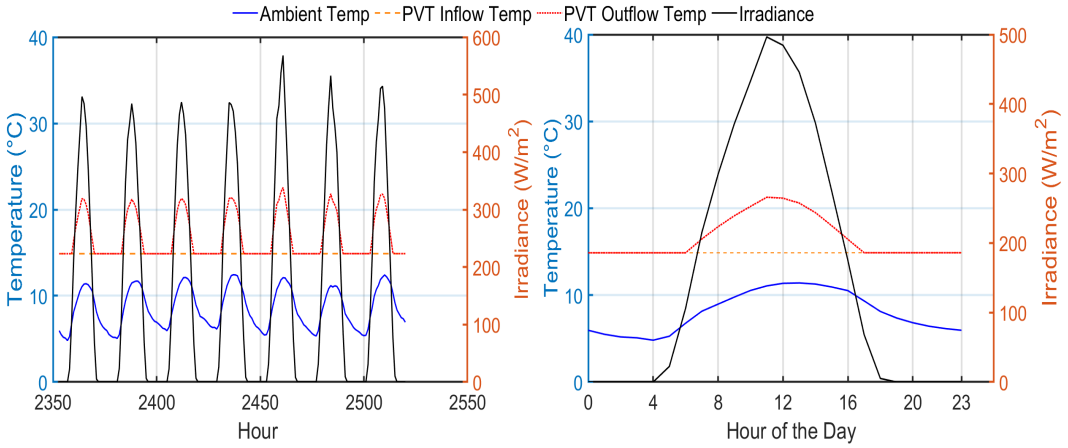

Figure 4.13: Spring season - Ambient temperature, Irradiance, and PVT collector inflow and outflow temperatures in Amsterdam (Week 15, April)

Performance analysis of the system for spring

The left side graph in figure 4.14 depicts performance across a span of approximately 180 hours (a full spring week), while the right side graph shows a 24-hour cycle (April 9th). In both cases, the COP PVT (blue line) exhibits significant fluctuations, oscillating between 0 and approximately 4.5. This cyclical pattern corresponds to daily solar irradiance variations, with peak efficiency occurring during daylight hours. Conversely, the COP ATES (orange line) and COP DHW (red line) remain constant at around 5.0 and 3.4, respectively, suggesting these systems maintain steady performance regardless of time. The stark contrast between the variable PVT system and the stable ATES and DHW systems underscores the impact of external factors such as solar availability.

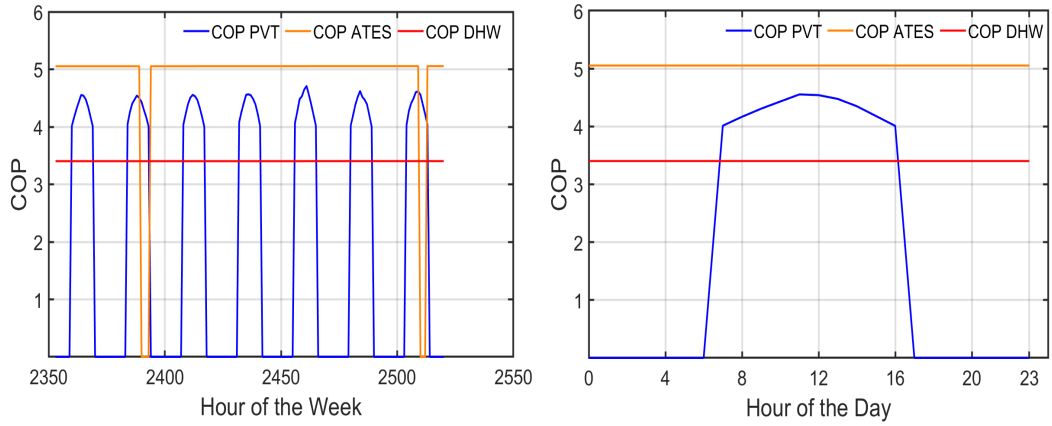

Figure 4.14: Spring season - Coefficient of Performance of heat pump for different sources and different demands (Week 15, April)

In summary, the seasonal analysis reveals a clear correlation between the outlet temperature of the PVT collector and the seasonal variations in solar irradiance and ambient temperature. Winter shows limited performance with brief peaks, summer demonstrates sustained high temperatures and optimal performance, while spring presents moderate and gradually improving conditions. Each season's characteristics directly impact the thermal efficiency and stability of the PVT system, crucial insights for optimizing its design and operation in Amsterdam's climate.

4.4 Comparative analysis of energy scenarios: Current, MT and LT

The case study in this section presents three different scenarios: Current, Medium Temperature and Low Temperature for the same buildings. It presents an overview of changes in the system inputs (demands) and how the system's dynamics change for various demands. Data for the hourly demands for the buildings (Oudebrugsteeg 3, Beursstraat 5, Beursstraat 21 and Warmoesstraat 96) which are modeled was provided by AMS Institute.

1. **Current:** Represents the present heat/cold demand of the house without any renovation.

2. **MT:** Represents the scenario after renovations, reducing the heat/cold demand, space heating demand is less than 80 kWh/m^2 yearly.

3. **LT:** Represents the best possible scenario with extensive renovations, resulting in a space heating demand of less than 50 kWh/m^2 yearly.

Table 4.6: Total and average demand for different scenarios for the buildings: Oudebrugsteeg 3, Beursstraat 5, Beursstraat 21 and Warmoesstraat 96, data provided by AMS Institute

Demand type	**Scenario**	**Total demand (kWh)**
Space heating	Current	197,217
	MT	102,365
	LT	50,713
Space cooling	Current	18,046
	MT	17,802
	LT	17,921
DHW	All scenarios	83,139

4.4.1 Demand comparison across scenarios

The comparative analysis of the demands through Figures 4.15, 4.16 and 4.17 across three different scenarios reveals distinct trends and implications for future energy planning. The space heating demand exhibits significant seasonal variation with notable reductions in future scenarios (MT and LT), with improvement in the insulations. In contrast, space cooling demand remains relatively constant across scenarios, with sharp peaks during summer, suggesting that it is not affected by the insulation in the buildings. DHW demand remains stable throughout the year, irrespective of better insulation. These insights underscore the importance of insulation for improving the building's energy performance and decreasing their demand especially space heating which is the most among the three for countries like the Netherlands.

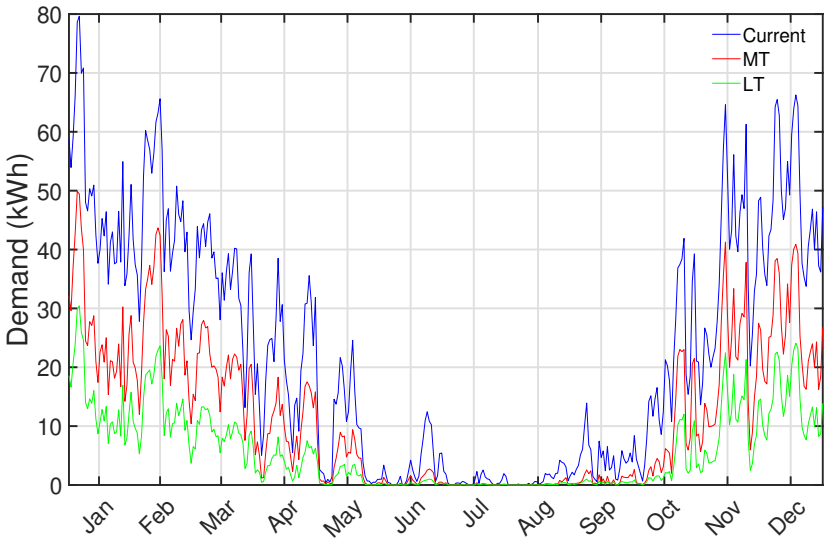

Figure 4.15: Comparison of daily average space heating demand for buildings under current conditions and projected MT and LT scenarios over a year. Peak demand is highest in the current scenario, with significant reductions observed in both MT and LT scenarios.

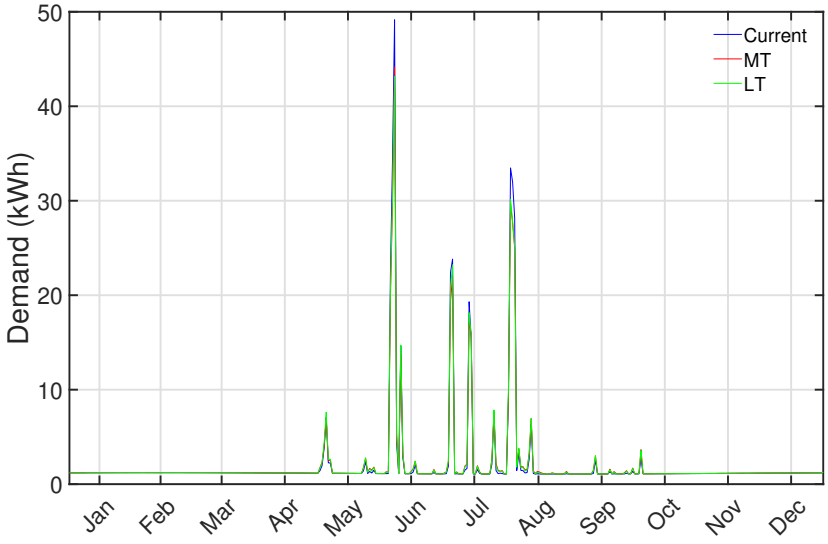

Figure 4.16: Daily space cooling demand throughout the year for buildings under current, MT and LT scenarios. The demand peaks sharply during the summer months (May to September), with minimal variation between the scenarios, indicating consistent cooling needs across all projections.

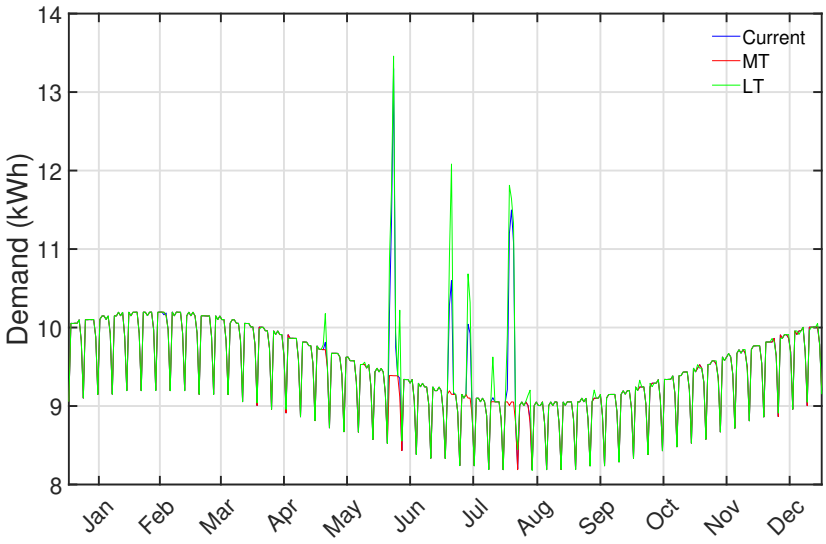

Figure 4.17: Annual daily average demand of domestic hot water for buildings under current, MT, LT scenarios. The demand remains stable throughout the year, with slight increases during colder months and minimal variation between scenarios.

4.4.2 System analysis for different scenarios

On analyzing the data presented in Table 4.7, we observe notable trends in the power consumption and aquifer temperatures across different scenarios—Current, MT, and LT. This analysis is pivotal in understanding the implications of varying space heating and cooling demands on energy consumption by heat pumps and aquifer thermal behavior.

Power consumed by heat pumps
The power consumed in the current scenario is 68.55 kW. This scenario represents the baseline energy usage without significant improvements in energy efficiency or changes in demand patterns. For the second scenario, there is a reduction in power consumed by heat pump by almost 25 %. It is due to the dip in demand for space heating which has decreased to almost half of the Current scenario demand and nominal changes in space cooling and DHW demand. For the best possible insulation for the buildings, the LT scenario provides more reduction in the power consumption by the heat pumps since the demand is one-fourth of the Current and half of the MT scenarios. It is quite surprising to see that the space cooling demand is higher than MT but slightly lower than the Current scenario. This might be because better insulations inadvertently lead to higher internal heat gains, necessitating additional cooling as found out by Fang et al. (2014).

Temperature of aquifers
The warm aquifer temperature in the current scenario is 26.58 °C. This temperature slightly decreases to 26.27 °C in the MT scenario and marginally increases to 26.29 °C in the LT scenario. The relatively stable temperature of the warm aquifer across different scenarios suggests that the energy extraction and storage processes maintain a consistent thermal environment.

The cold aquifer temperature increases from 15.62 °C in the current scenario to 16.54 °C in the MT scenario, and further to 17.28 °C in the LT scenario. The rising temperatures in the cold aquifer imply a gradual reduction in the efficiency of cooling cycles, due to the increased cooling demand.

Table 4.7: Comparison of power consumption by heat pump and aquifer temperatures for various scenarios

Scenario	Power consumed (kW)	Warm aquifer (°C)	Cold aquifer (°C)
Current	68.55	26.58	15.62
MT	48.50	26.27	16.54
LT	37.58	26.29	17.28

In conclusion, the transition from the current scenario to MT and LT scenarios demonstrates a clear reduction in overall power consumption, driven predominantly by decreased space heating demands. However, it is essential to consider the modest increase in cooling demand, which could impact the thermal management of the aquifers.

4.5 Impact of flow rates on PVT and ST collectors: Integrated energy system

To understand the modeled system under varying mass flow rates of water entering the collectors in the "Current" demand scenario, sensitivity analysis was conducted to assess how the system adapts (mode count) and also to assess based on energy supply by each component. A detailed explanation of each operational mode is provided in Section 3.4.

4.5.1 Operational mode analysis of collectors

This subsection presents an analysis of the change in the count of each designed operational mode with a change in the flow rate of collectors (PVT and ST).

Photovoltaic thermal collectors
The analysis of the modeled system with varying flow rates of unglazed PVT collectors is depicted in Figure 4.18. It is evident that there is a complex interaction between the mass flow rate of water entering the collectors and designed operational modes. As the mass flow rate increases from 0.005 to 0.025 kg/s, there's a distinct shift in the system's primary energy source from PVT to ATES for space heating. This transition is evidenced by the decreasing frequency of PVT primary modes (2a, 3a, 4a) and the corresponding increase in counts of modes 2b, 3b, and 4b where ATES is the main source of energy with little generation of thermal energy from PVT collectors. Notably, mode 3 (space heating > space cooling) consistently dominates across all configurations, suggesting an optimal operating condition or a frequent demand scenario. The constant high occurrence of mode 1c (no PVT output and ATES only supply, 1345 counts) across all flow rates indicates a baseline operation independent of flow rate, possibly representing a minimum system requirement.

The count of modes like 3a decreases with an increase in flow rate, indicating that at a lower limit, they produce water at lower temperatures which can easily satisfy the heat demand by the use of heat pumps. The absence of modes 1a, 5a, 1b, and 5b across all scenarios suggests these are the conditions which are unlikely to happen such as high irradiance and high outlet temperature when there is a space heating demand which is generally in winter months when the former conditions are the opposite.

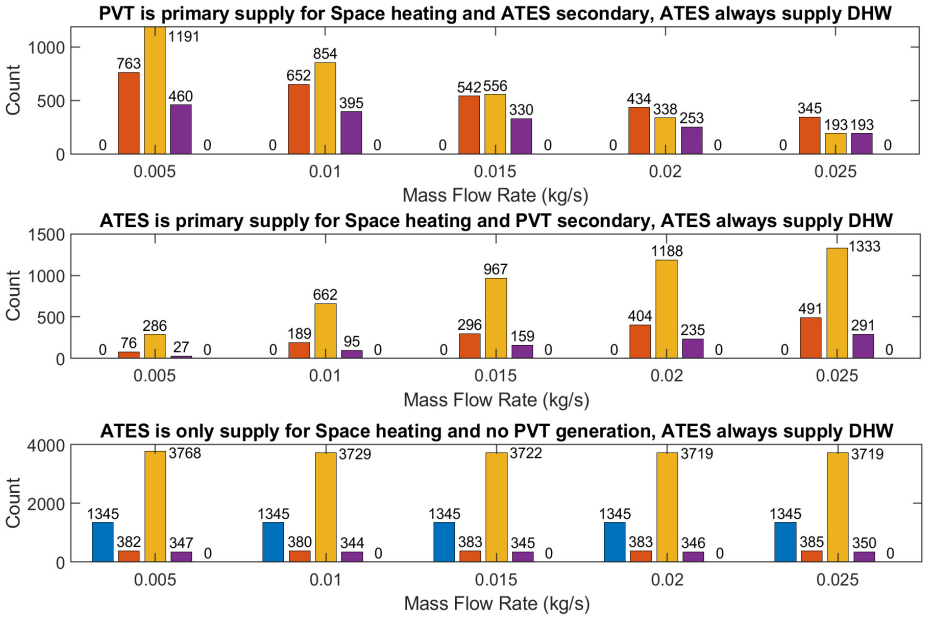

Figure 4.18: Mode counts with a varying flow rate of PVT collectors from 0.005 to 0.025 kg/s

Table 4.8 details the count of the most frequent mode (Mode 3) across different PVT collector flow rates. It reveals that as the flow rate increases, PVT becomes less capable of meeting demand (higher counts of mode 3b), leading to increased reliance on ATES.

Table 4.8: Most frequent modes and their count at different mass flow rates of PVT collectors

Mass flow rate (kg/s)	**0.005**	**0.010**	**0.015**	**0.020**	**0.025**
PVT Primary, ATES Secondary (Mode 3a)	1191	854	556	338	193
ATES Primary w/ PVT Secondary (Mode 3b)	286	662	967	1188	1333
ATES w/o PVT (Mode 3c)	3768	3729	3722	3719	3719

This behavior can be attributed to several factors:

- Thermal efficiency: At lower flow rates, the PVT collector can achieve higher thermal efficiencies due to prolonged contact time between the water and the thermal absorber. This enhances the heat transfer process, making the PVT a more effective primary heat source.

- System dynamics: Higher flow rates reduce the thermal gradient across the PVT collector, diminishing its efficiency and shifting the load towards ATES. Consequently, ATES can leverage its stored thermal energy more effectively at these higher flow rates.

- Operational flexibility: The relatively stable occurrence of Mode 3c suggests that the ATES system is capable of providing consistent thermal performance, irrespective of the operational status of the PVT collector.

Thus, it can be concluded that the mass flow rate of water for the PVT collectors is an important criterion, to influence the energy supplied by the collectors or aquifers.

Solar thermal collectors

Figure 4.19 presents operational mode distributions for a combined ST and ATES system under varied mass flow rates. Similar to PVT collectors, ST collectors show distinct mode shifts with increasing flow rates, emphasizing ATES's role as the flow rate rises.

With the increase in mass flow rate from 0.005 to 0.025 kg/s, we observe a significant shift in the operational modes. Mode 3a (likely representing optimal ST performance) shows a consistent decrease. This suggests that higher flow rates may reduce the outlet temperature of the water which in turn results in a decrease in the number of mode 3a and a surge in the count of mode 3b. Interestingly, modes 1a and 5a remain inactive across all flow rates, indicating potential system limitations or design constraints. In the scenario where ATES is supplying both space heating and DHW demand with energy generation via collectors, the number is constant across various flow rates. The minimal variations in other modes (1c, 2c, 4c) suggest that the ATES system's performance is less sensitive to flow rate changes when operating without PVT generation.

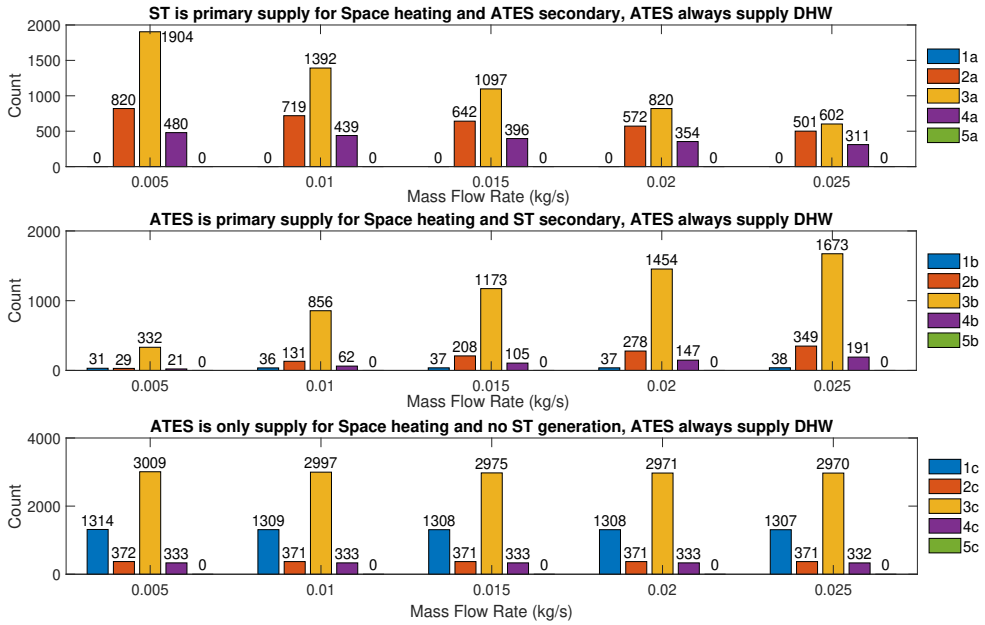

Figure 4.19: Mode counts with a varying flow rate of ST collectors from 0.005 to 0.025 kg/s

The count of the most frequent mode (Mode 3) with varying flow rates of water in the ST collector is presented in Table 4.9. It can be seen that with an increase in mass flow rate, this type of collector is not able to satisfy the demand (more counts of mode 3b) and most of the energy demand is satisfied by ATES.

Table 4.9: Most frequent modes and their count at different mass flow rates of ST collectors

Mass flow rate (kg/s)	**0.005**	**0.010**	**0.015**	**0.020**	**0.025**
ST Primary, ATES Secondary (Mode 3a)	1904	1392	1097	820	602
ATES Primary w/ ST Secondary (Mode 3b)	332	856	1173	1454	1673
ATES w/o ST (Mode 3c)	3009	2997	2975	2971	2970

The system's behavior is significantly influenced by mass flow rate, particularly in configurations involving ST generation. Higher flow rates tend to favor ATES-dominated operational modes, requiring a need to study whether this trend is true in the aspect of energy supply.

The system demonstrates greater stability when relying primarily on ATES without the generation of thermal energy by the collector, indicating a robust baseline performance. The absence of mode 5 across all scenarios suggests that space heating demand and space cooling demand are rarely present.

The analysis done for PVT and ST collectors for different flow rates shows that a lower flow

rate of water is needed to effectively use the thermal energy of these collectors and the ATES acts as a secondary source of thermal energy and also a medium to store it when needed.

4.5.2 Energy analysis of PVT/ST collectors

With the increase in mass flow rate, it has been observed that there is a continuous rise in energy supplied through the PVT/ST collectors, which is almost 105% and 87.70% of the initial value, respectively. The opposite is observed for the case of ATES where a drop of 3% and 5% occurs during the same change. On the other hand, the heat pump energy supply increases since the PVT/ST output temperature drops with flow rate, more work has to be done to reach the required space heating temperature showcasing a surge of 5.50% and 8.90%, respectively.

Table 4.10 presents the energy output of PVT collectors, warm aquifer, and heat pump at various mass flow rates. The data shows the relation between flow rate and various component's performance.

Table 4.10: Energy supplied by PVT collectors at various mass flow rates

Mass flow rate (kg/s)	PVT (MWh)	Warm aquifer (MWh)	Heat pump (MWh)
0.005	3.96	169	20.0
0.010	5.18	167	20.4
0.015	6.16	166	20.7
0.020	7.13	165	20.9
0.025	8.05	164	21.1

Figure 4.20 illustrates the percentage change in energy supply as the mass flow rate increases for both PVT and ST collectors. The two subfigures allow for a direct comparison of the systems' responses to flow rate variations.

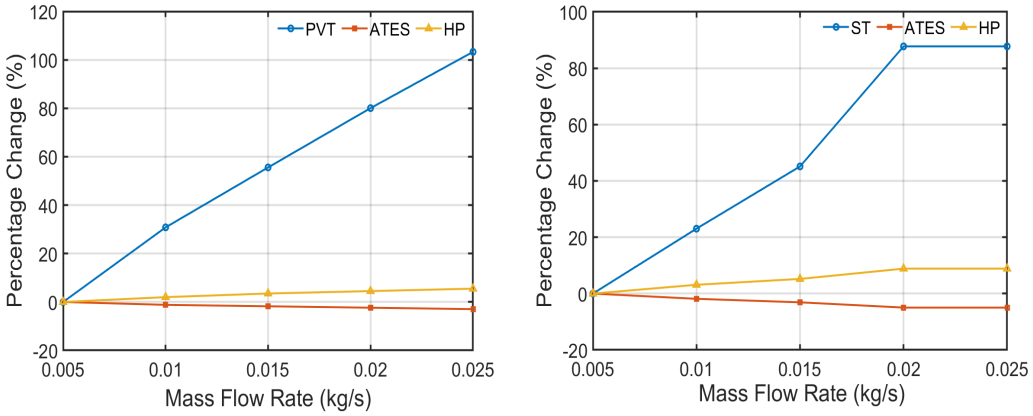

Figure 4.20: Percentage change of energy supply with change in PVT and ST mass flow rate

The energy output of ST collectors, warm aquifer, and heat pumps across different mass flow rates is displayed in Table 4.11. This data shows that the thermal energy production of ST collectors is better than PVT collectors.

Table 4.11: Energy supplied by ST collectors at various mass flow rates

Mass flow rate (kg/s)	ST (MWh)	Warm aquifer (MWh)	Heat pump (MWh)
0.005	7.51	161	19.2
0.010	9.24	158	19.8
0.015	10.9	156	20.2
0.020	14.1	153	20.9
0.025	14.1	153	20.9

4.6 Performance analysis of system: Underfloor heating

A case analysis is done to understand the performance of the integrated system in implementing underfloor heating and compare it with radiator heating through graphs and values.

Figure 4.21: Picture of pipes laid on the floor to provide underfloor heating in the room, Verbeterjehuis.nl (2024)

The main difference between both types of heating is temperature. For radiator heating, the water is supplied at around 50 °C and for underfloor heating it is calculated according to the expression: 30 - 0.5 * T_{am} where T_{am} is the ambient temperature for that hour of the year, derived by Aguilera (2024). Through this expression, we can see that the temperature requirement is never as high as 50 °C (radiator heating) which can be also seen in graph 4.22.

4.6.1 Underfloor heating temperature

Figure 4.22 illustrates the annual variation in ambient temperature and required temperature over 12 months. The blue line represents the ambient temperature, which follows a typical seasonal pattern with lower temperatures in winter months (November-December to January-February) and higher temperatures in summer months (May to September). The ambient temperature ranges approximately from 2 °C to 22 °C throughout the year. The orange line depicts the required temperature, which remains relatively constant at around 28 °C for most of the year (space heating demand).

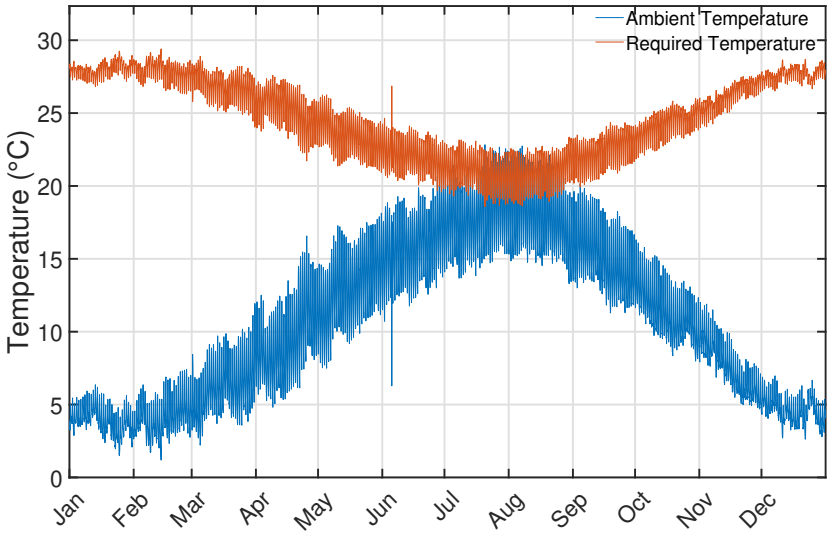

Figure 4.22: Underfloor heating temperature required for the full year.

The graph effectively demonstrates the inverse relationship between ambient temperature and heating requirements. As ambient temperature decreases, the gap between it and the required temperature widens, indicating a greater heating demand. Conversely, this gap narrows during warmer months, implying reduced or no heating needs.

4.6.2 Aquifer temperature over the year

On modeling it for the base case of 10 PVT collectors at 0.015 kg/s water flow rate, the two aquifer sizes were found to be 22,000 m^3 which relates to the hydraulic radius of 28.58 m and thermal radius of 18.86 m calculated using equations 3.4 and 3.5.

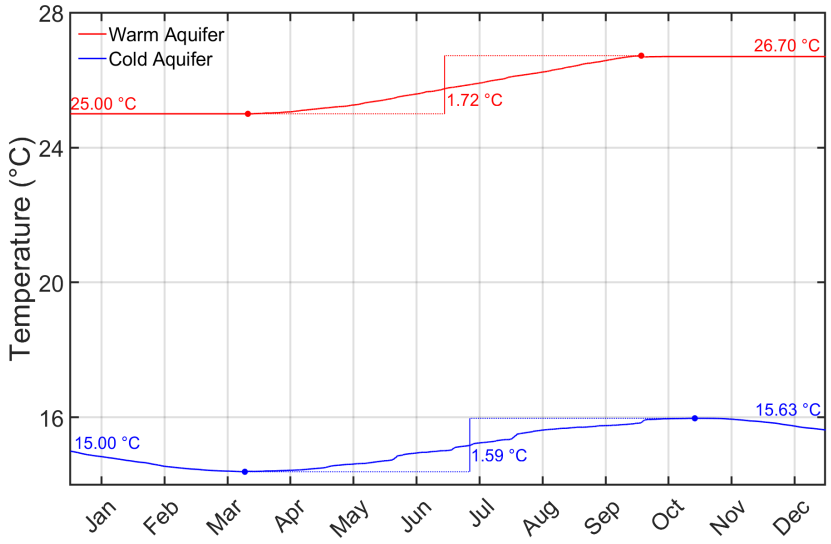

Figure 4.23: Temperature throughout the year of warm and cold aquifers

4.6.3 Coefficient of performance of ATES and PVT during the year

The heat pump's performance in underfloor heating is much higher than observed in Figure 4.4. It is due to the temperature required being lower than 50 °C due to which the heat pump doesn't have to perform much work to deliver the same energy. DHW curve of the heat pump doesn't change since there is no change in its demand or temperature.

COP of the heat pump when warm aquifer and PVT collectors are the sources have values above 8 and there is no change in COP value for the DHW case. In comparison, the COP values for the case of space heating for radiator type were 4.36 and 5.14 (almost half of the present case values). This indicates that the electricity consumption of the heat pump was reduced severely in this case.

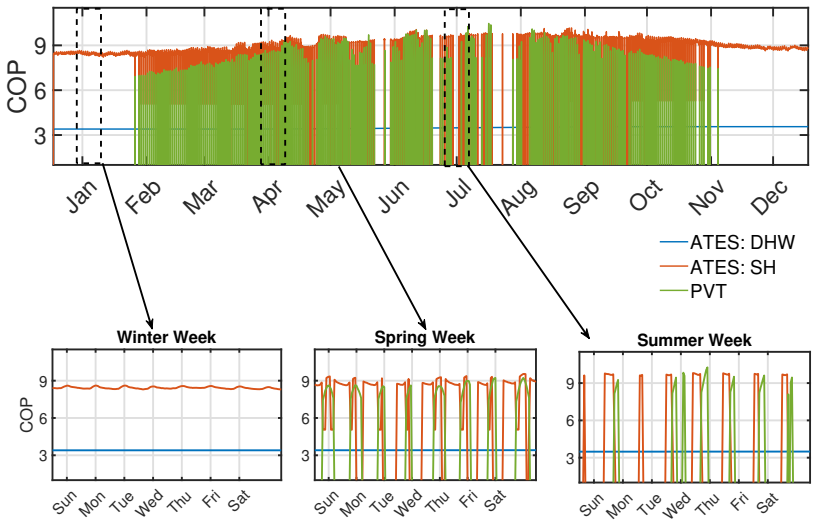

Figure 4.24: COP of Heat pump for the underfloor heating system using ATES and PVT.

Table 4.12: Coefficient of performance of heat pump for underfloor heating and DHW through sources: PVT, ATES for SH and ATES for DHW

System	Average COP	Maximum COP
PVT: SH	8.28	10.47
ATES: SH	8.45	10.21
ATES: DHW	3.48	3.58

4.6.4 Power consumed by heat pumps

The total power consumed by the heat pump is around 52.51 kW which is around 23% less than the base case scenario (68.55 kW). This means that the size of aquifers and power consumption are reduced with the shift to underfloor heating.

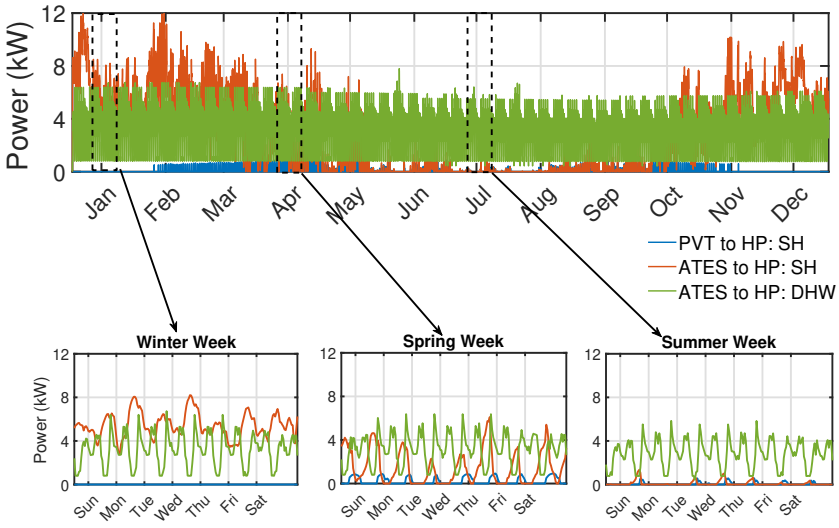

Figure 4.25: Power consumption of heat pumps (kW) for supplying energy from PVT and ATES to meet the building's demand (SH and DHW) throughout the year.

4.6.5 Pumping rate of water through ATES and PVT

Table 4.13 presents the average and maximum pumping rates for PVT collectors to HP for SH, ATES system to HP for SH, and ATES to HP for DHW over a year for underfloor heating. The PVT system for space heating maintains a consistent pumping rate of 1.08 m^3/h. This showcases that the maximum output is delivered most of the time of the year to HP by PVT. While the ATES system for space heating shows greater variability with an average of 1.67 m^3/h and a peak of 5.18 m^3/h This shows that ATES can increase the output when required and acts as primary and secondary supply of energy for SH throughout the year. The ATES system for domestic hot water has lower rates, averaging 0.457 m^3/h and peaking at 1.18 m^3/h, due to the variable demand.

Table 4.13: Average and maximum pumping rates (m^3/h) of PVT to HP for SH, ATES to HP for SH and ATES to HP for DHW over a year for underfloor heating

System	Average pumping rate (m^3/h)	Maximum pumping rate (m^3/h)
PVT: SH	1.08	1.08
ATES: SH	1.67	5.18
ATES: DHW	0.457	1.18

4.6.6 Energy supplied by ATES, heat pump and PVT throughout the year

Table 4.14 compares the energy supplied by each component (PVT, ATES and heat pump) of the modeled system before and after implementing underfloor heating. The PVT contribution increases slightly meaning more utilization of solar energy. There is a significant rise in ATES energy supplied which jumps from 166 to 183.35 MWh. The energy supplied by heat pumps is almost 25% of the radiator heating meaning that the heat pump requirement decreases. This is found due to the decrease in the required temperature for heating.

Table 4.14: Comparison of energy supplied by each component for radiator heating and underfloor heating

	PVT (MWh)	ATES (MWh)	Heat pump (MWh)
Radiator heating	6.16	166	20.70
Underfloor heating	6.38	183.35	4.57

These changes suggest that the transition to underfloor heating has led to a more efficient energy distribution system (higher COPs as seen in Table 4.12), particularly by leveraging the ATES system and reducing the load on the heat pump.

4.7 Costs of the integrated system

This section examines the economic aspects of an aquifer system integrated with heat pumps, heat exchanger, submersible pumps, PVT collectors, and PV modules. The analysis includes capital costs, operational costs, replacement costs, and an annual cost calculation. The study aims to assess the financial viability of the ATES system compared to conventional heating and cooling methods.

Table 4.15 outlines the lifetime and units of each component of the integrated system, including cold and warm wells, heat exchanger, submersible pumps, and heat pumps. The lifetimes of these components vary, with wells lasting 25 years and other components ranging from 5 to 30 years. The lifetime of the submersible pump is less than the total lifetime of the system indicating that more units are needed to replace the existing ones after their lifetime to run the system. This type of cost comes under replacement cost and is stated in subsubsection 4.7.3.

Table 4.15: Components of the integrated system with their number of units and their lifetime, VDI (2012), Ingenieurgesellschaft für Geo-und Umwelttechnik (2017), Bloomquist (2000), TripleSolar (2024)

Component	**Units**	**Lifetime (years)**
Cold well	1	25
Warm well	1	25
Heat exchanger	1	20-30
Submersible pumps	2	5-7
Heat pumps	2	20-30
PVT collectors	10	25
PV modules	190	25

4.7.1 Capital costs

The capital costs are those costs which are one-time costs while building the system. They consist of an investigation of the site where the aquifers are suitable. Once the site is decided comes the drilling costs, laying out the pipes in the wells, installing valves and meters to regulate and monitor water flow.

Figure 4.26: Laying of pipelines underground to connect aquifers and buildings, Getty images

Once this is done then the pipes are laid out as shown in figure 4.26 to connect them to buildings

and install pipes over there. Building integration consists of heat pumps and heat exchangers which are then connected to the PVT collectors. These all form a single system.

The electricity generation through the PV module of area 1.88 m^2 is around 366.23 kWh. There is a requirement of 69.03 MWh to power the heat pumps and submersible pumps for the demands. Therefore, there is a need for 190 PV modules and 10 PVT collectors to satisfy the electrical demand of the modeled system.

Table 4.16: Category-wise capital costs breakdown of ATES system, heat pump, heat exchanger and PVT collecotrs, Stadtwerke Waldkraiburg (2018), Stadtwerke Sindelfingen (2007), Landesamt für Natur, Umwelt und Verbraucherschutz Nordrhein-Westfalen (2015), Ingenieurgesellschaft für Geo-und Umwelttechnik (2017), Chiasson and Culver (2006), Vanhoudt et al. (2011), Seider (2006) and International Energy Agency, Solar Heating and Cooling Programme (2021)

Category	**Costs (€)**
Pre-investigation/ Feasibility	3,398
Preparation	6,220
Drilling	6,617
Well piping and well insulation	27,600
Controlling and Monitoring	5,920
Piping	139,230
Building integration	44,256
PVT collectors	20,000
PV modules	41,800
Total capital costs	295,041

4.7.2 Operational costs

Operating costs for ATES systems generally are 4% of capital costs as found out by Schüppler et al. (2019). The total operating costs in the lifetime of the integrated system are found out by multiplying by 25, summing to €295,041.

Table 4.17: Operational costs of the integrated system

Component	**Costs (€)**	**Total operational costs (€)**
ATES + Heat pump + Heat exchanger	11,801	295,041

4.7.3 Replacement costs

These costs occur when there is a need to replace a component before the lifetime of the system. In the modeled system, the submersible pump is the component whose lifetime is 5-7 years as stated in Table 4.15.

Table 4.18: Replacement costs of the integrated system, Pumpa.eu (2024)

Component	**Units**	**Costs (€)**	**Total replacement costs (€)**
Submersible pump	10	188	1,888

4.7.4 Cost calculations

This section presents the cost calculations for the integrated system. Three main cost components are considered: depreciation, replacement, and interest payments.

Equation 4.1 calculates the annual depreciation costs after dividing the total capital costs by the system's lifetime. This results in an annual depreciation of €11,801 (Equation 4.2).

Depreciation costs

$$\text{Annual depreciation} = \frac{\text{Capital costs}}{\text{Lifetime}} \tag{4.1}$$

$$\text{Annual depreciation} = \frac{295,041}{25} = €11{,}801 \tag{4.2}$$

Annual replacement costs (Equation 4.3) are determined by dividing the total replacement costs over the system's lifetime. The calculation yields an annual replacement cost of €75 (Equation 4.4).

Annual replacement cost

$$\text{Annual replacement cost} = \frac{\text{Total replacement costs}}{\text{Lifetime}} \tag{4.3}$$

$$\text{Annual replacement cost} = \frac{1,888}{25} = €75 \tag{4.4}$$

The annual interest payment is computed by multiplying the capital costs by the interest rate (Equation 4.5). This results in an annual interest payment of €14,752.05 considering 5% rate (Equation 4.6).

Annual interest payment

$$\text{Annual interest payment} = \text{Capital costs} \times \text{Interest rate} \tag{4.5}$$

$$\text{Annual interest payment} = 295,041 \times 0.05 = €14{,}752 \tag{4.6}$$

Table 4.19 summarizes the cost breakdown of the integrated system, including capital costs, annual depreciation, operational costs, replacement costs, and interest payments. The total annual costs amount to €38,430.

Table 4.19: Cost breakdown of the integrated system

Category	**Cost (€)**
Annual depreciation	11,801
Annual operational costs	11,801
Annual replacement costs	75
Annual interest payment	14,752
Total annual costs	38,430

The thermal demand delivered over a year is 298,400 kWh. By dividing the total annual costs by the delivered thermal demand, the levelized cost of thermal energy is calculated to be €0.128/kWh.

This economic analysis of the integrated system consisting of ATES, heat pumps, heat exchanger, submersible pumps, PVT collectors and PV modules, encompassing capital, operational, and replacement costs along with annual cost assessments, provides a detailed evaluation of its financial viability. The findings suggest that the integrated modeled system presents a cost-effective and sustainable alternative to conventional heating and cooling methods, with a levelized cost of thermal energy amounting to €0.128/kWh.

4.8 Carbon emissions reduction through integrated system

This section presents an analysis of the carbon emissions reduction achieved by the integrated system compared to conventional energy sources. The analysis considers gas-based sources for supplying space heating, space cooling and DHW demands. the systems utilise PV modules and PVT collectors to supply the systems' electricity demand to run heat pumps and submersible pumps. Carbon emissions supply the same electricity demand through a grid consisting of fossil fuels and green sources. This provides a comprehensive view of the environmental impact of the proposed system.

4.8.1 Emission factors

Table 4.20 presents the CO_2 emission factors for electricity and gas, as reported by for Standardization (2008). These emission factors are crucial for calculating the environmental impact of energy consumption. Specifically, fossil-fuel-based electricity has an emission factor of 617 kg CO_2/MWh, while gas has an emission factor of 277 kg CO_2/MWh. These values serve as the foundation for the subsequent emissions reduction analysis.

Table 4.20: CO_2 Emission factors

Energy source	CO_2 emission factor (kg/MWh)
Electricity (fossil-fuel)	617
Gas	277

4.8.2 Emissions reduction compared to gas-based systems

Table 4.21 illustrates the annual CO_2 emissions reduction achieved by the integrated system when compared to a gas-powered district heating system. The table details the energy demands alongside their respective emission factors and calculated emissions reductions. The integrated system results in significant annual emissions reductions: 54.63 tonnes for space heating, 5 tonnes for space cooling, and 23.03 tonnes for DHW. Over the 25-year lifetime of the system, these reductions accumulate to a total of 2066.40 tonnes of CO_2, demonstrating the substantial environmental benefits of the integrated system compared to conventional gas-based methods.

Table 4.21: Annual CO_2 emissions reduction compared to gas-based systems

Demand type	Energy demand (MWh)	Emission factor (kg/MWh)	Annual reduction (tonnes/year)	Lifetime reduction (tonnes)
Space heating	197.21	277	54.63	1365.70
Space cooling	18.04	277	5	125
DHW	83.14	277	23.03	575.73

The total emissions reduction over the system's 25-year lifetime, compared to a gas-powered district heating system, is calculated to be 2066.43 tonnes of CO_2.

4.8.3 Emissions reduction compared to grid electricity

The integrated system's electricity production is achieved through a combination of 190 PV modules and 10 PVT collectors. This configuration supports the electricity consumption of submersible pumps and heat pumps for various demands.

For this analysis, we assume that grid electricity is sourced 50% from coal and 50% from solar panels, resulting in an effective emissions factor of 308.50 kg/MWh.

Table 4.22: Annual CO_2 emissions reduction compared to grid electricity

Electricity demand (MWh)	Electricity produced (MWh)	Emission factor (kg/MWh)	Annual reduction (tonnes/year)	Lifetime reduction (tonnes)
69.04	69.99	308.50	21.60	539.80

The integrated system generates a slight surplus of 950 kWh of electricity annually. Over its 25-year lifetime, the system is projected to reduce CO_2 emissions by 539.80 tonnes compared to grid electricity consumption.

The analysis demonstrates significant environmental benefits of the integrated system. When compared to gas-based alternatives, the system reduces CO_2 emissions by 2066.43 tonnes over its lifetime. In comparison to grid electricity, it achieves a reduction of 539.80 tonnes, totalling 2606.23 tonnes of combined emissions savings. These findings underscore the substantial positive environmental impact of integrating renewable energy sources with traditional heating and DHW systems, supporting the viability of such integrated approaches in mitigating climate change.

4.9 Conclusion

This chapter presents the findings of the integrated system under various scenarios, accomplishing the third sub-objective of the thesis which is to examine the integrated system's performance in various scenarios to understand its applicability under various scenarios. Furthermore, compares its cost and carbon emissions with current commercial heat systems. Firstly, the considered parameters and constraints for modeling the system are discussed. The first case, which is the base case scenario of 10 PVT collectors with an aquifer volume of 27,000 m^3 is presented which highlights important parameters such as temperature changes in the aquifers, COP of heat pump, pumping rate and other parameters. This showcases the general performance of the system for the current insulation level. To validate the system, parameters L/R_{th} and V are compared with existing literature. The base case scenario generalizes the system analysis for a year, but it is important to understand it season-wise since system inputs such as irradiance and demands change accordingly. It was found out that the collectors are effective during summer with ATES being consistent in performance and energy delivery throughout the year with changing demands.

The model is simulated for different demands which are occurring due to varying insulation levels in the same four building models as in the base case. The system's performance improves with insulation level since total energy demand decreases drastically (space heating demand for the LT scenario is one-fourth of the current scenario). There are different collectors which are modeled: one is PVT and another one is ST. On comparing the performance of PVT and ST collectors under various flow rates, it is observed that at higher flow rates both PVT and ST collectors produce lower outlet temperatures of water. In contrast, on comparison of energy supplied by each collector at various flow rates, it was found that higher flow rates supply more energy due to higher mass flow. Moreover, in general, ST collectors perform better than PVT collectors. When the system was modeled for underfloor heating, a different type of heating than the radiator, it was found that there was around 75% reduction in energy utilisation by the heat pumps since the temperature required to heat the buildings is quite lower than 50 °C (radiator heating).

On the evaluation of the system in terms of cost, a levelised cost of thermal energy was found to be €0.128/kWh, for its lifetime of 25 years. In comparison to district heating, the costs are similar but there is no impact on the environment through these systems. Also, if these systems are scaled up then the levelised costs of energy will decrease considerably, making them cheaper than district heating systems. A total of 2606.23 tonnes of carbon can be saved in comparison to district heating in the system's lifespan of 25 years on implementing the integrated system.

5

Conclusions

This thesis investigated a sustainable energy system incorporating aquifer thermal energy storage (ATES), solar collectors, heat pumps, and heat exchangers. The primary objective of the thesis was to optimize the integrated energy system consisting of PVT collectors and ATES, with a focus on the Dutch climate. To accomplish the main objective, several sub-objectives were formulated. Firstly, the foundation of the components and their working was addressed in Chapter 2. Several system inputs were identified such as irradiance, ambient temperature, and energy demand, which can influence the system's performance and characteristics. Chapter 3 covers the individual models of solar collectors, heat pumps, ATES, and heat exchanger in detail. Heat exchanger and ATES models were developed from scratch as a part of the thesis sub-objective 1. Later in the same chapter, the optimization approach followed was discussed where the full year was divided into five modes each having three sub-modes. This is done to systematically size the system (ATES and PVTs) according to the demand and other system inputs. This makes the system robust and redundant for future applications. The second sub-objective was to validate the previously developed system consisting of ATES and PVT. This was performed by comparing the value of L/R_{th} and V with several other ATES systems around the world, through literature.

The third sub-objective of the thesis was covered in Chapter 4 which highlights the findings of the integrated system under various scenarios. The first case was the base case scenario modeled for the Current scenario energy demand, comprising 10 PVT collectors and the aquifers of volume 27,000 m^3. Several important parameters such as temperature changes in the aquifers, COP of heat pump, pumping rate, and power consumed are analysed showcasing the critical aspects of a complex energy system. To study the performance and other characteristics of the system in detail, season-wise system outputs such as COP and output water temperature were evaluated with changing system inputs such as irradiance, and ambient temperature with seasons. This analysis was critical as it explains that the collectors are effective during summer with ATES being consistent in performance and energy delivery throughout the year with changing demands.

Another case for which the system was simulated was of three different insulation levels (Current, MT and LT) for the same buildings. The system's performance improves in terms of power consumed and COP with insulation levels. It was due to the decrease in total energy demand drastically (space heating demand for the LT scenario is one-fourth of the current scenario). The findings indicate that with improvement in insulation level, not only the demand but the performance of the systems also improves. The thesis considered two types of collectors: PVT and ST. On comparing the performance of PVT and ST collectors under various flow rates, it was observed that at higher flow rates both PVT and ST collectors produce lower temperatures of water as outlet. In contrast, on comparison of energy supplied by each collector at various flow rates, it was found that higher flow rates supplied more energy due to higher mass flow. In general, the thermal performance of ST is better than PVT collectors.

Radiator type of heating was considered in the system and the system's performance was assessed. In another type of heating, underfloor heating when considered it was found that there was a reduction of 75% in energy utilisation by the heat pumps. It was due to the fact the temperature required to heat the buildings is quite lower than 50 °C (radiator heating). Furthermore, a comparison of the integrated system's cost and emissions with district heating system is examined in (Chapter 4). On evaluation of the system in terms of cost, a levelised cost of thermal energy was found to be €0.128/kWh, throughout its lifetime of 25 years. In comparison to district heating, the costs are similar but there is no impact on the environment through these systems which is present in gas-powered district heating systems. Moreover, if these systems are scaled up to the larger number of buildings then the levelised costs of energy will decrease considerably, making them cheaper than district heating systems. A total of 2606.23 tonnes of carbon can be saved in comparison to district heating in the system's lifespan of 25 years on implementing the integrated system.

In conclusion, this research demonstrates the significant potential of integrated energy systems utilizing ATES, solar collectors, heat pumps, and heat exchangers to provide heating and cooling to buildings. The system's high performance, substantial environmental benefits, and long-term economic viability present a compelling case for its adoption in sustainable building designs. These systems have a lot of scope in the Netherlands due to ATES feasibility, around 90% of the ATES systems in the world are installed in the Netherlands. While challenges remain, particularly in initial costs and system sizing, the overall performance suggests that such systems could play a crucial role in our transition to a more sustainable energy future. The interdisciplinary nature of this research underscored the importance of holistic approaches in addressing complex energy challenges.

6

Recommendations

The findings of this thesis underscore the significant potential of integrating aquifer thermal energy storage (ATES), solar collectors, heat pumps, and heat exchangers into a comprehensive energy system. While the results are promising, they also highlight the need for further improvement to fully benefit from such systems in a changing environment. This chapter presents a number of recommendations aimed at enhancing the system's performance and understanding. These recommendations are intended to guide future research, policy development, and practical implementation, ensuring that the full potential of this innovative energy solution can be effectively harnessed.

1. **Evaluation of MT-ATES and HT-ATES applicability:** Perform a thorough analysis of the suitability of High-Temperature (HT) and Medium-Temperature (MT) ATES systems under various geographic and climatic conditions. This evaluation should identify optimal scenarios for each type of ATES while considering factors such as energy demand, aquifer characteristics, and local environmental conditions. Understanding the suitability of MT-ATES and HT-ATES in different contexts will help in tailoring energy solutions to specific needs, thereby enhancing system efficiency and effectiveness.

2. **Feasibility studies in diverse climates:** Perform feasibility studies in various geographic locations and climates to assess the adaptability and performance of the system under different environmental conditions and demands, of countries such as Spain, France, China, and India.

3. **Degradation analysis of solar collectors:** A thorough analysis needs to be carried out to quantify the effect of cooling on the modules as well as the collectors. This analysis will open more scope for lifetime analysis of these collectors, to determine the cooling effect on these systems while enhancing their performance.

4. **Economic analysis for different scales:** Advised to conduct additional economic analysis to determine the cost-effectiveness of implementing the system at various scales, from residential to commercial buildings, to identify different demands and challenges.

5. **Utilization of advanced simulation software:** Utilise advanced energy simulation software such as EnergyPlus, Modelica, TRNSYS, SIM-VICUS, and QGIS, used by leading energy companies. These tools can be instrumental in modeling and optimizing the performance of integrated energy systems, allowing for more accurate predictions and enhanced design strategies. Encouraging collaboration with these companies could also provide valuable industry insights and access to cutting-edge technology.

Bibliography

Aguilera, D. M. (2024). *Integration and optimization of a solar collector heat pump system model for households in the netherlands* [Master's thesis]. Electrical Engineering, Mathematics and Computer Science.

Ali, H. M., Mahmood, M., Bashir, M. A., Ali, M., & Siddiqui, A. M. (2016). Outdoor testing of photovoltaic modules during summer in taxila, pakistan. *Thermal Science*, *20*(1), 165–173. https://doi.org/10.2298/TSCI1401165A

Alsaqoor, S., Alqatamin, A., Alahmer, A., Nan, Z., & Al-Husban, Y. (2023). The impact of phase change material on photovoltaic thermal (pvt) systems: A numerical study. *International Journal of Thermofluids*, *18*.

Association, E. H. P. (2018). *European heat pump market and statistics*. http://www.stats.ehpa.org/hp_sales/country_cards/

Aste, N., Chiesa, G., & Verri, F. (2008). Design, development and performance monitoring of a photovoltaic-thermal (pv/t) air collector. *Renewable Energy*, *33*(5), 914–927.

Bakema, G., Snijders, A. L., & Nordell, B. (1994). *International energy agency: Implementing agreement for a programme of research and development on energy conservation through energy storage. evaluation underground thermal energy storage state of the art*. International Energy Agency.

Bakker, M., Zondag, H., Elswijk, M., Strootman, K., & Jong, M. (2005). Performance and costs of a roof-sized pv/thermal array combined with a ground coupled heat pump. *Solar Energy*, *78*, 331–339.

Bird, L., Lew, D., Milligan, M., Carlini, E., Estanqueiro, A., Flynn, D., Gomez-Lazaro, E., Holttinen, H., Menemenlis, N., Orths, A., Eriksen, P., Smith, J., Soder, L., Sorensen, P., Altiparmakis, A., Yasuda, Y., & Miller, J. (2016). Wind and solar energy curtailment: A review of international experience. *Renewable and Sustainable Energy Reviews*, *65*, 577–586.

Blaas, M. (2022). D2.9 plan for balancing geothermal heat-cold storage system by using surface water. https://ruggedised.eu/fileadmin/repository/Publications/D2.9_-_Plan_for_balancing_geothermal_heat-cold_storage_system_by_using_surface_water.pdf

Bloemendal, M., & Hartog, N. (2018). Analysis of the impact of storage conditions on the thermal recovery efficiency of low-temperature ates systems. *Geothermics*, *71*, 306–319. https://doi.org/10.1016/j.geothermics.2017.10.009

Bloemendal, M., & Olsthoorn, T. (2018a). The effect of a density gradient in groundwater on ates system efficiency and subsurface space use. *Advances in Geosciences*, *45*, 85–103. https://adgeo.copernicus.org/articles/45/85/2018/

Bloemendal, M., Van Esch, M. S., Vardon, P. J., Pape, J. J., & Hartog, N. (2022). Novel ates triplet system for autarkic space heating and cooling. *IOP Conference Series: Earth and Environmental Science*, *1085*(1), 012028. https://doi.org/10.1088/1755-1315/1085/1/012028

Bloemendal, M., Jaxa-Rozen, M., & Olsthoorn, T. (2018). Methods for planning of ates systems. *Applied Energy*, *216*, 534–557. https://doi.org/https://doi.org/10.1016/j.apenergy.2018.02.068

Bloemendal, M., & Olsthoorn, T. (2018b). Ates systems in aquifers with high ambient groundwater flow velocity. *Geothermics*, *75*, 81–92. https://doi.org/https://doi.org/10.1016/j.geothermics.2018.04.005

Bloomquist, R. G. (2000). Geothermal heat pumps: Five plus decades of experience in the united states. *Proceedings of the World Geothermal Congress 2000*, 1–7.

Branker, K., Pathak, M., & Pearce, J. M. (2011). A review of solar photovoltaic levelized cost of electricity. *Renewable and Sustainable Energy Reviews*, *15*(9), 4470–4482.

Buonomano, A., Calise, F., & Vicidomini, M. (2016). Design, simulation and experimental investigation of a solar system based on pv panels and pvt collectors. *Energies*, *9*(7), 497. https://doi.org/10.3390/en9070497

Carotenuto, A., Ruocco, G., & Reale, F. (1990). Thermal storage in aquifers and energy recovery for space heating and cooling. *Heat Recovery Systems and Chp*, *10*, 555–565. https://api.semanticscholar.org/CorpusID:111211137

Chiasson, A., & Culver, G. (2006). *Final report feasibility study for hvac retrofit with a geothermal system mount grant general hospital* (Report on HVAC retrofit feasibility with a geothermal system). Mount Grant General Hospital. Hawthorne, NV.

Chow, T. T., Pei, G., Fong, K. F., et al. (2009). Energy and exergy analysis of photovoltaic-thermal collector with and without glass cover. *Applied Energy*, *86*(2), 310–316.

Chow, T. (2010). A review on photovoltaic/thermal hybrid solar technology. *Applied Energy*, *87*(2), 365–379. https://doi.org/https://doi.org/10.1016/j.apenergy.2009.06.037

Chow, T., Tiwari, G., & Ménézo, C. (2012). Hybrid solar: A review on photovoltaic and thermal power integration. *International Journal of Photoenergy*, *2012*. https://doi.org/10.1155/2012/307287

Cole, W. J., Powell, K. M., & Edgar, T. F. (2012). Optimization and advanced control of thermal energy storage systems. https://api.semanticscholar.org/CorpusID:101028745

Connection, C. E. (2024, January). Heat pump [Accessed: April 15, 2024]. https://www.cleanenergyconnection.org/article/heat-pump-water-heater-vs-tankless-which-better

Curve Tracing, S. E. (2024). https://www.seaward.com/gb/support/solar/faqs/29495-curve-tracing-faq-s/

Danehkar, S., & Yousefi, H. (2022). A comprehensive overview on water-based energy storage systems for solar applications. *Energy Reports*, *8*, 8777–8797. https://doi.org/10.1016/j.egyr.2022.06.057

Díaz, S. R. (2022). A generalized theoretical approach for solar cells fill factors by using shockley diode model and lambert w-function: A review comparing theory and experimental data. *Physica B: Condensed Matter*, *624*, 413427. https://doi.org/https://doi.org/10.1016/j.physb.2021.413427

Dinçer, I., Rosen, M., & Ahmadi, P. (2017). Modeling and optimization of heat pump systems. In *Optimization of energy systems* (pp. 183–198). John Wiley & Sons, Ltd.

Doughty, C., Hellström, G., Tsang, C. F., & Claesson, J. (1982). A dimensionless parameter approach to the thermal behavior of an aquifer thermal energy storage system. *Water Resources Research*, *18*(3), 571–587. https://doi.org/10.1029/WR018i003p00571

Dubey, S., & Tiwari, G. (2008). Life cycle cost analysis and carbon credit earned by hybrid pv/t solar water heater for delhi climatic conditions. *Open Environmental Sciences Journal*, *2*, 15–25. https://doi.org/10.2174/1876325100802010015

Duijff, R., Bloemendal, M., & Bakker, M. (2021). Interaction effects between aquifer thermal energy storage systems. *Groundwater*, *61*. https://doi.org/10.1111/gwat.13163

EIA. (2022). Solar thermal collectors. https://www.eia.gov/energyexplained/solar/solar-thermal-collectors.php

European Commission. (2020). *National climate assessment 2020: Netherlands* (tech. rep.). European Commission. https://energy.ec.europa.eu/system/files/2021-03/nl_ca_2020_en_0.pdf

Fang, Z., Li, N., Li, B., Luo, G., & Huang, Y. (2014). The effect of building envelope insulation on cooling energy consumption in summer. *Energy and Buildings*, *77*, 197–205. https://doi.org/https://doi.org/10.1016/j.enbuild.2014.03.030

Fischer, D., Wolf, T., Wapler, J., Hollinger, R., & Madani, H. (2017). Model-based flexibility assessment of a residential heat pump pool. *Energy*, *118*(100), 853–864. https://EconPapers.repec.org/RePEc:eee:energy:v:118:y:2017:i:c:p:853-864

Fleuchaus, P., Schüppler, S., Bloemendal, M., Guglielmetti, L., Opel, O., & Blum, P. (2020). Risk analysis of high-temperature aquifer thermal energy storage (ht-ates). *Renewable & Sustainable Energy Reviews*, *133*, 110153. https://api.semanticscholar.org/CorpusID:224925054

for Standardization, E. C. (2008). Energy performance of buildings – Overall energy use and definition of energy ratings [Available at: https://www.en-standard.eu/en-15603-2008-energy-performance-of-buildings-overall-energy-use-and-definition-of-energy-ratings/]. *European Committee for Standardization*.

Fossoul, F., Orban, P., & Dassargues, A. (2011). Numerical simulation of heat transfer associated with low enthalpy geothermal pumping in an alluvial aquifer. *Geologica Belgica*, *14*(1-2), 45–54.

Gagliano, A., & Aneli, S. (2017). Energy analysis of hybrid solar thermal plants (pv/t). *Energies*, *3*, 1320–1334.

Grubišić-Čabo, F., Nižetić, S., & Tina, G. (2016). Photovoltaic panels: A review of the cooling techniques. *Transactions of FAMENA*, *40*, 63–74.

Günther, D., Miara, M., Langnner, R., Helmling, S., & Madani, H. (2014). *WP Monitor - Feldmessung von Wärmepumpenanlagen [WP Monitor - Field Measurements of Heat Pumps]* (Final Project Report). Fraunhofer ISE.

Heating and cooling systems. (2022, April). https://mienergy.ca/geothermal/

Hoekstra, N., Pellegrini, M., Bloemendal, M., Spaak, G., Andreu Gallego, A., Rodriguez Comins, J., Grotenhuis, T., Picone, S., Murrell, A., Steeman, H., Verrone, A., Doornenbal, P., Christophersen, M., Bennedsen, L., Henssen, M., Moinier, S., & Saccani, C. (2020). Increasing market opportunities for renewable energy technologies with innovations in aquifer thermal energy storage. *Science of The Total Environment*, *709*, 136142. https://doi.org/https://doi.org/10.1016/j.scitotenv.2019.136142

Huang, B. J., Lin, T. H., Hung, W. C., et al. (1999). Solar photo-voltaic/thermal co-generation collector. *ISES Solar World Congress*.

Huang, B. J., Lin, T. H., Hung, W. C., & Sun, F. S. (2001). Performance evaluation of solar photovoltaic/thermal systems. *Solar Energy*, *70*(5), 443–448.

Ibrahim, A., Othman, M. Y., Ruslan, M. H., et al. (2011). Recent advances in flat plate photovoltaic/thermal (pv/t) solar collectors. *Renewable and Sustainable Energy Reviews*, *15*(1), 352–365.

Ingenieurgesellschaft für Geo-und Umwelttechnik. (2017). *Kostenschätzung geothermieanlage*. Ingenieurgesellschaft für Geo- und Umwelttechnik.

International Energy Agency, Solar Heating and Cooling Programme. (2021). Task 60: Pvt systems [Accessed: 2024-08-02]. https://www.iea-shc.org/Data/Sites/1/publications/2021-07-Task60-PVT-Systems.pdf

Kalogirou, M. (2019). A review of solar thermal technologies. *Energy and Buildings*, *188-189*, 46–57. https://doi.org/10.1016/j.enbuild.2018.12.042

Kangas, M., & Lund, P. (1994). Modeling and simulation of aquifer storage energy systems. *Solar Energy*, *53*(3), 227–237. https://doi.org/10.1016/0038-092X(94)90630-0

Katz, E. A., Fairman, D., Tuladhar, S. M., et al. (2001). Temperature dependence for the photovoltaic device parameters of polymer-fullerene solar cells under operating conditions. *Journal of Applied Physics*, *90*(10), 5343–5350.

Klampaftis, E., et al. (2009). Enhancing the performance of solar cells via luminescent down-shifting of the incident spectrum: A review. *Solar Energy Materials and Solar Cells*, *93*(8), 1182–1194.

Kolhe, M., Bin, D., & Hu, E. (2012). Water cooled concentrated photovoltaic system. *International Journal of Smart Grid and Clean Energy*, *2*(1), 2–6.

Kozak-Jagieła, E., Cisek, P., & Ocłoń, P. (2023). Cooling techniques for pv panels: A review. *SciRad Journal*, *2*(1), 47–68. https://doi.org/10.58332/scirad2023v2i1a03

Kranz, S., & Bartels, J. (2010). Simulation and data based optimisation of an operating seasonal aquifer thermal energy storage. https://api.semanticscholar.org/CorpusID:110425287

Kranz, S., Bloecher, G., & Saadat, A. (2015). Improving aquifer thermal energy storage efficiency. https://api.semanticscholar.org/CorpusID:113845116

Kribus, A., Kaftori, D., Mittelman, G., et al. (2006). A miniature concentrating photovoltaic and thermal system. *Energy Conversion and Management*, *47*(15), 3582–3590.

Landesamt für Natur, Umwelt und Verbraucherschutz Nordrhein-Westfalen. (2015). Leistungsbuch altlasten und flächenentwicklung [Accessed 29 Jan 2019]. http://www.leistungsbuch.de/Frontend/lbuKatalog/KatalogForm.aspx

Lee, K. S. (2010). A review on concepts, applications, and models of aquifer thermal energy storage systems. *Energies*, *3*(6), 1320–1334.

Lund, H., Østergaard, P., Connolly, D., Ridjan, I., Mathiesen, B., Hvelplund, F., Thellufsen, J., & Sorknæs, P. (2016). Energy storage and smart energy systems. *Int J Sustainable Energy Plan Manage*, *11*, 3–14.

Lyden, A., Brown, C. S., & Strachan, N. (2022). Seasonal thermal energy storage in smart energy systems: District-level applications and modelling approaches. *Renewable and Sustainable Energy Reviews*, *167*, 112760.

Matias, C. A., Santos, L., Alves, A., & Calixto, W. (2017). Increasing photovoltaic panel power through water cooling technique. *Journal of Renewable Energy and Environmental Sustainability*, *3*(1), 012345. https://doi.org/10.1234/jreees2017v3i1a01

Matuška, T. (2014). Performance and economic analysis of hybrid pvt collectors in solar dhw system. *International Conference on Solar Heating and Cooling for Buildings and Industry*, 1–10.

Moharram, K. A., Eltawil, M. A., & Omara, Z. M. (2013). Enhancing the performance of photovoltaic panels by water cooling. *Ain Shams Engineering Journal*, *4*(4), 869–877.

Mustafa Omer, A. (2008). Ground-source heat pumps systems and applications. *Renewable and Sustainable Energy Reviews*, *12*(2), 344–371. https://doi.org/https://doi.org/10.1016/j.rser.2006.10.003

Nižetić, S., Čoko, D., Yadav, A., & Grubišić-Čabo, F. (2016). Water spray cooling technique applied on a photovoltaic panel: The performance response. *Energy Conversion and Management*, *108*, 287–296.

Nordbotten, J. M. (2017). Analytical solutions for aquifer thermal energy storage. *Water Resources Research*, *53*, 1354–1368. https://api.semanticscholar.org/CorpusID:133117434

Nordell, B., & Snijders, A. (2015). The use of aquifers as thermal energy storage (tes) systems. *Renewable and Sustainable Energy Reviews*, *51*, 988–1001. https://doi.org/10.1016/j.rser.2015.06.008

Odeh, S., & Behnia, M. (2009). Improving photovoltaic module efficiency using water cooling. *Heat Transfer Engineering*, *30*(6), 499–505.

Østergaard, D., & Svendsen, S. (2017). Space heating with ultra-low-temperature district heating – a case study of four single-family houses from the 1980s [15th International Symposium on District Heating and Cooling, DHC15-2016, 4-7 September 2016, Seoul, South Korea]. *Energy Procedia*, *116*, 226–235. https://doi.org/https://doi.org/10.1016/j.egypro.2017.05.070

Othman, M. Y. H., Yatim, B., Sopian, K., et al. (2005). Performance analysis of a double-pass photovoltaic/thermal (pv/t) solar collector with cpc and fins. *Renewable Energy*, *30*(13), 2005–2017.

Pang, W., Zhang, Q., Wilson, G. J., Yang, Q., & Yan, H. (2020). Empirical influence of various environmental conditions and mass flow rates on hybrid photovoltaic thermal modules. *Applied Thermal Engineering*, *171*, 114965. https://doi.org/10.1016/j.applthermaleng.2020.114965

Patel, H., & Agarwal, V. (2008). Matlab-based modeling to study the effects of partial shading on pv array characteristics. *Energy Conversion, IEEE Transactions on*, *23*, 302–310. https://doi.org/10.1109/TEC.2007.914308

Pinel, P., Cruickshank, C. A., Beausoleil-Morrison, I., & Wills, A. (2011). A review of available methods for seasonal storage of solar thermal energy in residential applications. *Renewable and Sustainable Energy Reviews*, *15*(7), 3341–3359. https://doi.org/https://doi.org/10.1016/j.rser.2011.04.013

Prasad, M., & Bansal, R. (2021). Solar thermal and pv systems: Performance, energy prediction and integration. *Solar Energy*, *215*, 108–120. https://doi.org/10.1016/j.solener.2020.12.036

Pumpa.eu. (2024). *Leo 5dwm submersible borehole pump* [Accessed: 2024-08-05]. https://www.pumpa.eu/en/leo-5dwm-submersible-borehole-pump/

Radziemska, E., & Klugmann, E. (2002). Thermally affected parameters of the current-voltage characteristics of silicon photocell. *Energy Conversion and Management*, *43*(15), 1889–1900.

Rahimi-Ahar, Z., Khiadani, M., Ahar, L. R., & Shafieian, A. (2023). Performance evaluation of single stand and hybrid solar water heaters: a comprehensive review. *Clean Technologies and Environmental Policy*, *25*(7), 2157–2184. https://doi.org/10.1007/s10098-023-02556-6

Rahman, T., Mansur, A. A., Lipu, M. S. H., Rahman, M. S., Ashique, R. H., Houran, M. A., Elavarasan, R. M., & Hossain, E. (2023). Investigation of degradation of solar photovoltaics: A review of aging factors, impacts, and future directions toward sustainable energy management. *Energies*, *16*(9), 3706. https://doi.org/10.3390/en16093706

Razak, A., Irwan, Y., Leow, W., Irwanto, M., Safwati, I., & Zhafarina, M. (2016). Investigation of the effect temperature on photovoltaic (pv) panel output performance. *International Journal on Advanced Science, Engineering and Information Technology*, *6*(5), 682–688. https://doi.org/10.18517/IJASEIT.6.5.938

Redko, A., Redko, O., & DiPippo, R. (2020). Effective use of heat pumps for various heating applications. In *Low-temperature energy systems with applications of renewable energy* (pp. 87–133). Academic Press. https://doi.org/https://doi.org/10.1016/B978-0-12-816249-1.00003-0

Rezvanpour, M., & Chen, Y. (2023). Space cooling energy potential of domestic cold water before household consumption in cold-climate regions. *Buildings*, *13*, 1491. https://doi.org/10.3390/buildings13061491

Ronquillo, R. (2023, March). Understanding heat exchangers. https://www.thomasnet.com/articles/process-equipment/understanding-heat-exchangers/

Rosa-Clot, M., Rosa-Clot, P., Tina, G. M., & Scandura, P. F. (2010). Submerged photovoltaic solar panel: Sp2. *Renewable Energy*, *35*(8), 1862–1865.

Ruhnau, O., Hirth, L., & Praktiknjo, A. (2019). Time series of heat demand and heat pump efficiency for energy system modeling. *Scientific data*, *6*(1), 1–10.

Ruiz Delgado, D., Hendriks, E., & Toimil Matesanz, M. (2010). *Open systems technical guide*. https://www.fenercom.com/publicacion/guia-tecnica-de-sistemas-geotermicos-abiertos-2010

Sadeghi, G., Mehrali, M., Shahi, M., Brem, G., & Mahmoudi, A. (2022). Progress of experimental studies on compact integrated solar collector-storage retrofits adopting phase change materials. *Solar Energy*, *237*, 62–95. https://doi.org/10.1016/j.solener.2022.03.070

Sarbu, I., & Sebarchievici, C. (2018). A comprehensive review of thermal energy storage. *Sustainability*, *10*(1), 191.

Sauty, J. P., Gringarten, A. C., Menjoz, A., & Landel, P. A. (1982). Sensible energy storage in aquifers: 1. theoretical study. *Water Resources Research*, *18*, 245–252. https://api.semanticscholar.org/CorpusID:119824362

Schüppler, S., Fleuchaus, P., & Blum, P. (2019). Techno-economic and environmental analysis of an aquifer thermal energy storage (ates) in germany. *Geothermal Energy*, *7*(11). https://doi.org/10.1186/s40517-019-0127-6

Seider, W. (2006). *Product and process design* [Book on equipment sizing and capital cost estimation]. University of Pennsylvania.

Sharaf, M., Yousef, M. S., & Huzayyin, A. S. (2022). Review of cooling techniques used to enhance the efficiency of photovoltaic power systems. *Environmental Science and Pollution Research*. https://doi.org/10.1007/s11356-022-18719-9

Singh, P., et al. (2008). Temperature dependence of i-v characteristics and performance parameters of silicon solar cell. *Solar Energy Materials and Solar Cells*, *92*(12), 1611–1616.

Smith, K. L., El-Gohary, M. A., & Ibrahim, A. M. (2014). Water cooling method to improve the performance of field mounted, insulated, and concentrating photovoltaic modules. *Journal of Solar Energy Engineering*, *136*, 034503–034512.

Sommer, W. (2015, June). *Modelling and monitoring of aquifer thermal energy storage : Impacts of soil heterogeneity, thermal interference and bioremediation* [internal PhD, WU]. Wageningen University [WU thesis 6052]. Wageningen University.

Stadtwerke Sindelfingen. (2007). *Planbare kosten—die hausanschlusspauschalen* (Report on planned costs and connection fees). Stadtwerke Sindelfingen. Sindelfingen.

Stadtwerke Waldkraiburg. (2018). *Preisblatt geothermale fernwärmeversorgung* (Report on geothermal district heating pricing). Stadtwerke Waldkraiburg GmbH. Waldkraiburg.

Sun, V., Asanakham, A., Deethayat, T., & Kiatsiriroat, T. (2022). Performance analysis on combined heat and power of photovoltaic-thermal module integrated with phase change material-water storage. *Journal of Energy Storage*, 103614.

Talavera, D. L., Nofuentes, G., Aguilera, J., et al. (2007). Tables for the estimation of the internal rate of return of photovoltaic grid-connected systems. *Renewable and Sustainable Energy Reviews*, *11*(3), 447–466.

Tian, Y., & Zhao, C. (2013). A review of solar collectors and thermal energy storage in solar thermal applications. *Applied Energy*, *104*, 538–553. https://doi.org/https://doi.org/10.1016/j.apenergy.2012.11.051

TripleSolar. (2024). *The pvt system* [Accessed: 2024-08-05]. https://triplesolar.eu/en/the-pvt-system/

Ul Abdin, Z., & Rachid, A. (2021). A survey on applications of hybrid pv/t panels. *Energies*, *14*(4), 1205. https://doi.org/10.3390/en14041205

Ul Abdin, Z., Rachid, A., & Korkut, T. B. (2022). Design and analysis of an innovative photovoltaic-thermal collector with embedded tank. *Solar Energy*, *245*, 290–298. https://doi.org/https://doi.org/10.1016/j.solener.2022.09.018

Ul-Abdin, Z., Zeman, M., Isabella, O., & Santbergen, R. (2024). Investigating the annual performance of air-based collectors and novel bi-fluid based pv-thermal system. *Solar Energy*, *276*, 112687. https://doi.org/https://doi.org/10.1016/j.solener.2024.112687

Union, E. (2009). Directive 2009/28/ec of the european parliament and of the council of 23 april 2009 on the promotion of the use of energy from renewable sources.

van der Roest, E., Beernink, S., Hartog, N., van der Hoek, J. P., & Bloemendal, M. (2021). Towards sustainable heat supply with decentralized multi-energy systems by integration of subsurface seasonal heat storage. *Energies*, *14*(23), 7958.

Van Doorninck, M. (2020). Amsterdam heat guide. https://issuu.com/gemeenteamsterdam/docs/the-amsterdam-heat-guide

Vanhoudt, D., Desmedt, J., van Bael, J., Robeyn, N., & Hoes, H. (2011). An aquifer thermal storage system in a belgian hospital: Long-term experimental evaluation of energy and cost savings. *Energy and Buildings*, *43*, 3657–3665. https://doi.org/10.1016/j.enbuild.2011.09.040

van-Rossum, A. (2024). Developing and implementing toolbox integrations for storing excess heat generated by a PVT system. https://repository.tudelft.nl/islandora/object/uuid%3Ab4066b14-7087-4ab7-8628-e7a2af4a2b83?collection=education

VDI. (2012). *Economic efficiency of building installations: Fundamentals and economic calculations.*

Verbeterjehuis.nl. (2024). Energiesubsidiewijzer [Accessed: 2024-08-02]. https://www.verbeterjehuis.nl/energiesubsidiewijzer

Vogt, M. R., Tobon, C. R., Alcañiz, A., Procel, P., Blom, Y., Din, A. N. E., Stark, T., Wang, Z., Goma, E. G., Etxebarria, J., Ziar, H., Zeman, M., Santbergen, R., & Isabella, O. (2022). Introducing a comprehensive physics-based modelling framework for tandem and other PV systems. *Solar Energy Materials and Solar Cells*, *247*, 111944. https://doi.org/10.1016/j.solmat.2022.111944

Vorushylo, I., Keatley, P., Shah, N., Green, R., & Hewitt, N. (2018). How heat pumps and thermal energy storage can be used to manage wind power: A study of ireland. *Energy*, *157*, 539–49. https://doi.org/10.1016/j.energy.2018.03.001

Ward, J., Simmons, C., & Dillon, P. (2007). A theoretical analysis of mixed convection in aquifer storage and recovery: How important are density effects? *Journal of Hydrology*, *343*, 169–186.

Weiss, W., & Spörk-Dür, M. (2023). *Solar heat worldwide: Global market development and trends 2022, detailed market figures 2021.* IEA Solar Heating Cooling Programme. https://www.iea-shc.org/Data/Sites/1/publications/Solar-Heat-Worldwide-2022.pdf

West, B. G. (2004). Open architecture ate: Prospects and problems. *2004 International Conference on Test*, 1410–. https://api.semanticscholar.org/CorpusID:1618498

Xie, K., Nian, Y.-L., & Cheng, W.-l. (2018). Analysis and optimization of underground thermal energy storage using depleted oil wells. *Energy*. https://api.semanticscholar.org/CorpusID:115283970

Yang, T., Liu, W., Kramer, G. J., & Sun, Q. (2021). Seasonal thermal energy storage: A techno-economic literature review. *Renewable and Sustainable Energy Reviews*, *139*, 110692.

Zaini, N., Kadir, M. A. A., Izadi, M., Ahmad, N. I., Radzi, M. A. M., & Azis, N. (2015). The effect of temperature on a mono-crystalline solar pv panel. *2015 IEEE Conference on Energy Conversion (CENCON)*.

Zhang, X., Wang, Y., Wang, J., Wang, S., & Wang, Q. (2022). Model predictive control for the performance improvement of air source heat pump heating system via variable water temperature difference. *Building and Environment*, *208*, 108614. https://doi.org/10.1016/j.buildenv.2021.108614

Zhao, R., Zhang, X., & Liu, J. (2019). A review on the air-source heat pump. *Applied Energy*, *239*, 514–525. https://doi.org/10.1016/j.apenergy.2019.01.172

Zondag, H., Vries, D., Helden, W., Zolingen, R., & Steenhoven, A. (2003). The yield of different combined pv-thermal collector designs. *Solar Energy*, *74*, 253–269. https://doi.org/10.1016/S0038-092X(03)00121-X

A

Modes and Equations

A.1 Brief explanation of Operational Modes

1. **Mode 1: Space Heating and Domestic Hot Water**

   - Mode 1a: When outflow water temperature from collectors is more than 20°C and PVT output $\geq$ 0.5 kW, the system prioritizes PVT for both space heating and DHW, supplemented by the warm aquifer.

   - Mode 1b: For outflow temperatures between 14°C and 20°C with sufficient PVT output ($\geq$ 0.5 kW), the warm aquifer becomes the primary source for both demands and the PVT thermal energy is stored in the cold aquifer.

   - Mode 1c: When PVT output is low ($<$ 0.5 kW), the system relies entirely on the warm aquifer for space heating and dhw demand.

2. **Mode 2: Space Cooling and Domestic Hot Water**

   - Mode 2a: Under favorable PVT conditions, cooling is provided by the cold aquifer while dhw is met through a combination of the warm aquifer and HP. The thermal energy extracted from PVT and building is stored in the warm aquifer.

   - Modes 2b: This mode is similar to Mode 2a, but in this case, the PVT thermal energy is stored in the cold aquifer and the building's energy in the warm aquifer because the temperature does not meet the threshold for the warm aquifer. As PVT output decreases, the system increasingly relies on the aquifers for both cooling and dhw.

   - Mode 2c: This mode fully supplies the demand, and there is no generation of thermal energy from PVT.

3. **Mode 3: Space Heating > Cooling and Domestic Hot Water**
   This mode addresses scenarios where there is a simultaneous need for both heating and cooling, along with a demand for domestic hot water. The system supplies the heating since it is higher than the cooling. The sub-modes are similar to Mode 1 where PVT produces sufficient output water temperature then it provides or else a warm aquifer satisfies the demand for heating. The system balances resources between PVT, and warm and cold aquifers to meet all demands efficiently.

4. **Mode 4: Space Cooling > Heating and Domestic Hot Water**
   This mode addresses scenarios where there is a simultaneous need for both heating and cooling, along with a demand for domestic hot water. The system supplies the cooling since

it is higher than the heating. The sub-modes are similar to Mode 2 where PVT produces sufficient output water temperature and is stored in the warm aquifer and the cold aquifer satisfies the demand for cooling. The system balances resources between PVT, and warm and cold aquifers to meet all demands efficiently.

5. **Mode 5: Domestic Hot Water Only**
   When only domestic hot water is required, the system prioritizes PVT use when available, and the warm aquifer acts as a secondary source when needed.

A.2 Detailed Explanation of Modes

Mode 1a: Space Heating, DHW Demand and PVT Generation : High
In this mode, the outflow temperature from the PVT system is above 20 °C, and the PVT system's output is significant ($\geq$ 0.5 kW). The code performs the following steps:

Calculates the volume flow rate of water extracted from the cold aquifer and injected into the warm aquifer after passing through the PVT system. Calculates the heat demand of the building ($Q_{supplied}$) in Wh. Utilizes a heat pump model to determine the heat output (Q_{room}), power consumption (P_{hp}), outlet temperature (T_{hp}), and mass flow rate ($dm_{f,hp}$) when using the PVT system's output as the heat source. Checks if the heat pump output is sufficient to meet the building's heat demand. If not, it uses the warm aquifer as an additional heat source and calculates the corresponding heat pump output ($Q_{roomATES}$), power consumption ($P_{hp,ATES}$), outlet temperature ($T_{hp,ATES}$), and mass flow rate ($dm_{f,hp,ATES}$). Calculates the domestic hot water (DHW) demand and uses the warm aquifer as the heat source to meet this demand, determining the corresponding heat pump output ($Q_{room,DHW}$), power consumption ($P_{hp,DHW}$), outlet temperature ($T_{hp,DHW}$), and mass flow rate ($dm_{f,hp,DHW}$). Updates the volumes (V1 and V2) and temperatures $T_{aquifer,1}$ and $T_{aquifer,2}$ of the warm and cold aquifers based on the water flow rates and temperatures involved.

Mode 1b: Space Heating, DHW Demand and PVT Generation : Low
In this mode, the outflow temperature from the PVT system is between 14 °C and 20 °C, and the PVT system's output is significant ($\geq$ 0.5 kW). The code follows steps similar to Mode 1a, with the following differences:

The water from the PVT system is directly injected into the cold aquifer instead of being sent to the heat pump. The warm aquifer's water is used as the heat source for both the building's heating demand and the DHW demand.

Mode 1c: Space Heating, DHW Demand and No PVT Generation
In this mode, the PVT system's output is negligible ($\leq$ 0.5 kW). The code performs the following steps:

Calculates the heat demand of the building ($Q_{supplied}$) in Wh. Utilizes the heat pump model with the warm aquifer as the sole heat source to meet the building's heating demand, determining the heat pump output ($Q_{roomATES}$), power consumption (P_{hpATES}), outlet temperature ($T_{hp,ATES}$), and mass flow rate ($dm_{f,hp,ATES}$). Calculates the DHW demand and uses the warm aquifer as the heat source to meet this demand, determining the corresponding heat pump output ($Q_{room,DHW}$), power consumption ($P_{hp,DHW}$), outlet temperature ($T_{hp,DHW}$), and mass flow rate ($dm_{f,hp,DHW}$). Updates the volumes (V1 and V2) and temperatures ($T_{aquifer,2}$) of the warm and cold aquifers based on the water flow rates and temperatures involved. The warm aquifer temperature ($T_{aquifer,1}$) remains unchanged in this mode.

Mode 2a: Space Cooling, DHW Demand and PVT Generation : High

The volume flow rate of water extracted from the cold aquifer and injected into the warm aquifer after passing through the PVT system is calculated. The cooling demand of the building ($Q_{supplied}$) is calculated in Wh. The flow rate of water from the cold aquifer to the building

(m_b) is determined based on the cooling demand and the temperature difference between the building and the desired space cooling temperature. The outlet temperature of the water sent to the building ($T_{cold,2}$) is calculated. The DHW demand is calculated, and the heat pump model is used with the warm aquifer as the heat source to meet this demand, determining the heat pump output ($Q_{room,DHW}$), power consumption ($P_{hp,DHW}$), outlet temperature ($T_{hp,DHW}$), and mass flow rate ($dm_{f,hp,DHW}$). The volumes (V1 and V2) and temperatures ($T_{aquifer,1}$) and $T_{aquifer,2}$ of the warm and cold aquifers are updated based on the water flow rates and temperatures involved.

Mode 2b: Space Cooling, DHW Demand and PVT Generation : Low

The volume flow rate of water extracted from the cold aquifer and injected into the warm aquifer after passing through the PVT system is calculated. The cooling demand of the building ($Q_{supplied}$) is calculated in Wh. The flow rate of water from the cold aquifer to the building (m_b) is determined based on the cooling demand and the temperature difference between the building and the desired space cooling temperature. The outlet temperature of the water sent to the building ($T_{cold,2}$) is calculated. The DHW demand is calculated, and the heat pump model is used with the warm aquifer as the heat source to meet this demand, determining the heat pump output ($Q_{room,DHW}$), power consumption ($P_{hp,DHW}$), outlet temperature ($T_{hp,DHW}$), and mass flow rate ($dm_{f,hp,DHW}$). The volumes (V1 and V2) and temperatures $T_{aquifer,1}$ and $T_{aquifer,2}$ of the warm and cold aquifers are updated based on the water flow rates and temperatures involved.

Mode 2c: Space Cooling, DHW Demand and No PVT Generation

The cooling demand of the building ($Q_{supplied}$) is calculated in Wh. The flow rate of water from the cold aquifer to the building (m_b) is determined based on the cooling demand and the temperature difference between the building and the desired space cooling temperature. The outlet temperature of the water sent to the building ($T_{cold,2}$) is calculated. The DHW demand is calculated, and the heat pump model is used with the warm aquifer as the heat source to meet this demand, determining the heat pump output ($Q_{room,DHW}$), power consumption ($P_{hp,DHW}$), outlet temperature ($T_{hp,DHW}$), and mass flow rate ($dm_{f,hp,DHW}$). The volumes (V1 and V2) and temperatures (($T_{aquifer,1}$) and $T_{aquifer,2}$) of the warm and cold aquifers are updated based on the water flow rates and temperatures involved.

In all three modes, the code ensures the proper interaction between the PVT system, ATES system, and the building, while updating the aquifer volumes and temperatures accordingly to meet the cooling and DHW demands efficiently.

Mode 3a: Space Heating > Space Cooling, DHW Demand and PVT Generation : High

The volume flow rate of water extracted from the cold aquifer and injected into the cold aquifer after passing through the PVT system is calculated. The heating demand of the building ($Q_{supplied}$) is calculated in Wh. The heat pump model is used with the PVT system as the primary heat source to determine the heat output (Q_{room}), power consumption (P_{hp}), outlet temperature (T_{hp}), and mass flow rate ($dm_{f,hp}$). If the heat pump output is insufficient to meet the heating demand, the warm aquifer is used as a supplementary heat source, and the corresponding heat pump output ($Q_{roomATES}$), power consumption ($P_{hp,ATES}$), outlet temperature ($T_{hp,ATES}$), and mass flow rate ($dm_{f,hp,ATES}$) are calculated. The DHW demand is calculated, and the heat pump model is used with the warm aquifer as the heat source to meet this demand, determining the heat pump output ($Q_{room,DHW}$), power consumption ($P_{hp,DHW}$), outlet temperature ($T_{hp,DHW}$), and mass flow rate ($dm_{f,hp,DHW}$). The volumes (V1 and V2) and temperatures ($T_{aquifer,1}$ and $T_{aquifer,2}$) of the warm and cold aquifers are updated based on the water flow rates and temperatures involved.

Mode 3b: Space Heating > Space Cooling, DHW Demand and PVT Generation : Low
The steps are similar to Mode 3a, with the difference being the temperature range of $T_{outflow}$ from 14 °C to 20 °C.

Mode 3c: Space Heating > Space Cooling, DHW Demand and No PVT Generation

The volume flow rate of water extracted from the cold aquifer and injected into the cold aquifer after passing through the PVT system is calculated (negligible contribution from the PVT system). The heating demand of the building ($Q_{supplied}$) is calculated in Wh. The heat pump model is used with the warm aquifer as the sole heat source to meet the heating demand, determining the heat pump output ($Q_{roomATES}$), power consumption ($P_{hp,ATES}$), outlet temperature ($T_{hp,ATES}$), and mass flow rate ($dm_{f,hp,ATES}$). The DHW demand is calculated, and the heat pump model is used with the warm aquifer as the heat source to meet this demand, determining the heat pump output ($Q_{room,DHW}$), power consumption ($P_{hp,DHW}$), outlet temperature ($T_{hp,DHW}$), and mass flow rate ($dm_{f,hp,DHW}$). The volumes (V1 and V2) and temperatures $T_{aquifer,1}$ and $T_{aquifer,2}$) of the warm and cold aquifers are updated based on the water flow rates and temperatures involved.

In all three modes, the code ensures the proper interaction between the PVT system, ATES system, and the building, while updating the aquifer volumes and temperatures accordingly to meet the heating, cooling, and DHW demands efficiently when the heating demand is greater than the cooling demand. The mode 4 and 5 are similar to the three modes.

A.3 Temperature and Volume dynamics during space cooling

The equations presented in this section represent the case when water from the cold aquifer is utilized for space cooling the buildings for an hour. Equations for the case of space cooling are presented in Appendix A.3.

A.3.1 Volume dynamics of aquifers

The volume changes in both warm and cold aquifers are governed by the following equations:

For the warm aquifer:

$$V1(i) = V_1 - V_{ext}(i) + V_b(i) \tag{A.1}$$

For the cold aquifer:

$$V2(i) = V_2 - V_{cc} + V_{inj}(i) - V_b(i) \tag{A.2}$$

where:
V_1 and V_2 are the volumes of warm and cold aquifers at time step i, respectively.
$V1$ and $V2$ are the initial volumes of warm and cold aquifers, respectively.
V_{ext} is the volume extracted for space heating and DHW at time step i.
V_{cc} is the volume used for cooling the collectors.
V_{inj} is the volume injected from heat pumps and collectors at time step i.
V_b is the volume injected from the heat exchanger at time step i.

A.3.2 Temperature dynamics of aquifers

The temperature changes in the aquifers are described by:

For the warm aquifer:

$$T_{\text{aquifer},1}(i) = \frac{V_1 \cdot T_{\text{aquifer},1}(i-1) + V_{\text{inj}}(i) \cdot T_{\text{inj water}}(i) + V_{\text{b}}(i) \cdot T_{\text{c}}(i)}{V_1(i)} \tag{A.3}$$

For the cold aquifer:

$$T_{\text{aquifer},2}(i) = \frac{V_2 \cdot T_{\text{aquifer},2}(i-1) + V_{\text{inj}}(i) \cdot T_{\text{inj water}}(i)}{V_2(i)} \tag{A.4}$$

where:
$T_{\text{aquifer},1}(i)$ and $T_{\text{aquifer},2}(i)$ are the temperatures of warm and cold aquifers at time step i.
$T_{\text{aquifer},1}(i-1)$ and $T_{\text{aquifer},2}(i-1)$ are the temperatures of warm and cold aquifers at time step i-1.
$T_{\text{inj water}}(i)$ is the temperature of injected water at time step i.

This equation provides insights into the thermal dynamics of the aquifer system for an hour of the year, indicating how the injection and extraction processes influence the temperature distribution within the cold aquifer.

Equations A.1 to A.4 facilitate the analysis of volume and temperature dynamics in response to injection and extraction of water in these aquifers, over the year. They serve as fundamental concepts in understanding the thermal and hydraulic behaviour of these aquifers.

A.3.3 Electrical performance of PVT collectors

On comparing the electrical efficiency of the PVT collector with and without cooling, it can be observed that cooling with cold aquifer water improves its efficiency, leading to better performance. This can be seen in the graph A.1.

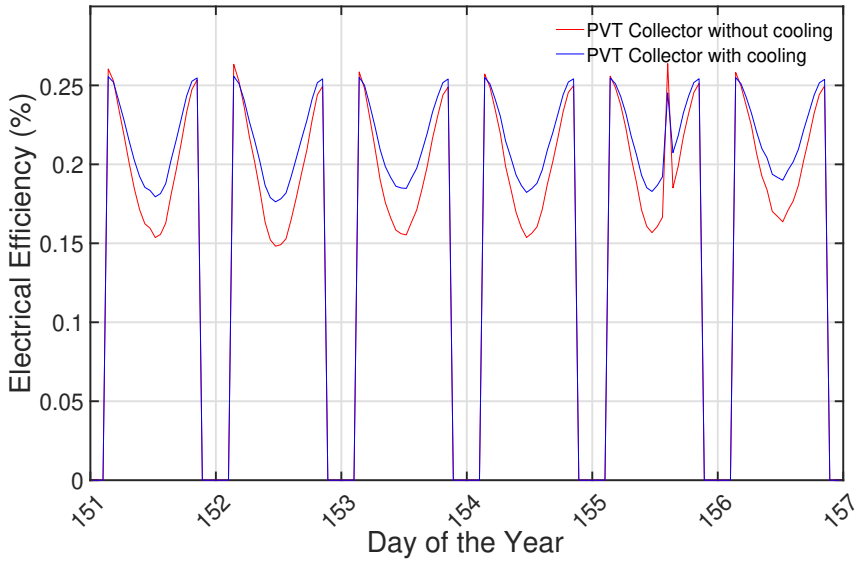

Figure A.1: Electrical efficiency of PVT collector with and without cooling

The graph is plotted for the June week from day 151th to day 157th of the year.